Instruments and Observing Methods
Report No. 140

Report on the WMO International Pyrheliometer Comparison (IPC-XIII)

(27 September - 15 October 2021, Davos, Switzerland)

W. Finsterle

WEATHER CLIMATE WATER

WORLD
METEOROLOGICAL
ORGANIZATION

This publication is available in pdf format, from the WMO Library website:
https://library.wmo.int/

Chair, Publications Board
World Meteorological Organization (WMO)
7 bis, avenue de la Paix
P.O. Box 2300
CH-1211 Geneva 2, Switzerland

Tel: +41 (0) 22 730 8403
Fax: +41 (0) 22 730 8117
E-mail: Publications@wmo.int

NOTE

FOREWORD

The World Meteorological Organization (WMO) strategic plan recognizes the increasing demand for accessible and authoritative information on the changing states of the entire Earth. High-quality fit-for-purpose traceable measurements are essential to meet this demand.

The WMO Technical Commission for Observation, Infrastructure and Information Systems (INFCOM) has set up a Standing Committee on Measurement, Instrumentation and Traceability (SC-MINT) that coordinates activities that enable the traceability of measurement to international standards in the context of the WMO Integrated Global Observing System (WIGOS). The intercomparison presented in this report is one of those key activities.

The organization and hosting of the WMO International Pyrheliometer Comparisons (IPCs) at the Physikalisch-Meteorologisches Observatorium Davos/World Radiation Centre (PMOD/WRC) has a long and important history. It aims at ensuring the traceability of solar radiation measurements around the world using the World Radiometric Reference (WRR) by verifying its stability and disseminating the reference to national and/or regional standard instruments, and other participating instruments such as those of universities and instrument manufacturers.

The 5-year regularity of IPCs is key to the traceability of solar radiation measurements around the world using the WRR. Exceptionally, the WMO Executive Council at its Seventy-second session agreed to the postponement of the Thirteenth International Pyrheliometer Comparison (IPC-XIII) by one year because of the pandemic and inherent travel restrictions. Organizing IPC-XIII in 2021 remained a challenge in view of the ongoing COVID-19 pandemic. Fortunately, many participants were able to travel to Davos and took part in the campaign.

This report summarizes the outcomes of the IPC-XIII and demonstrates the stability of the WRR in providing a worldwide metrological reference. Favourable weather conditions enabled acquisition of a large number of the calibration points, what increased confidence in the traceability dissemination. On the days without weather conditions appropriate to take the measurements, a symposium on radiation measurement was organized. Many presentations delivered at the symposium facilitated the experience exchange and knowledge transfer.

It has been shown that there is an apparent offset of the WRR relative to the International System of Units (SI) and that recent technological developments enable to significantly reduce the uncertainties of potential new reference instruments for solar irradiance measurements, such as the Cryogenic Solar Absolute Radiometer (CSAR) and Monitor to Measure the Integral Transmittance of Windows (MITRA). INFCOM is envisaging a reference change to ensure stable and accurate measurements for the future while minimizing the impacts that such a change will have on climate datasets. The outcomes of this intercomparison and of the next intercomparison to be held in 2025 will be critical elements to consider towards this reference change. It is anticipated that such a reference change could be approved by the 20th World Meteorological Congress in 2027.

I wish to express my sincere appreciation to all those who contributed to the success of this intercomparison. Particularly to the staff of the World Radiation Centre for organizing this intercomparison and ensuring a safe environment for all participants, to the members of the IPC-XIII Ad-hoc committee for their review of the report and to all those who contributed to the symposium, sharing their expertise with other participants.

President of the Infrastructure Commission

Michel Jean

WMO International Pyrheliometer Comparison
IPC-XIII
27 September - 15 October 2021
Davos Dorf, Switzerland

Wolfgang Finsterle

PMOD/WRC, Davos Dorf
WMO IOM Report No. 140
2023

Contents

Chapter 1 Organization and Procedures

1.1 Introduction

The 13^{th} International Pyrheliometer Comparison (IPC-XIII) was held together with Regional Pyrheliometer Comparisons (RPCs) of all WMO Regional Associations (RA I to RA VI) from 27 September through 15 October 2021 at the Physikalisch-Meteorologisches Observatorium Davos/World Radiation Centre (PMOD/WRC) in Davos Dorf, Switzerland. The IPC-XIII was delayed by 1 year because of international travel restrictions in response to the COVID-19 pandemic in 2020. Held concurrently with the IPC-XIII were the fifth Filter Radiometer Comparisons (FRC-V) and the third International Pyrgeometer Comparisons (IPgC-III). Results from the FRC-V and IPgC-III will be presented in separate reports.

The results presented in this report are based on the measurements carried out during the three weeks assigned to the IPC-XIII. The weather conditions allowed acquisition of a large number of calibration points for most participating instruments. Seminar presentations were given on days when the weather conditions did not allow measurements to be taken.

1.2 Participation

Due to the on-going COVID-19 restrictions not all Regional Radiation Centres (RRC) were able to delegate a representative to the IPC-XIII. Instead, pyrheliometers sent from RRCs without operators were operated by WRC staff, resulting in 103 pyrheliometers from 40 institutions (1 WRC, 9 RRCs, 12 NRCs, 6 manufacturers, 3 National Metrology Institutes (NMI), 3 universities, 6 solar energy industry) representing 26 countries and the European Commission that were present for the comparison. The six World Standard Group (WSG) instruments (PMO2, PMO5, CROM2L, PAC3, HF18748, MK67814) and the Cryogenic Solar Absolute Radiometer (CSAR), were operated by the WRC staff. See Tables 1.1 and 1.2 for a complete list of all participating centres and institutions. Two representatives of WMO attended the first couple of days of IPC-XIII.

Table 1.1: IPC-XIII Participants: *WMO World, Regional and National Radiation Centres*

Country	*Type*	*Institution*	*Operator(s)*	*Instrument(s)*
World Radiation Center				
Switzerland	WRC	Physikalisch-Meteorologisches Observatorium Davos, World Radiation Centre, Davos	Wolfgang Finsterle Ricco Soder Natalia Engler Christian Thomann David Schweizer Julian Gröbner Stelios Kazadzis Natalia Kouremeti	**PMO2**[1] **PMO5** **CROM2L** **PAC3** **HF18748** **MK67814** NIP-31144E6 EPAC11402 PMO6-79-122 AHF32455 CSAR PMO6-0304 PMO6-0401 PMO6-0803 SIAR-2A PMO8-F201-007A PMO6-7 (Meteoswiss, NRC) PMO6-0808 (China, NRC) PMO6-1109 (Croatia, NRC) PMO6-1603 (Japan, RRC) PMO6-1610 (Indonesia, NRC)
RA I (Africa)				
Algeria	RRC	Office National de la Météorologie	Ben Mohammed	AHF29225
Egypt	RRC	Egyptian Meteorolgical Auth., Cairo	Khaled Wael	AHF31103
Libya	NRC	Libyan Center for Solar Energy Research and Studies, Tripoli	Akram Essnid	CHP1-131107

[1]The WSG pyrheliometers are printed in **boldface**. In normal print are other WRC pyrheliometers, unless indicated otherwise.

Table 1.1: (continued)

Country	*Type*	*Institution*	*Operator(s)*	*Instrument(s)*
RA II (Asia)				
Saudi Arabia	NRC	K.A.CARE, Riyadh	Abdullah Al Adwani Saad Al Qahtani Abdulhakim Bin Dayil	AHF30110
RA III (South America)				
Uruguay	NRC	Laboratorio de Energía Solar, Universidad de la República, Salto	Augustín Laguarda Paola Russo	CHP1-150261
RA IV (North America, Central America and the Caribbean)				
Mexico	RRC	Instituto de Geofísica, UNAM México, DF	Adirana Elizabeth Gonzalez	AHF29223 PMO6-1102
RA V (South-West Pacific)				
RA VI (Europe)				
Belgium	RRC	Royal Meteorological Institute, Uccle	Christian Conscience Joannes Nevens Julien Amand Pierre Malcorps Luca Schifano	CR05L CR09R
Czech Republic	NRC	Czech. Hydromet. Institute, Hradec Kralove	Jiri Pokorny	HF30497
Germany	RRC	DWD Met. Obs. Lindenberg, Tauche OT Lindenberg	Stefan Wacker Lionel Doppler	AHF29221[2] HF27157 PMO6-5 PMO6-0405
Russian Federation	RRC WRDC	Voeikov MGO, St. Petersburg	Vladislav Iakovlev Artem Rodionov	PMO6-0817
Slovakia	NRC	SHMI, Poprad-Ganovce	Anna Pribullová	AHF37814
Slovenia	NRC	Slovenian Environment Agency, Ljubljana	Marko Svetličič Iztok Miklavžina	PMO6-1103 CHP1-140049
Sweden	RRC	SMHI, Norrköping	Thomas Carlund	PMO8-F201-006A AWX 33393

[2]This pyrheliometer was operated in active mode with the LINARD controller s/n P00.

Table 1.1: (continued)

Country	*Type*	*Institution*	*Operator(s)*	*Instrument(s)*
The Netherlands	NRC	KNMI, De Bilt	Wouter Knap Izzy Hendriks	AHF27159 CHP1-200837 CHP1-200838
United Kingdom of Great Britain and Northern Ireland	NRC	Met Office, Exeter, Devon	David Hiscock Sanghera Sandeep	AHF31110 AHF37813

Table 1.2: IPC-XIII Participants: *Manufacturers, metrology, research, and industrial institutions*

Country	*Institution*	*Participant(s)*	*Instrument(s)*
Chile	Universidad de Santiago de Chile, Santiago	Edgardo Sepúlveda José Jorgue Torres	PMO6-1602 SHP1-195181
Denmark	Technical University of Denmark, Kgs. Lyngby	Adam Jensen	SHP1-185163 SHP1-205241
Germany	PTB, Braunschweig (NMI)	Dirk Friedrich	PMO6-1104 PMO8-F201-001 PMO8-F201-002 SHP1-130042 SHP1-175109 SHP1-175110
Italy	European Commission JRC, Ispra, Varese	Willem Zaaiman Diego Pavanello Harald Müllejans	PMO6-81109 PMO6-911204 AHF0000 NIP-21451E6 NIP-23927E6 NIP-25738E6 NIP-26626E5 CH1-060460 CH1-930018 CH1-040370 CHP1-110533 MS56-12036 MS56-12039 MS57-1702504 TMI67604 TMI68835
The Netherlands	EKO Instruments, The Hague	Mario Po	PMO6-0816 MS56-P12023

Table 1.2: (continued)

Country	*Institution*	*Participant(s)*	*Instrument(s)*
Japan	Ishikawa Trading Co., Ltd., Tokyo	Kazuhiko Ohkubo	IRS04-2101 (AIST, RENRC) IRS04-2102 AHF33396 (AIST, RENRC)
Sweden	RISE Research Institute of Sweden (NMI), Borås	Anne Andersson Stefan Källberg Mikael Lindgren	HF15744
Spain	CIEMAT, Madrid	Jose Balenzategui	AHF28486 PMO6-0301 PMO6-1609 SNIP-37886E6
Switzerland	Davos Instruments	Markus Suter Jon Buchli Valeria Büchel	PMO6-1611 PMO8-F211-001 PMO8-F211-002 PMO8-F201-009 (Argentina, RRC)
The Netherlands	Hukseflux Thermal Sensors, Delft	Kees van den Bos Chiel Donkers Jürgen Konings	CP20C-101 CP20C-102 CP20U-101 CP20U-102 DR02-9210 DR20-65033 DR30-65005
The Netherlands	Kipp & Zonen BV (Ott Hydromet), Delft	Erik Nagel Joop Mees	PMO6-0103 SHP33-01 CHP1-REF2 PH1-999991
USA	Argonne National Lab, Billings OK	Craig Webb	AHF28968
USA	National Renewable Energy Lab., Golden CO	Ibrahim Reda Afshin Andreas	AHF23734 AHF29220 AHF30713 TMI68018
USA	The Eppley Laboratory Inc., Newport RI	Tom Kirk	AHF14915 AHF27798 AHF32449 AHF37812 (Korea)
USA	ISO-CAL North America, LCC, Phoenix AZ	Erik Naranen	AHF37816 AHF28560

Table 1.2: (continued)

Country	*Institution*	*Participant(s)*	*Instrument(s)*
USA	University of Oregon, Solar Radiation Monitoring Lab, Eugene	Josh Peterson	AHF34926

1.3 Data Acquisition and Evaluation

The signals from the WSG instruments and additional WRC and RRC radiometers were acquired by a data acquisition system based on 18 National Instruments PXI-4065 6.5-digit digital multimeters with NI PXI-2501 24-channel multiplexers. The system was controlled by a LabView application ("DAQ2010") running on an industrial PC and operated flawlessly. A separate LabView application triggered the aural and visual timing signals on the measurement field as well as the initialization and readout of the data entry forms for manually operated instruments (see below). This system is very robust and flexible, allowing pyrheliometers to be added/removed to/from the comparison without re-initializing the DAQ2010 software. All measurements were analyzed and visualized with an IDL software package on a separate PC in near-real-time.

The participating pyrheliometers were operated with their standard pointing and data acquisition equipment, either manually or automated.

The data from the manually operated instruments were typed into a web application by the operators. WLAN connections were used to initialize the web application and to upload the readings to a dedicated directory on the PMOD/WRC FTP server, from where it was fetched by the data analysis and visualisation computer (IDL). Written records were kept for backup purposes and to double-check for typing errors in the web application.

Computer controlled data acquisition systems had to run on CET (Central European Standard Time) and be synchronized to the basic measurement cadence (see below). Participants could up-load their data files to the dedicated directory on the FTP server from where they were fetched by the IDL computer. The prescribed file naming and format convention with three columns corresponding to date, time, and irradiance was observed by most participants. All data were ingested into the data acquisition and evaluation system at the end of each measurement day.

1.3.1 Timing of the Measurements

The measurements were taken in series of 21 minutes with a basic interval of 90 seconds. The starting time of each series was either on the full hour or the minute xx:30. Where needed, electrical calibrations and/or zero readings were completed *before* the starting time[3]. Voice announcements and acoustic signals together with a visual indicator on the measurement field informed the participants about the starting times and progress of the measurement series. A network time server or a digital reference clock on the measurement field could be used to synchronize all data acquisition systems.

[3]Manually operated radiometers which were using the web interface for submitting the data started their calibration sequence and/or zero reading on the starting time of the series. Hence they acquired slightly fewer irradiance readings per series.

The time until the next measurement was also indicated on the web interface for manual operators. The timing for each type of instrument was as follows[4]:

- PAC3: the calibration phase started with the shutter closed and the electrical heater[5] switched on for 40 seconds (this was introduced after IPC-III in order to have a well defined thermal state of the instrument independent of the operation sequence before the run). The zero of the thermopile was read 90 seconds after the heater had been switched off again. Then the heater was switched on for another 90 seconds before the heater voltage, current and the thermopile signal were read. The calibration sequence ends with the shutter open command 90 seconds before the starting time of the series. Each series produced 14 irradiance readings at 90-second interval. After the last reading the shutter was closed.
- HF- and TMI-type pyrheliometers: the calibration phase started with the shutter closed, after 90 seconds the thermopile zero was read and the electrical heater[5] turned on during 90 seconds. At the end of the heating phase the heater voltage, current and thermopile signal were read. The calibration sequence ends with the shutter open command, 90 seconds before the starting time of the series. Each series produced 14 irradiance readings at 90-second interval (11 irradiance readings via the web interface). After the last reading the shutter was closed.
- PMO-, SIAR- and CROM-type pyrheliometers: The measurements started with a reference phase (shutter closed) of 90 seconds, followed by a measurement phase (shutter open) of 90 seconds. The closed and open heater voltage and current are read at the end of each reference or measurement phase[6]. This reference/measurement sequence was repeated seven times, followed by an additional reference phase, yielding 7 open and 8 closed readings during each run (6 open and 7 closed via the web interface). PMO2 was read at twice that pace, with a reference phase of 45 seconds and a measurement phase of 45 seconds, producing 13 irradiance values per series. Note that for PMO2 the *open* heater current and voltage were read 6 times in rapid succession ($200\ \mathrm{ms}$ interval) to assess the atmospheric stability.
- Field pyrheliometers with thermopile sensor (NIP, CHP1, MS56, DR0x, etc.): These pyrheliometers started with a zero reading 90 seconds before the starting time of the series, followed by the shutter open command. The thermopile signal was then recorded every 90 seconds[6], yielding 14 irradiance readings (13 irradiance readings via web interface).
- Computerized and prototype pyrheliometers (e.g. CSAR, see Sect. 1.4) were using various modes of operation which are specific to their design. Their measurements were synchronized to the 90-seconds base cadence. The irradiance values were calculated according to the instrument-specific algorithms before being submitted to the FTP server in the standardized format.

1.3.2 Data Evaluation

For each instrument the irradiance was calculated according to the appropriate evaluation procedure as listed below. After each day a graphical print-out of the ratios to PMO2 was put on the FTP server to be reviewed by the participants. This simple but effective measure of quality control revealed instrumental problems in several cases which subsequently could be fixed quickly.

"Quick-look" print-outs were also produced at any time during the measurement day when an instrument was suspected to malfunction.

[4] This timing scheme applies to all WRC radiometers and radiometers that were connected to the WRC data acquisition system. Radiometers which were controlled by their own computer may have deviated partially from this scheme.

[5] The heater voltage was manually selected before each series to match the expected level of solar irradiance.

[6] The integration time varies between instrument types and between individual instruments from instantaneous up to 2 seconds.

The procedure used to calculate the irradiance *S* of each instrument type is described below. The notations are:

V_{th}	output of the thermopile
U_h, U_i	voltage across the heater (index h) or across the standard resistor (index i)
R_n	standard resistor (For PMOx-type radiometers R_n is often included in C_1.)
C_1	calibration factor (see Table 2.2)
C_2	correction factor for lead heating (see Table 2.2)
P	electrical power in the active cavities

- PAC3, HF, and TMI type pyrheliometers: the irradiance was calculated from the thermopile output V_{th}(irrad) when the receiver was irradiated. The sensitivity was determined by the calibration during which the cavity was shaded and electrically heated and U_h and U_i were measured together with the corresponding thermopile output V_{th}(cal). Furthermore, the zero of the thermopile V_{th}(zero) was measured and subtracted from all thermopile readings.

$$S = C_1 \frac{V_{th}(\text{irrad}) - V_{th}(\text{zero})}{V_{th}(\text{cal}) - V_{th}(\text{zero})} \frac{U_i}{R_n} \left(U_h - \frac{U_i}{R_n} C_2 \right)$$

- PMO-, SIAR- and CROM-type pyrheliometers: the irradiance was obtained from P(closed) averaged from the closed values before and after the open reading P(open).

$$S = C_1(P(\text{closed}) - P(\text{open}))$$

  The power calculation was done according to the prescription of the instrument type with

$$P = U_h^2 \qquad \text{or} \qquad P = U_h U_i \qquad \text{or} \qquad P = U_h \frac{U_i}{R_n}$$

  The SIAR-type radiometers slightly deviate from this scheme in that they subtract the open power from the *preceding* closed power rather than the average of the preceding and successive closed reading.

- Field Pyrheliometers with thermopile sensor: the thermopile reading was divided by the calibration factor after subtraction of the zero point reading[7].

- PMO2: As during preceding IPCs, PMO2 was used as the reference instrument for the daily summaries because it can be operated fast enough to provide an irradiance value every 90 seconds. The values of PMO2 were obtained with the algorithm for PMO-type pyrheliometers. At the end of the open phase, 6 readings were taken in rapid succession within 1 second. The standard deviation of the 6 readings was used during the final evaluation as a quality control parameter to assess the atmospheric stability during each acquisition sequence (see Sect. 2.1).

1.3.3 Auxiliary Data

The meteorological parameters (air temperature, relative humidity, atmospheric pressure) were obtained from the MeteoSwiss' automated weather station SwissMetNet located at PMOD/WRC (see Sect. 4.4). Two anemometers were measuring wind speed and direction, one on the measurement field and one above the WSG tracker.

The WRC's Infrared Cloud Camera (IRCCAM) was used to flag all measurements when clouds were too close to the sun (see Sect, 2.1.

Precision Filter Radiometers (PFR) were used to determine Aerosol Optical Depth (AOD) at four wavelengths (367.6 nm, 412.0 nm, 501.2 nm, and 862.4 nm, see Sect. 4.2).

[7]Some operators assumed a vanishing zero signal. They did not perform zero readings.

1.4 The Cryogenic Solar Absolute Radiometer (CSAR)

The CSAR is a prototype pyrheliometer which aims at exploiting the benefits of cryogenic radiometry in a pyrheliometer that directly measures solar irradiance. Thanks to the CSAR's traceability to SI primary standards its irradiance measurements are expected to have a 10-fold improved uncertainty compared to the WRR. The CSAR is operated in a mode which is similar to HF- and TMI-type pyrheliometers, although its reference block is actively stabilized at 30 K by a PID controller. After each operation of the shutter the PID controller requires up to 15 minutes to stabilize the reference block. Therefore, the standard 20-minutes measurement series are not feasible for the CSAR. It was thus operated separately from the rest of the pyrheliometers. After the reference block was stabilized, irradiance readings were carried out every 7 seconds. This cadence is limited by the precision thermometry bridge (ISOTECH microK) reading the Cernox® thermistors on the CSAR cavity and reference block.

In a next step, the attenuation of the solar irradiance by the Suprasil® entrance window to the CSAR's vacuum tank needs to be corrected. The attenuation factor depends on the spectral composition of the solar irradiance – and thus the atmospheric conditions – at the time of the measurement. The Monitor for Integrated Transmittance (MITRA) is a 2-channel differential ambient-temperature radiometer which measures the attenuation factor of an identical window simultaneously with each irradiance reading by the CSAR. The MITRA attenuation factors are then used to correct the CSAR irradiance measurements.

In order to detect and account for a possible non-equivalence of both windows the optical path of the CSAR is equipped with a vacuum gate which allows to swap the CSAR and MITRA windows in the course of the day. The swapping procedure requires roughly 1 hour, during which the CSAR cannot measure the solar irradiance.

Unfortunately the measurement conditions and the operational stability of the CSAR did not offer opprotunities to swap the windows during IPC-XIII without risking the loss too much data. However, the non-equivalence between the two windows was determined several times. It was found that the attenuation factor of the CSAR window is consistently 0.16% lower than the MITRA window. The attenuation factors measured by MITRA were corrected accordingly before being applied to the CSAR irradiance measurements.

1.5 Agreement of Procedures

Based on the eleventh session of the Commission for Instruments and Methods of Observation (CIMO-11), resolution 1, on the evaluation of calibration factors resulting from international pyrheliometer comparisons, an ad-hoc working group has been established at IPC-XIII. The ad-hoc working group met several times during the comparisons to discuss preliminary results, evaluate the performance of the World Radiometric Reference (WRR) and recommend the updating of the calibration factors of the participating instruments. The group approved the procedure to compute the new WRR factors of the WSG as well as the calibration factors of the participating instruments. In addition, the group discussed and recommended the future of IPCs and RPCs. The ad-hoc group was chaired by Stefan Wacker, (Germany, RA VI) and composed as follows: Khaled Wael (Egypt, RA I), Nozomu Ohkawara and Shun Sasaki(Japan, RA II), Edgardo Sepúlvedo (Chile, RA III), Adriana Elizabeth Gonzalez (Mexico, RA IV), Michael Milner (Australia, RA V), Thomas Carlund (Sweden, RA VI), Ibrahim Reda and Tom Kirk (USA), Bruce Forgan (Austalia, vice president of INFCOM), Wolfgang Finsterle (PMOD/WRC). Dirk Fehse (PTB, Germany) and Markus Suter (Davos Instruments AG) participated as observers in some meetings of the ad-hoc group.

The procedures used to compute the new WRR factors of the WSG and participating instruments are explained in Section 2.3.

Chapter 2 Irradiance Measurements and Results

Measurements were taken on 11 days (2021 September 27, 28, 30, October 1, 2, 8 - 11, 14, 15). Up to 17 series of 21 minutes duration were acquired during the sunniest days of the intercomparison. In total 141 series were acquired. The best observing conditions were experienced from October 8 - 14. Therefore, only the measurements from those days were used to transfer the WRR and to determine the new WRR factors for the WSG. Restricting the WSG evaluation to the best observing conditions not only reduces the scatter in the WRR factors of the WSG, but also avoids the first couple of days, when CROM2L experienced problems with the mechanical shutter, thus allowing for a consistent statistical representation of the all valid WSG instruments in the new WRR. All measurement days were accepted to calculate the WRR factors of participating pyrheliometers. Applying the same restriction as for the WSG seems unreasonable and would result in very few data points for some of the participating pyrheliometers. The following data selection criteria were applied, according the recommendation by the ad-hoc group, resulting in 1441 valid irradiance readings for the WRR.

2.1 Data Selection Criteria for the Final Evaluation

The Ad-hoc Group responsible for the approval of the final evaluation procedure (c.f. Sect. 1.5) agreed on the following criteria for the acceptance of IPC-XIII data:

1. That no measurements be used for the absolute cavity radiometers (field of view = 5 degrees) if a cloud is within 8 degrees of the sun. A thermal imager will facilitate the detection of clouds near the sun.
2. The irradiance as measured by PMO2 must exceed $700\ \mathrm{Wm^{-2}}$.
3. That no measurements be used if the wind speed is greater than $2.5\ \mathrm{ms^{-1}}$.
4. That no data be used if the 500 nm AOD is greater than 0.120.
5. That an individual point be excluded from the series if the standard deviation of the solar irradiance in a 1-second period is greater than $1\ \mathrm{Wm^{-2}}$ (based on the 6 fast readings by PMO2).
6. That an individual point be excluded if it is not in a contiguous stretch of 6 valid points.
7. That the minimum number of acceptable data points be 150 for the PMO2 taken over a minimum of three days during the comparison period.

2.2 Status of the WSG and Transfer of the WRR

The main objective of the periodic IPCs is the dissemination of the World Radiometric Reference (WRR) in order to ensure worldwide homogeneity of solar radiation measurements. The WRR is realized by the World Standard Group (WSG) at PMOD/WRC, which is frequently inter-compared to detect possible deviations of individual WSG-radiometers with respect to the group average and to ensure the stability of the WRR. In addition to this *internal* stability check the stability of the WRR is assessed during IPCs by comparing the WSG to other pyrheliometers that have participated in previous IPCs.

Since IPC-XII, which was held in 2015 [7], only one member instruments of the WSG has failed in internal stability check. The instrument PMO5 slowly drifted with respect to the WSG average during the last inter-IPC period. A reason for the drift could not be determined. It was therefore not considered for the calculation of the new WRR but will hopefully help to transfer the WRR to the next IPC. Starting on June 6, 2017, PAC3 was suddenly reading $\sim 0.4\%$ low because of an insect in the cavity. The readings returned to the normal level after the insect was removed on August 11, 2021. PAC3 was not considered for calculating the WRR during the affected period.

The remaining four WSG instruments (PMO2, HF18748, MK67814, CROM2L) did not show any irregularities and are thus considered stable over the past five years[1]. The new WRR is calculated based on the average readings of these five radiometers.

2.3 Computation of the New WRR Factors

2.3.1 WSG Instruments

The WRR factor $WRR_{i,IPC}$ for the WSG instrument i, $i \in \{$PMO2, CROM2L, MK67814, HF18748, PAC3, PMO5$\}$, by definition is the ratio of the WRR to the WSG instrument i averaged over the selected days during the IPC (October 8 to 14, see top of page 15):

$$WRR_{i,IPC} = \left\langle \frac{WRR(t)}{WSG_i(t)} \right\rangle_t ,$$

where $WRR(t)$ is the reference irradiance and $WSG_i(t)$ irradiance measured by WSG instrument i at the time t, and $\langle x(t) \rangle_t$ denotes the temporal average of $x(t)$. The reference irradiance (WRR) is defined as the mean value of the simultaneous readings of at least four WSG instruments, multiplied by their corresponding WRR factors from the previous IPC. Because the ratios of PMO5 with respect to the WRR was unstable during the past five years it was not used to compute the reference irradiance during IPC-XIII. A new WRR factor was determined for PMO5 and it will be considered to transfer the WRR for the coming inter-IPC period. With $j \in \{$PMO2, CROM2L, PAC3, HF19748, MK67814$\}$ we calculate the reference irradiance as

$$WRR(t) = \langle WSG_j(t) * WRR_{j,\text{IPC}-\text{XII}} \rangle_j .$$

We thus get

$$WRR_{i,\text{IPC}-\text{XIII}} = \left\langle \frac{\langle WSG_j(t) * WRR_{j,\text{IPC}-\text{XII}} \rangle_j}{WSG_i(t)} \right\rangle_t ,$$

where $i \in \{$PMO2, CROM2L, MK67814, HF18748, PAC3, PMO5$\}$ and $j \in \{$PMO2, CROM2L, PAC3, HF18748, MK67814$\}$.

2.3.2 Participating Instruments

For each participating instrument k the new WRR factor is calculated according to

$$WRR_{k,\text{IPC}-\text{XIII}} = \left\langle \frac{WRR(t)}{Irr_k(t)} \right\rangle_t ,$$

where $Irr_k(t)$ is the irradiance measured by the instrument k at the time t and $WRR(t)$ the reference irradiance at time t.

[1] CROM2L did experience problems with the mechanical shutter, which could be fixed with kind support from the manufacturer (IRMB).

Table 2.1: New WRR-factors for the WSG instruments computed using PMO2, HF18748, MK67814, CROM2L, and PAC3.

Instrument	*WRR factor IPC-XII*	**WRR Factor IPC-XIII**	*standard uncertainty* $\frac{\sigma}{\sqrt{N-1}}$ *[ppm]*	*# of points N*	*Relative Change of WRR Factor [ppm]*
PMO2	0.998189	**0.998477**	25	628	289
PMO5	0.999395	**1.000595**	35	337	1201
CROM2L	1.003118	**1.003431**	29	336	312
MK67814	1.001702	**1.002200**	18	628	497
PAC3	1.002190	**1.001741**	15	623	-448
HF18748	0.998258	**0.997719**	16	629	-540

Temporal averaging is done by fitting a gaussian to the distribution of WRR-to-instrument ratios. The largest outliers are successively removed until a χ^2 test confirms the hypothesis that the measured WRR-to-instrument ratios follow a normal distribution with 10% significance, or until all ratios are within ± 0.002 of their arithmetic mean value. The new WRR factors for the WSG and all participating instruments are listed in Table 2.2.

Table 2.2: The new WRR factors for the participating instruments

Instrument	C_1	C_2	R_n Ω	**WRR Factor**	σ ppm	*N*	*Country/ Owner*
AHF0000	2.0355			**1.003171**	760	802	JRC Italy
AHF14915	20010	0.065	10	**0.999827**	971	848	Eppley USA
AHF23734	2.002			**0.998671**	763	1080	NREL USA
AHF27159	20030			**0.999429**	791	973	KNMI The Netherlands
AHF27798	20020	0.066	10	**1.001000**	1972	691	Eppley USA
AHF28486	2.001	0.066	10	**0.999378**	1447	1004	CIEMAT Spain
AHF28560	2.0028			**1.000298**	1040	793	ISO-Cal North America USA
AHF28968	19980.2			**0.998019**	714	1066	ARM/SGP USA
AHF29220	19999			**0.997793**	696	1060	NREL USA
AHF29221	20000			**1.001690**	740	634	Germany
AHF29221-W	20000			**1.069136**	871	313	Germany
AHF29223	19998			**0.999456**	642	739	Mexico
AHF29225	20004.2			**0.996624**	1020	791	Algeria
AHF30110	1.9999			**1.072222**	6718	914	KACARE Saudi Arabia
AHF30713	19989			**0.997596**	668	1058	NREL USA
AHF31103	19989	0.066	10000	**1.007017**	4053	373	Egypt
AHF31110	19989			**0.997137**	581	719	United Kingdom of Great Britain and Northern Ireland
AHF32449	200592	0.066	10	**0.997746**	811	856	Eppley USA
AHF32455	20009.2			**1.001471**	751	1140	WRC

Table 2.2: (continued)

Instrument	C_1	C_2	R_n Ω	**WRR Factor**	σ ppm	*N*	*Country/ Owner*
AHF33396	1.9988			**0.997946**	1338	807	AIST Japan
AHF34926	1			**1.001361**	784	687	UO USA
AHF37812	19903	0.066	10	**1.001411**	1020	846	KIER Korea
AHF37813	1.9979			**1.000846**	668	873	United Kingdom of Great Britain and Northern Ireland
AHF37814	2.013			**1.001447**	636	986	Slovakia
AHF37816	1.9998			**0.999522**	797	780	ISO-Cal North America USA
AWX33393	2.0009	0.066	10	**1.001048**	845	917	Sweden
CH1-040370	10.48			**1.002201**	1760	884	JRC Italy
CH1-060460	10.07			**1.001348**	1773	897	JRC Italy
CH1-930018	10.85			**1.000590**	2458	907	JRC Italy
CHP1-110533	7.8			**0.995962**	2463	891	JRC Italy
CHP1-131107	7.6874			**0.998671**	2427	793	Libya
CHP1-140049	8.27			**0.995478**	734	833	Slovenia
CHP1-150261	8.29			**0.987260**	2762	778	LES Uruguay
CHP1-200837	9.32			**1.014874**	5658	1053	KNMI The Netherlands
CHP1-200838	8.7			**1.007458**	1412	1023	KNMI The Netherlands
CHP1-REF2	7.94			**1.005724**	1424	604	Kipp&Zonen The Netherlands
CP20C-101	1			**0.061661**	2535	497	Hukseflux The Netherlands
CP20C-102	1			**0.061228**	2382	465	Hukseflux The Netherlands
CP20U-101	1			**0.061695**	1564	494	Hukseflux The Netherlands
CP20U-102	1			**0.061344**	1384	461	Hukseflux The Netherlands
CR05L	1			**0.998807**	1712	382	Belgium
CR09L	1			**1.001980**	1832	381	Belgium
CSAR	1			**1.003115**	1302	64	WRC
DR02-9210	10.739			**1.001386**	1707	659	Hukseflux The Netherlands
DR20-65033	21.70166			**0.982803**	1223	645	Hukseflux The Netherlands
DR30-65005	17.968			**0.999679**	1381	652	Hukseflux The Netherlands
EPAC11402	10024			**1.006732**	3074	747	WRC
HF15744	20020			**0.998696**	805	783	RISE Sweden
HF27157	20037.6			**0.996712**	887	749	Germany
HF30497	19943.8			**1.000001**	657	1019	Czech Republic
IRS04-2101	1			**1.001449**	1234	695	AIST Japan
IRS04-2102	1			**1.001043**	1573	703	Ishikawa Japan

Table 2.2: (continued)

Instrument	C_1	C_2	R_n Ω	**WRR Factor**	σ ppm	*N*	*Country/ Owner*
MS56-12036	7.3			**0.972244**	3064	906	JRC Italy
MS56-12039	7.08			**0.994387**	2782	904	JRC Italy
MS56-P12023	1			**1.021953**	1980	1151	EKO Japan
MS57-1702504	7.36			**1.001764**	4271	912	JRC Italy
NIP-21451E6	8.42			**1.003161**	4070	916	JRC Italy
NIP-23927E6	8.54			**0.998800**	6748	918	JRC Italy
NIP-25738E6	7.92			**0.994990**	6147	919	JRC Italy
NIP-26626E6	8.24			**0.994483**	4821	916	JRC Italy
NIP-31144E6	8.04			**0.993855**	5722	1205	WRC
PH1-999991	1			**0.997332**	3176	504	Kipp&Zonen The Netherlands
PMO6-0103	51183.3			**0.998913**	609	611	Kipp&Zonen The Netherlands
PMO6-0301	51161.5			**1.000435**	988	976	CIEMAT Spain
PMO6-0304	50000			**1.023841**	614	572	WRC
PMO6-0401	50000			**1.021649**	702	1072	WRC
PMO6-0405	50936			**0.999130**	693	911	Germany
PMO6-0803	51221			**1.000287**	568	597	WRC
PMO6-0808	50479			**0.999958**	465	393	China
PMO6-0816	51037			**0.999191**	1260	575	EKO Japan
PMO6-0817	51141			**0.999957**	762	941	Russian Federation
PMO6-1102	51295.5			**0.999367**	802	777	Mexico
PMO6-1103	51396.9			**0.999661**	557	596	Slovenia
PMO6-1104	51231.9			**1.000427**	881	580	PTB Germany
PMO6-1104-L	51231.89			**0.999903**	1058	408	PTB Germany
PMO6-1109	51250.1			**0.999154**	601	579	Croatia
PMO6-1602	50925			**1.003889**	716	731	USACH Chile
PMO6-1603	51178			**0.999802**	568	584	Japan
PMO6-1609	51110			**1.000318**	747	621	CIEMAT Spain
PMO6-1609-L	51110			**1.000538**	748	236	CIEMAT Spain
PMO6-1610	50997			**0.999805**	482	500	Indonesia
PMO6-1611	50917			**1.003372**	669	1066	Davos Instruments Switzerland
PMO6-5	50894			**0.999562**	890	959	Germany
PMO6-7	132.79			**0.999504**	2335	339	Switzerland
PMO6-79-122	600			**1.002051**	2647	637	WRC
PMO6-81109	600.0345			**0.998599**	706	872	JRC Italy
PMO6-911204	601.7356			**1.000612**	871	862	JRC Italy
PMO8-F201-001	51851.1			**0.999959**	757	878	PTB Germany
PMO8-F201-002	51806			**1.000068**	765	932	PTB Germany
PMO8-F201-006A	51510			**1.000082**	702	947	Sweden
PMO8-F201-007A	51400			**1.006331**	721	877	WRC
PMO8-F201-009	51809			**0.999853**	663	981	Argentina

Table 2.2: (continued)

Instrument	C_1	C_2	R_n Ω	**WRR Factor**	σ ppm	*N*	*Country/ Owner*
PMO8-F211-001	51588			**0.999772**	688	859	Davos Instruments Switzerland
PMO8-F211-002	51892			**1.000106**	743	931	Davos Instruments Switzerland
SHP1-130042	7.85467			**0.988180**	1358	2967	PTB Germany
SHP1-175109	9.07728			**0.995921**	1394	2969	PTB Germany
SHP1-175110	9.05247			**0.998466**	1326	2962	PTB Germany
SHP1-185163	8.91			**1.000623**	1307	1876	DTU Denmark
SHP1-195181	9.9011			**0.999353**	1397	1618	USACH Chile
SHP1-205241	9.14			**1.010177**	823	1857	DTU Denmark
SHP33-01	6.53			**1.004188**	1877	815	Kipp&Zonen The Netherlands
SIAR-2A	1			**0.990934**	2617	43	WRC
SNIP-37886E6	8.556			**0.997286**	1360	781	CIEMAT Spain
TMI67604	1.0052			**0.999402**	937	842	JRC Italy
TMI68018	1.0046			**0.996851**	738	1108	NREL USA
TMI68835	1.00383			**1.000427**	1319	882	JRC Italy

2.4 External stability check of the WSG

In Section 2.2 the stability of the WSG was checked by analyzing the trends of individual members of the WSG with respect to the group's average. Here we present an external assessment of the stability of the WSG with respect to all cavity radiometers which have participated in at least two consecutive IPCs since 1980 (c.f. Fig. 2.1). This analysis confirms the long-term stability of the WSG within the required uncertainty level of $3000\ \mathrm{ppm}$ (0.3%). Compared to IPC-XII [7] the WRR factors of 38 cavity radiometers have changed by $650\ \mathrm{ppm}$ on average, with a statistical uncertainty of $707\ \mathrm{ppm}$ (2-σ). We thus conclude that the WSG has not significantly drifted over the past five years. For completeness the history of WRR factors since 1980 (IPC-V) is given in Table 2.3 for all participating instruments. Note that in this table the actual WRR factors are listed while normalized factors (with respect to C_1) were used for assessing the stability of the WSG. Normalization was necessary because some instruments changed their calibration factors C_1, which produces spurious changes in their WRR factors.

Table 2.3: The history of WRR factors. In this table the actual WRR factors are listed. They depend on the calibration constant C_1 which was used and which may have changed over time. In the WSG-stability analysis presented in Section 2.4 and Figure 2.1 these factors were re-normalized accordingly. Note that only pyrheliometers which have participated in more than one IPC are listed here.

Instrument	*IPC-V*	*IPC-VI*	*IPC-VII*	*IPC-VIII*	*IPC-IX*	*IPC-X*	*IPC-XI*	*IPC-XII*	*IPC-XIII*
A7	1.02210	1.00011	1.00109	1.00160					
A24	1.02323	0.99896							
A171	1.00903	0.99843	1.00042	0.99967	1.003				
A212	1.01912	0.99932	1.00154	1.00175	1.00065	1.003381	0.996482		
A507	1.02143	0.99964							
A561	1.02572	0.99770							
A564	1.02415	0.99908	1.00190	0.99655					
A567					0.99914	1.000240			
A568	1.02732	0.99823	1.00099						
A576	1.020130	1.005233	1.001071	1.000460	0.997370	1.000050	0.990369	0.990848	
A578	1.02538	0.99941	1.00225	1.00171	1.00571				
A583	1.00096	1.00202							
A702				1.0291	1.00394	1.005965	0.998769		
A708	1.03027	1.00396							
A7190	1.02029		1.00419	1.00092					
A7636	1.02381	0.99987	1.00151	1.00163	1.001121				
A9003	1.00122	0.99278	0.99978						
A12578				1.04137	1.00599	1.006532	1.00858		
A13439				1.022990	1.002370	1.003291	1.001350	1.0034568	
A15192			0.99913	1.00189	1.00157	1.002165		1.0304138	
A16491			0.99571	0.99644					
A18020		0.99870				1.004923	1.00265		
A18587		1.00524	1.00505	1.00605	1.0021	0.997646			
AHF00000							0.997352	1.000307	1.003171
AHF14915	0.998751	0.998421	0.999980	1.000460	1.000260	0.999640	0.999682	0.999542	0.999827
AHF17142	0.998801	0.997733	0.998901	0.998860	0.998930	0.999141	0.998358	0.997946	
AHF18742						1.003773	1.002280	1.004506	

Table 2.3: (continued)

Instrument	*IPC-V*	*IPC-VI*	*IPC-VII*	*IPC-VIII*	*IPC-IX*	*IPC-X*	*IPC-XI*	*IPC-XII*	*IPC-XIII*
AHF23734							0.998281	0.998187	0.998671
AHF27159			0.999271	0.998880		0.998004	1.000020	0.999438	
AHF27160			0.997267	0.997090	0.996770	0.996910	0.996467	0.997424	
AHF27798			0.998363	0.998980	0.999880	0.999410	0.999018	0.998654	1.001000
AHF28486							0.997308	0.997318	0.999378
AHF28553				0.997560	0.997330	0.996105	0.996842	0.997739	
AHF28560								0.999283	1.000298
AHF28968				0.998720	0.998660	0.997765	0.997734	0.997627	0.998019
AHF29220				0.998620	0.998460	0.997556	0.997691	0.997482	0.997793
AHF29223				0.997450	0.997470	0.996761	0.997352	1.003219	0.999456
AHF29225					0.99709	0.996105	0.996896		0.996624
AHF30110-W								1.063471	1.072222
AHF30497					0.997740	0.999350	0.999623	0.999589	
AHF30713					0.998610	0.997512	0.997548	0.997228	0.997596
AHF31041					0.998130	0.996294	0.996286	0.996392	
AHF31103					0.998990	0.999640		0.999345	1.007017
AHF31105						1.001649	0.999964	0.998656	
AHF31110					0.997890	0.997211	0.996431	0.997038	0.997137
AHF31117							0.998861	0.999042	
AHF32455						0.999090	1.000280	1.001380	1.001471
AHF33396						0.997951	0.998079	0.997184	0.997946
AHF36011							0.998226[2]	1.000005	
AHF36013							1.058110	0.999802	
AHF37813								1.000461	1.000846
AHF37814								1.001054	1.001447
AHF37816								0.999458	0.999522
AWX31114							1.001240	1.001209	
AWX32448					1.00031	0.999874	0.999939	0.999986	
AWX33393						0.997281	0.999362	0.999885	1.001048
CH1-040370								0.998163	1.002201
CH1-050392							1.000250	1.010940	
CH1-020283							0.997677	0.993818	
CH1-060460							1.002330	1.004743	1.001348
CH1-930018							1.000750	1.001243	1.000590
CH1-940072						1.005958	1.007580	1.0093218	
CHP1-100245							1.000490	1.0011568	
CHP1-110533								0.998562	0.995962
CHP1-REF2								1.004987	1.005724
CR09R					0.999123	0.999111	0.998363		
CSAR							0.992123	1.002100	1.003115
EPAC11402					0.999250	1.000560	1.000680	1.0362658	1.006732
HF15744	1.000640	1.000030	0.999650	0.999470	0.999160	0.998034	0.998085	0.9982018	0.998696

[2] This WRR factor results from a re-evaluation of the IPC-XI data after excluding all measurements from October 3^{rd} and 7^{th}, 2010, because a wrong calibration factor was used on those days. The IPC-XI report erroneously included the affected data and states a WRR factor of 0.996933.

Table 2.3: (continued)

Instrument	*IPC-V*	*IPC-VI*	*IPC-VII*	*IPC-VIII*	*IPC-IX*	*IPC-X*	*IPC-XI*	*IPC-XII*	*IPC-XIII*
HF19746	0.999520	0.999940	1.001603	0.999190	0.999660	0.998782	0.998886	1.000022	
HF27157				1.000380	0.999020	0.998722	0.999647	0.999084	0.999429
HF27162			1.000370	1.000960	1.000820	1.000180	0.999212	0.999543	
HF27796					0.996910	0.996979	0.997204	0.996033	
MAR-1-3				0.999610			0.999991	0.999953	
NIP-21451E6							0.999193	1.005957	1.003161
NIP-23927E6								1.000885	0.998800
NIP-25738E6							0.998843	0.991889	0.994990
NIP-26626E6								1.000334	0.994483
NIP-31144E6							0.997184	0.9968248	0.993855
PMO6-5	1.006756	1.000100	0.998602	0.997980	1.000530	0.999960	0.999116	0.998288	0.999562
PMO6-7								0.999681	0.999504
PMO6-79-122			0.996890	0.999970	0.999860	1.000390	0.999401	1.000051	1.002051
PMO6-80022		1.000230	0.996890	0.996130	0.996990	0.997944	1.003080	0.997891	
PMO6-811108		0.999210	0.999970	1.000110	0.999970	0.998114	1.000660	1.000083	
PMO6-81109					0.999460	0.998412	0.998577	0.998315	0.998599
PMO6-850405				1.000370	0.999290	0.999191	1.000560	0.998919	
PMO6-850406					1.000320	0.999440	1.000200	1.001992	
PMO6-850410				1.001800	1.015280	0.987030	0.990890	0.990976	
PMO6-911204					1.000810	0.999011	0.999711	0.999445	1.000612
PMO6-0103						0.999424		0.997916	0.998913
PMO6-0301							1.000588	1.000183	1.000435
PMO6-0401							1.021527	1.020979	1.021649
PMO6-0403							1.000160	0.999753	
PMO6-0405							0.999684	0.999265	0.999130
PMO6-0803							1.000364	1.000335	1.000287
PMO6-0804							0.999914	0.999908	
PMO6-0808								0.999421	0.999958
PMO6-0817								0.999516	0.999957
PMO6-1102								0.999389	0.999367
PMO6-1104								1.000194	1.000427
PMO6-1109								0.998732	0.999154
SIAR-2A						1.000623	0.991696	0.991360	0.990934
SIAR-2B						0.998620	1.000290	1.000895	
SIAR-2C						1.000087	0.999839	0.998949	
TMI67502	0.999290	0.998471	1.000390	0.998660	0.999660	0.999480	0.999294	1.000999	
TMI67604	1.00238	1.00093	1.000140	1.00239	0.99928	0.998792	0.998226		0.999402
TMI68018			0.998692		0.998480	0.997138	0.996804	0.996601	0.996851
TMI68025			0.999460	0.999860	1.000060	0.998135	0.998613	0.998133	
TMI68835							1.000980	1.000723	1.000427

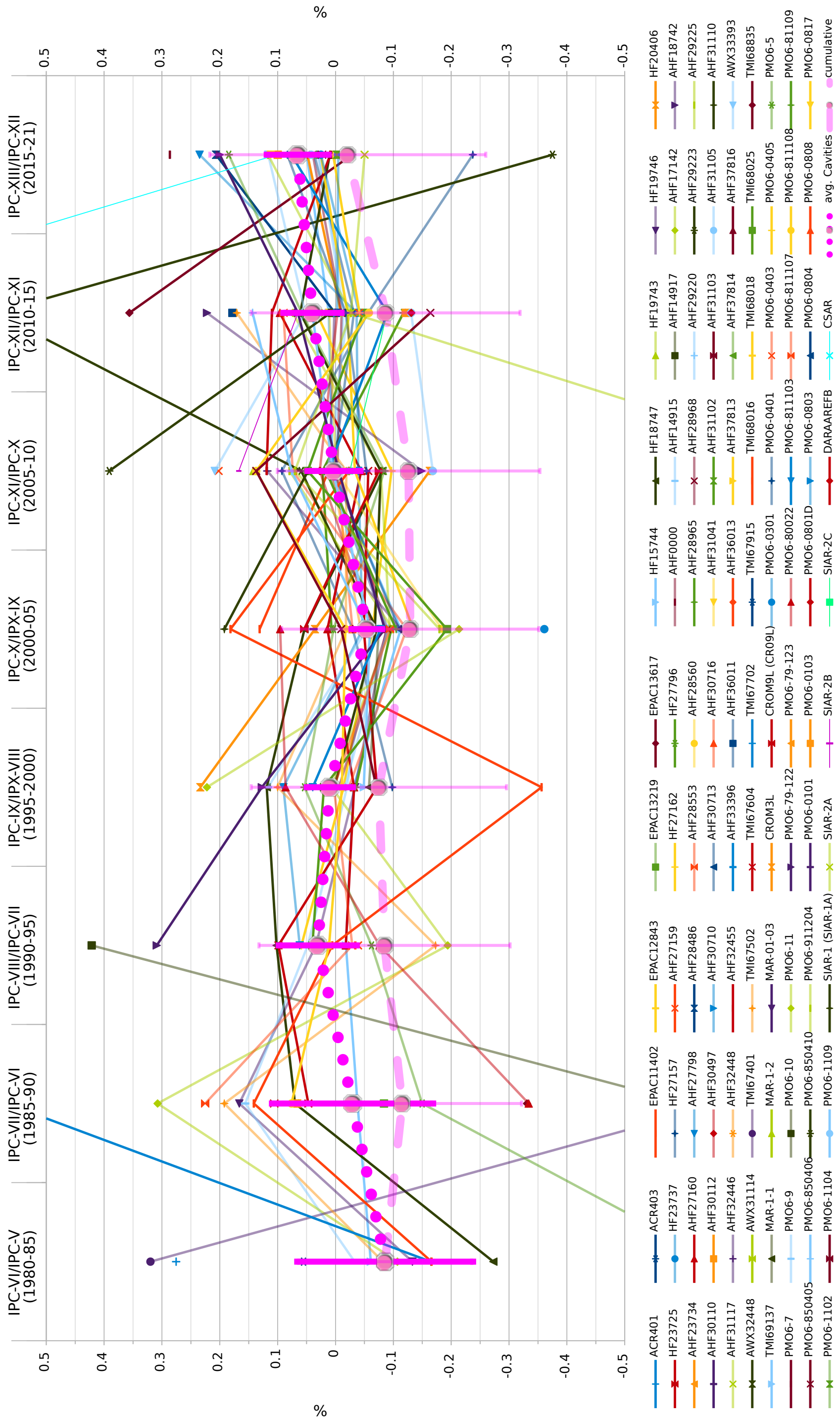

Figure 2.1: The historic evolution of the WRR factors of all cavity radiometers which have participated in at least two consecutive IPC's since 1980 (IPC-V). Note that in this analysis all WRR factors are normalized to the calibration constant C_1 which was used at the time. The thick magenta line is the average of all plotted data points. The most recent data point was calculated from 38 open cavity pyrheliometers that have participated in IPC-XII and IPC-XIII. In this metric the drift of the WRR between IPC-XII (2015) [7] and IPC-XIII (2021) was 650 ± 540 ppm $(k = 2)$. The cumulated drift since IPC-V (1980) is -210 ± 2400 ppm $(k = 2)$ shown by the semi-transparent dashed magenta line.

Chapter 3 Conclusions and Recommendations

The WRR is considered stable within the limits required by the Guide to Instruments and Methods of Observation (WMO-No. 8). The new WRR factors are calculated based on the average readings of PMO2, HF18478, MK67814, CROM2L, and PAC3.

3.1 Graphical Representation of the Results

On the following pages are the data plots for each instrument. The deviation from WRR is plotted. All the points which were used for the analysis (i.e. the points fulfilling the selection criteria listed in Sect. 2.1) have been plotted with a corresponding histogram on the side.

AHF0000: WRR factor=1.003171, σ= 760 ppm, n= 802

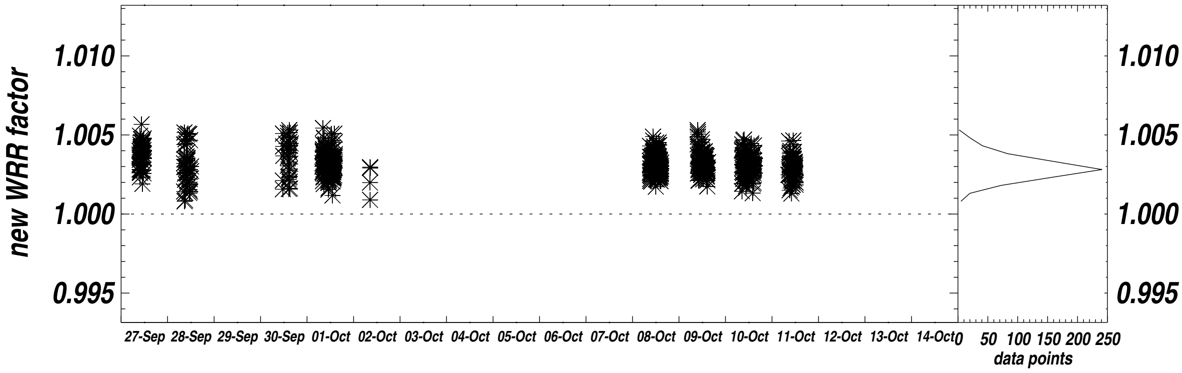

AHF14915: WRR factor=0.999827, σ= 971 ppm, n= 848

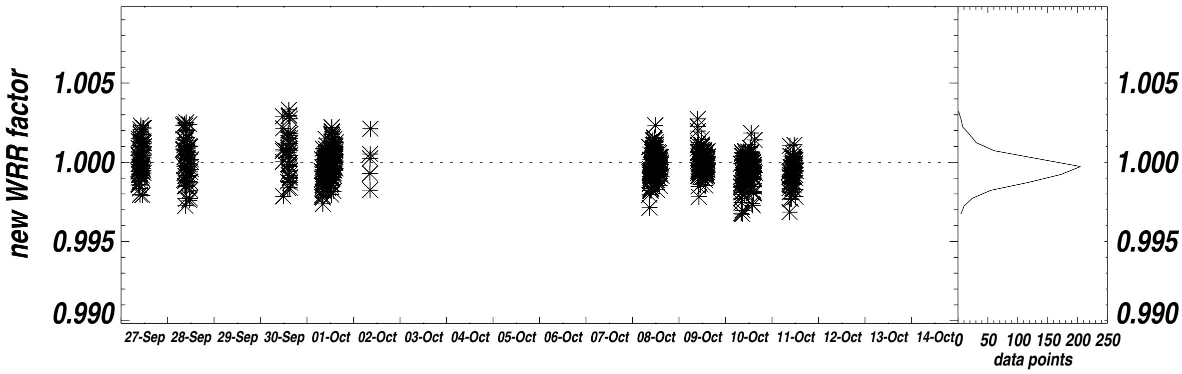

AHF23734: WRR factor=0.998671, σ= 763 ppm, n=1080

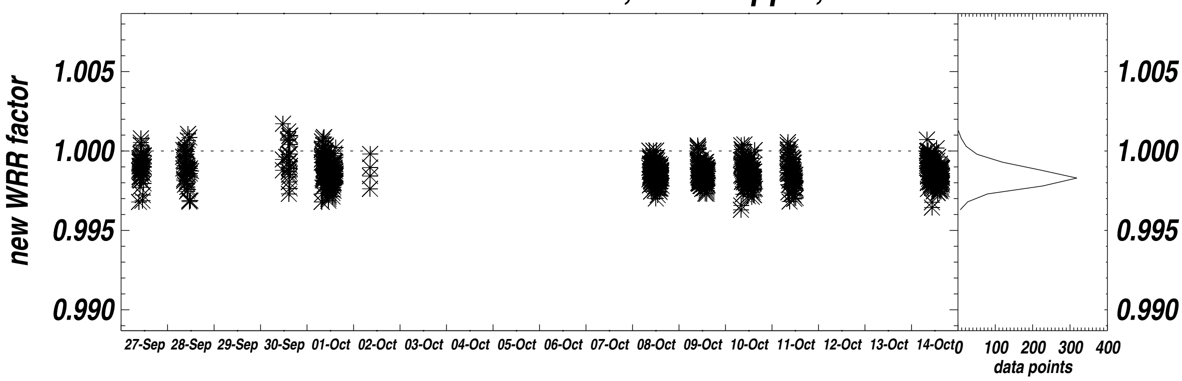

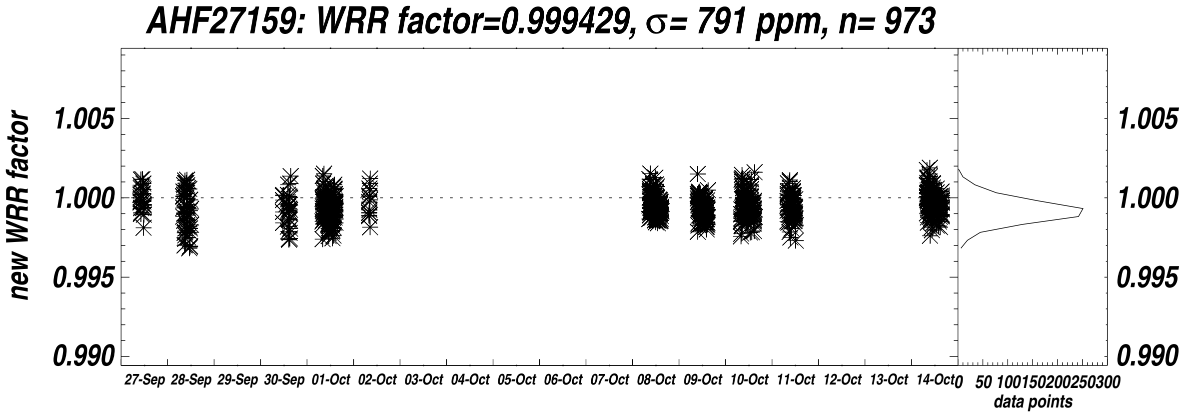
AHF27159: WRR factor=0.999429, σ= 791 ppm, n= 973
new WRR factor
1.005
1.000
0.995
0.990
27-Sep 28-Sep 29-Sep 30-Sep 01-Oct 02-Oct 03-Oct 04-Oct 05-Oct 06-Oct 07-Oct 08-Oct 09-Oct 10-Oct 11-Oct 12-Oct 13-Oct 14-Oct
0 50 100150200250300
data points

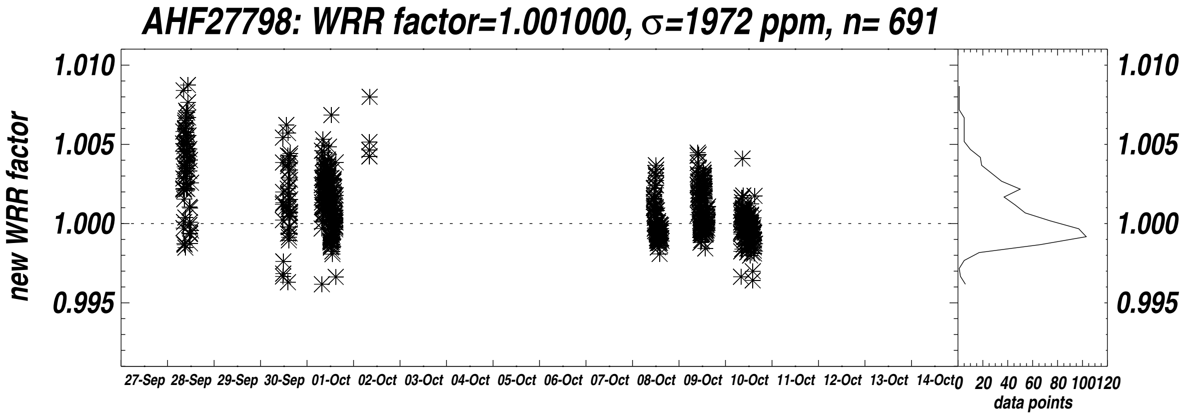
AHF27798: WRR factor=1.001000, σ=1972 ppm, n= 691
new WRR factor
1.010
1.005
1.000
0.995
27-Sep 28-Sep 29-Sep 30-Sep 01-Oct 02-Oct 03-Oct 04-Oct 05-Oct 06-Oct 07-Oct 08-Oct 09-Oct 10-Oct 11-Oct 12-Oct 13-Oct 14-Oct
0 20 40 60 80 100120
data points

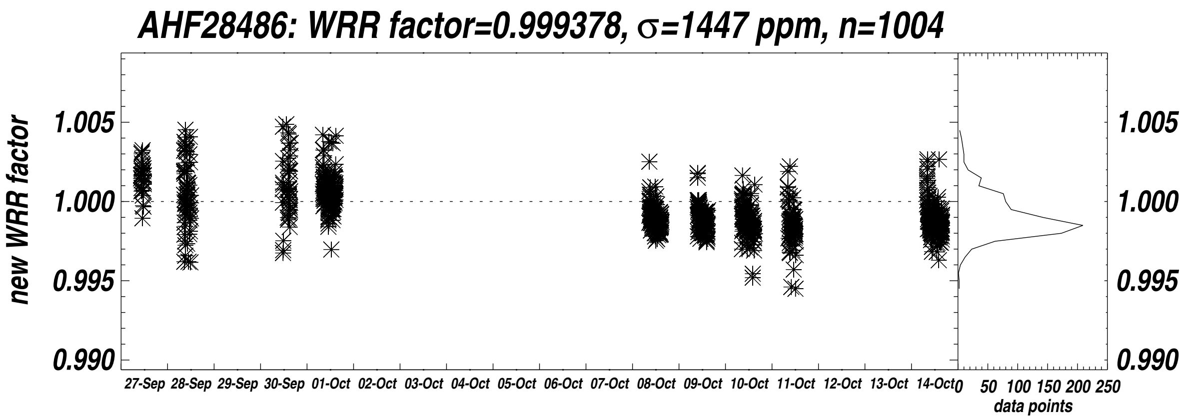
AHF28486: WRR factor=0.999378, σ=1447 ppm, n=1004
new WRR factor
1.005
1.000
0.995
0.990
27-Sep 28-Sep 29-Sep 30-Sep 01-Oct 02-Oct 03-Oct 04-Oct 05-Oct 06-Oct 07-Oct 08-Oct 09-Oct 10-Oct 11-Oct 12-Oct 13-Oct 14-Oct
0 50 100 150 200 250
data points

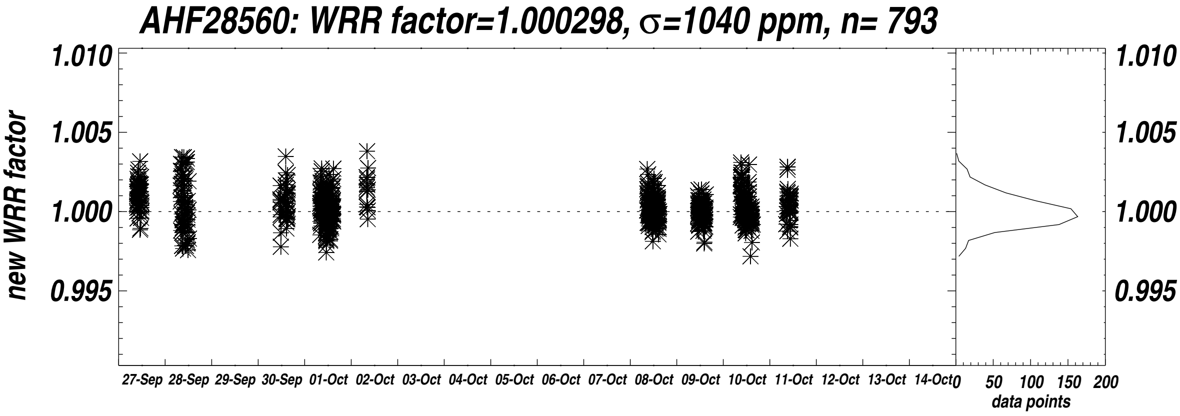
AHF28560: WRR factor=1.000298, σ=1040 ppm, n= 793
new WRR factor
1.010
1.005
1.000
0.995
27-Sep 28-Sep 29-Sep 30-Sep 01-Oct 02-Oct 03-Oct 04-Oct 05-Oct 06-Oct 07-Oct 08-Oct 09-Oct 10-Oct 11-Oct 12-Oct 13-Oct 14-Oct
0 50 100 150 200
data points

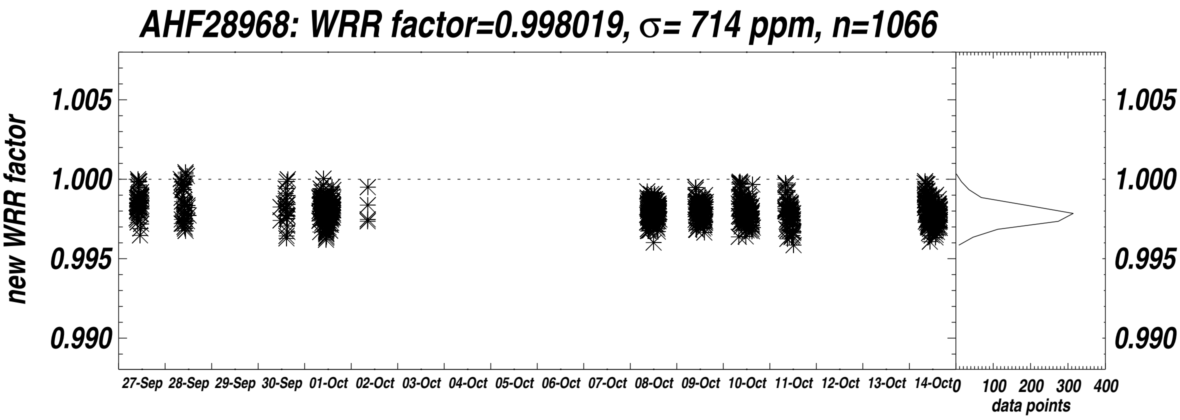
AHF28968: WRR factor=0.998019, σ= 714 ppm, n=1066
new WRR factor
1.005
1.000
0.995
0.990
27-Sep 28-Sep 29-Sep 30-Sep 01-Oct 02-Oct 03-Oct 04-Oct 05-Oct 06-Oct 07-Oct 08-Oct 09-Oct 10-Oct 11-Oct 12-Oct 13-Oct 14-Oct
0 100 200 300 400
data points

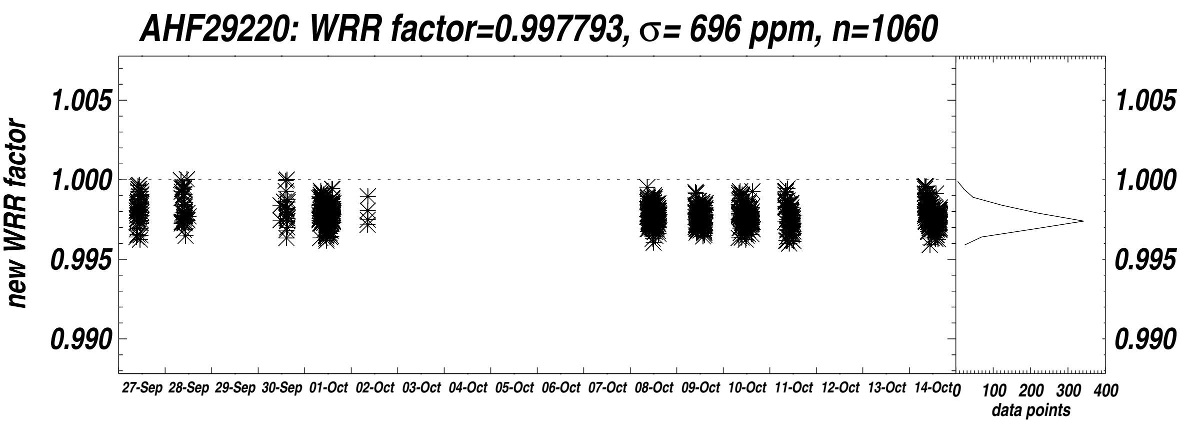
AHF29220: WRR factor=0.997793, σ= 696 ppm, n=1060
new WRR factor
1.005
1.000
0.995
0.990
27-Sep 28-Sep 29-Sep 30-Sep 01-Oct 02-Oct 03-Oct 04-Oct 05-Oct 06-Oct 07-Oct 08-Oct 09-Oct 10-Oct 11-Oct 12-Oct 13-Oct 14-Oct
0 100 200 300 400
data points

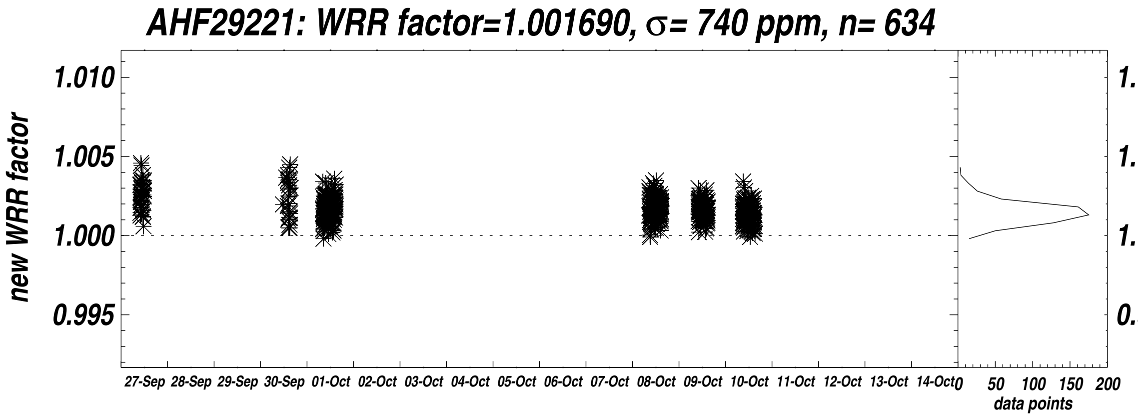
AHF29221: WRR factor=1.001690, σ= 740 ppm, n= 634
new WRR factor
1.010
1.005
1.000
0.995
27-Sep 28-Sep 29-Sep 30-Sep 01-Oct 02-Oct 03-Oct 04-Oct 05-Oct 06-Oct 07-Oct 08-Oct 09-Oct 10-Oct 11-Oct 12-Oct 13-Oct 14-Oct
0 50 100 150 200
data points

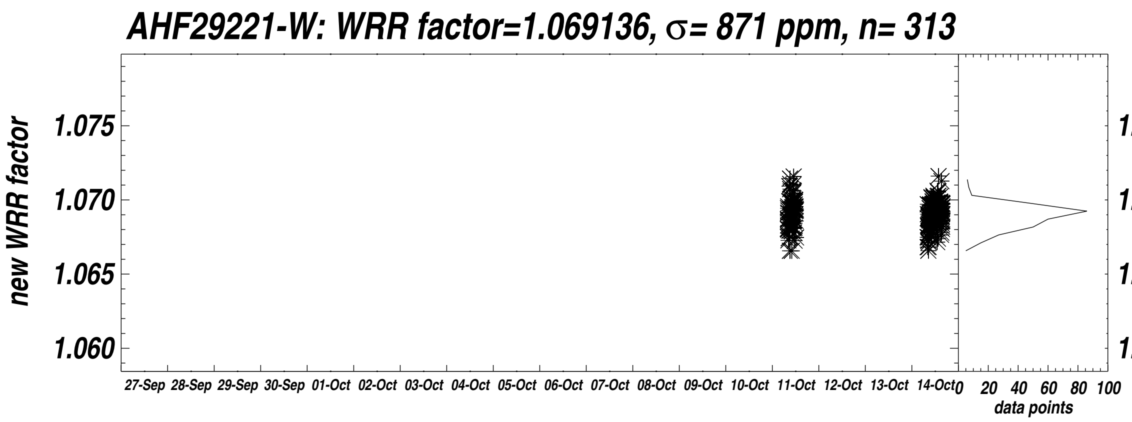
AHF29221-W: WRR factor=1.069136, σ= 871 ppm, n= 313
new WRR factor
1.075
1.070
1.065
1.060
27-Sep 28-Sep 29-Sep 30-Sep 01-Oct 02-Oct 03-Oct 04-Oct 05-Oct 06-Oct 07-Oct 08-Oct 09-Oct 10-Oct 11-Oct 12-Oct 13-Oct 14-Oct
0 20 40 60 80 100
data points

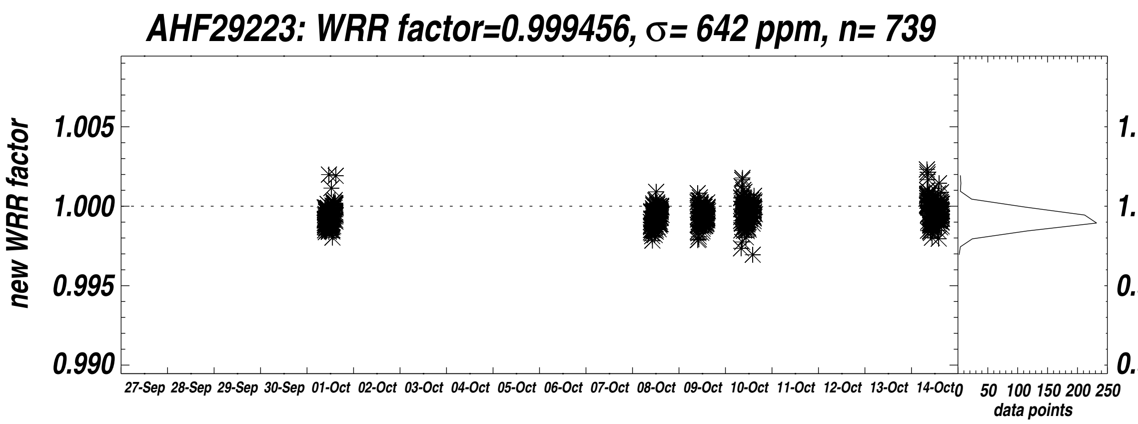
AHF29223: WRR factor=0.999456, σ= 642 ppm, n= 739
new WRR factor
1.005
1.000
0.995
0.990
27-Sep 28-Sep 29-Sep 30-Sep 01-Oct 02-Oct 03-Oct 04-Oct 05-Oct 06-Oct 07-Oct 08-Oct 09-Oct 10-Oct 11-Oct 12-Oct 13-Oct 14-Oct
0 50 100 150 200 250
data points

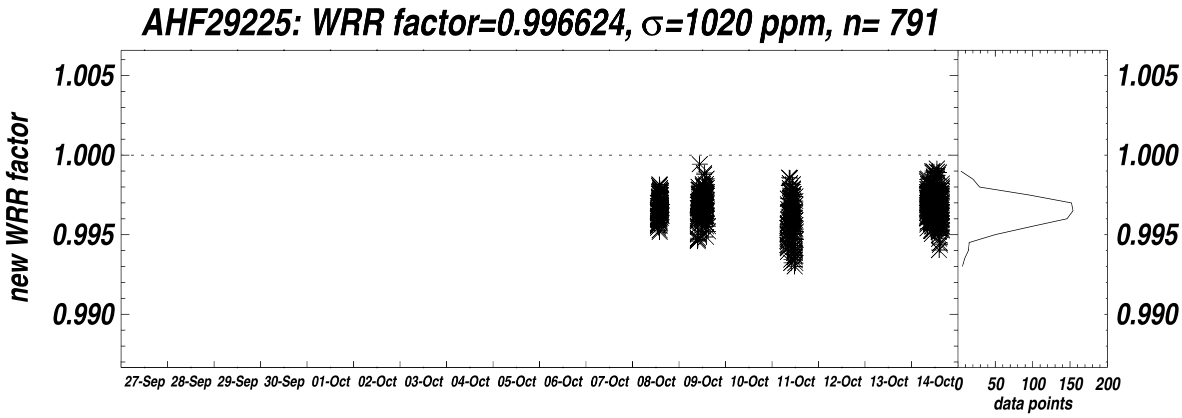
AHF29225: WRR factor=0.996624, σ=1020 ppm, n= 791
new WRR factor
1.005
1.000
0.995
0.990
27-Sep 28-Sep 29-Sep 30-Sep 01-Oct 02-Oct 03-Oct 04-Oct 05-Oct 06-Oct 07-Oct 08-Oct 09-Oct 10-Oct 11-Oct 12-Oct 13-Oct 14-Oct
0 50 100 150 200
data points

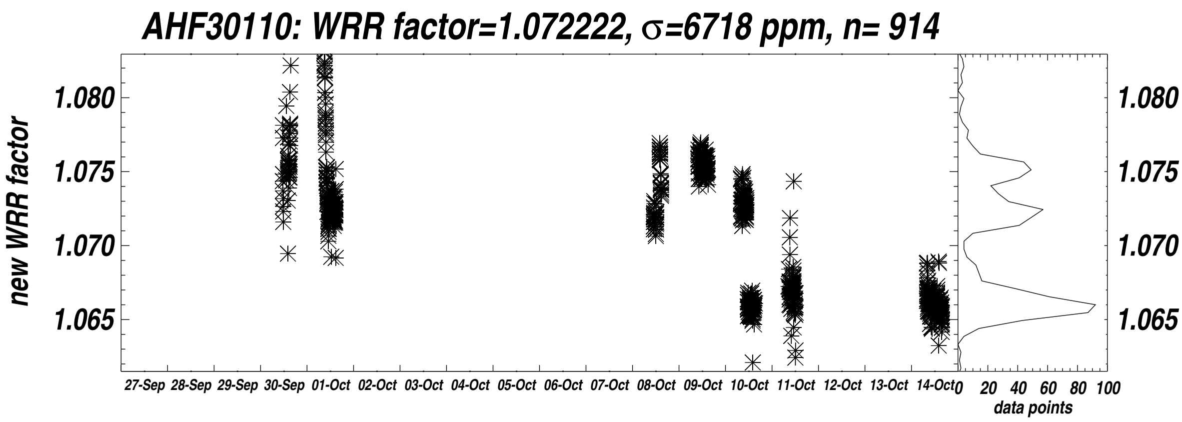
AHF30110: WRR factor=1.072222, σ=6718 ppm, n= 914
new WRR factor
1.080
1.075
1.070
1.065
27-Sep 28-Sep 29-Sep 30-Sep 01-Oct 02-Oct 03-Oct 04-Oct 05-Oct 06-Oct 07-Oct 08-Oct 09-Oct 10-Oct 11-Oct 12-Oct 13-Oct 14-Oct
0 20 40 60 80 100
data points

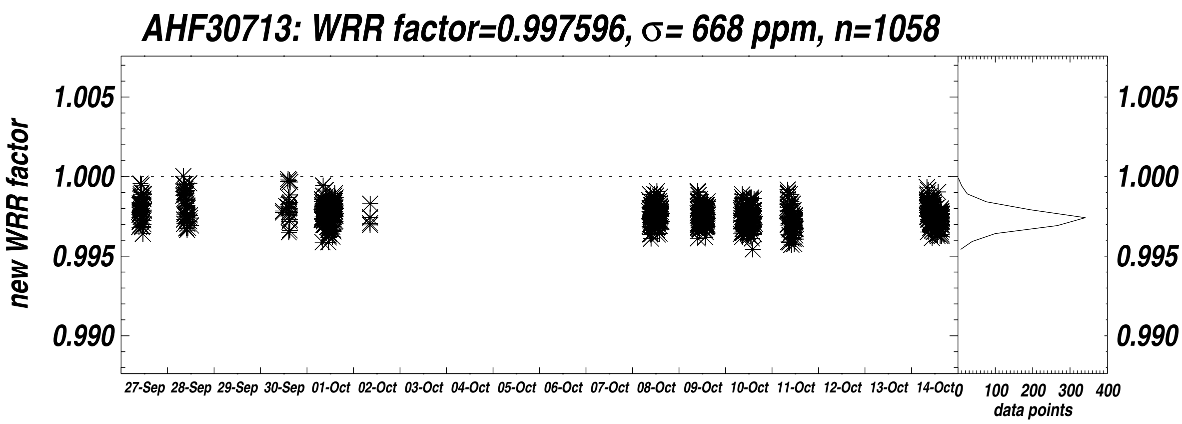
AHF30713: WRR factor=0.997596, σ= 668 ppm, n=1058
new WRR factor
1.005
1.000
0.995
0.990
27-Sep 28-Sep 29-Sep 30-Sep 01-Oct 02-Oct 03-Oct 04-Oct 05-Oct 06-Oct 07-Oct 08-Oct 09-Oct 10-Oct 11-Oct 12-Oct 13-Oct 14-Oct
0 100 200 300 400
data points

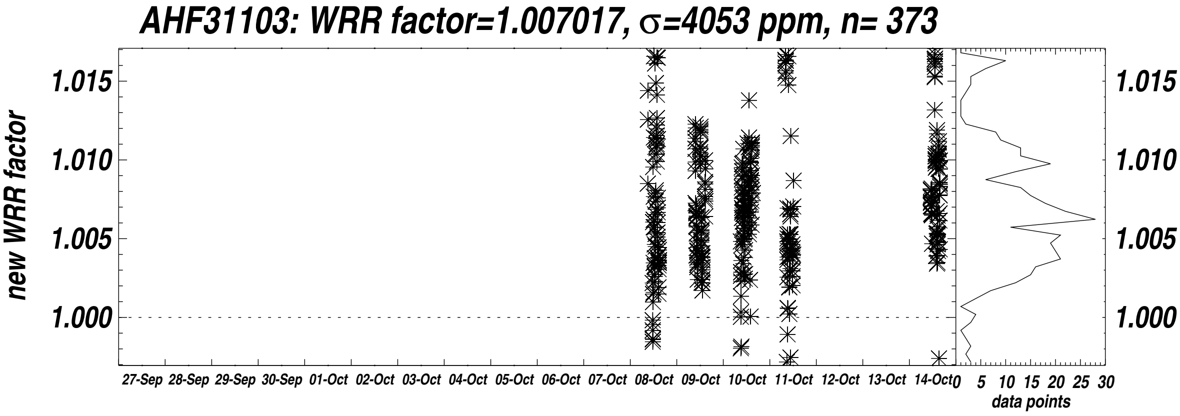
AHF31103: WRR factor=1.007017, σ=4053 ppm, n= 373
new WRR factor
1.015
1.010
1.005
1.000
27-Sep 28-Sep 29-Sep 30-Sep 01-Oct 02-Oct 03-Oct 04-Oct 05-Oct 06-Oct 07-Oct 08-Oct 09-Oct 10-Oct 11-Oct 12-Oct 13-Oct 14-Oct
0 5 10 15 20 25 30
data points

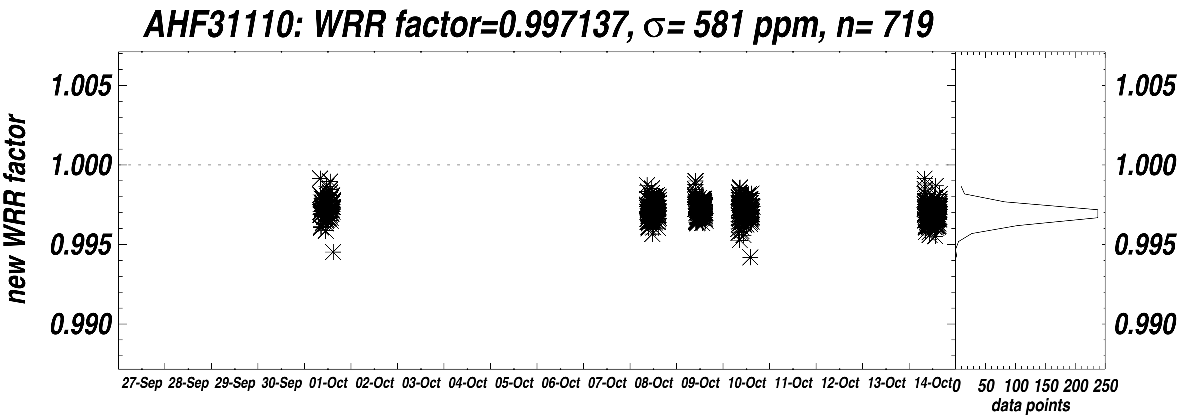
AHF31110: WRR factor=0.997137, σ= 581 ppm, n= 719
new WRR factor
1.005
1.000
0.995
0.990
27-Sep 28-Sep 29-Sep 30-Sep 01-Oct 02-Oct 03-Oct 04-Oct 05-Oct 06-Oct 07-Oct 08-Oct 09-Oct 10-Oct 11-Oct 12-Oct 13-Oct 14-Oct
0 50 100 150 200 250
data points

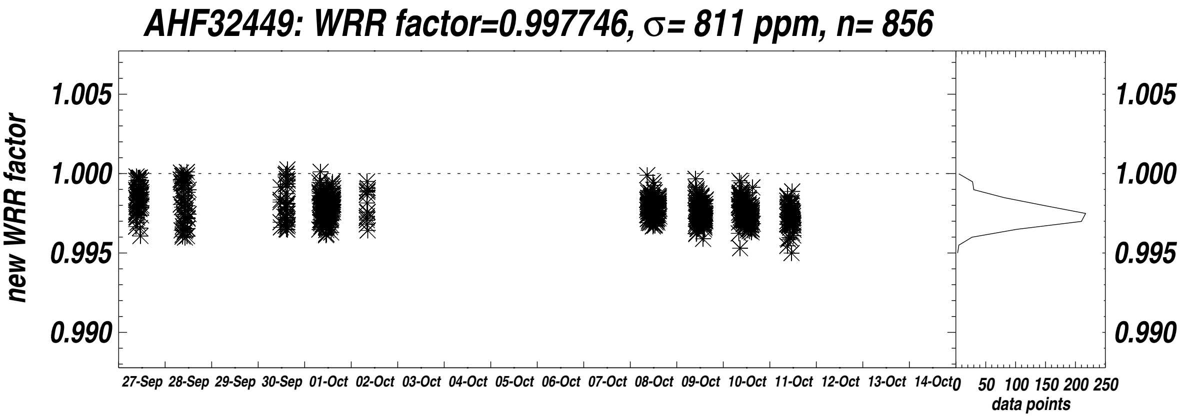
AHF32449: WRR factor=0.997746, σ= 811 ppm, n= 856
new WRR factor
1.005
1.000
0.995
0.990
27-Sep 28-Sep 29-Sep 30-Sep 01-Oct 02-Oct 03-Oct 04-Oct 05-Oct 06-Oct 07-Oct 08-Oct 09-Oct 10-Oct 11-Oct 12-Oct 13-Oct 14-Oct
0 50 100 150 200 250
data points

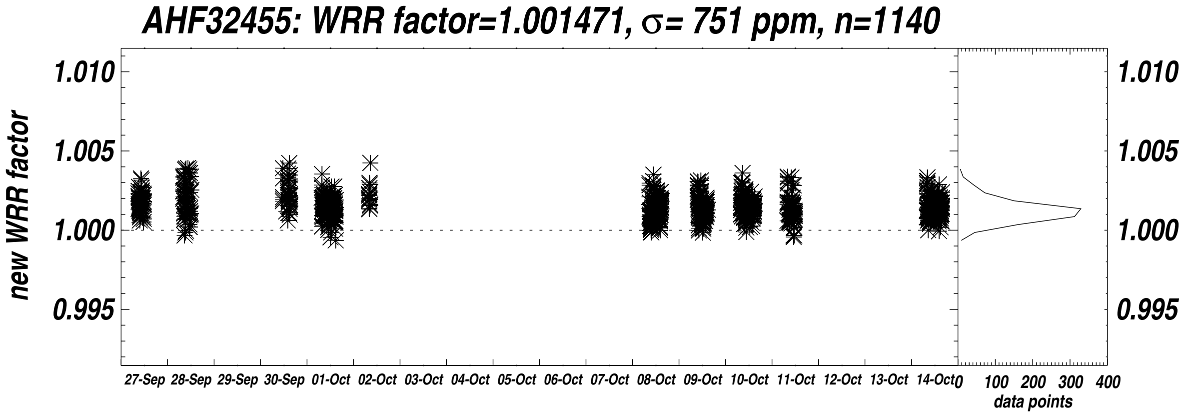
AHF32455: WRR factor=1.001471, σ= 751 ppm, n=1140
new WRR factor
1.010
1.005
1.000
0.995
27-Sep 28-Sep 29-Sep 30-Sep 01-Oct 02-Oct 03-Oct 04-Oct 05-Oct 06-Oct 07-Oct 08-Oct 09-Oct 10-Oct 11-Oct 12-Oct 13-Oct 14-Oct
0 100 200 300 400
data points

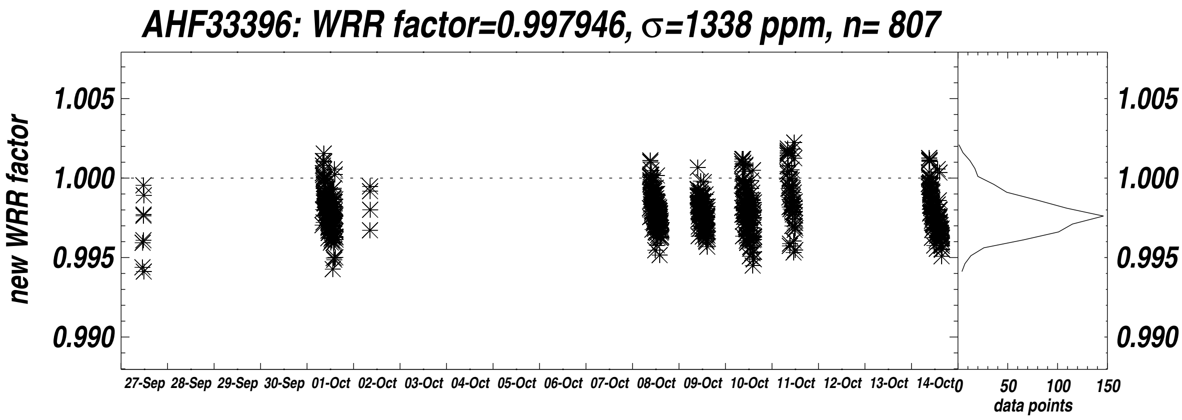
AHF33396: WRR factor=0.997946, σ=1338 ppm, n= 807
new WRR factor
1.005
1.000
0.995
0.990
27-Sep 28-Sep 29-Sep 30-Sep 01-Oct 02-Oct 03-Oct 04-Oct 05-Oct 06-Oct 07-Oct 08-Oct 09-Oct 10-Oct 11-Oct 12-Oct 13-Oct 14-Oct
0 50 100 150
data points

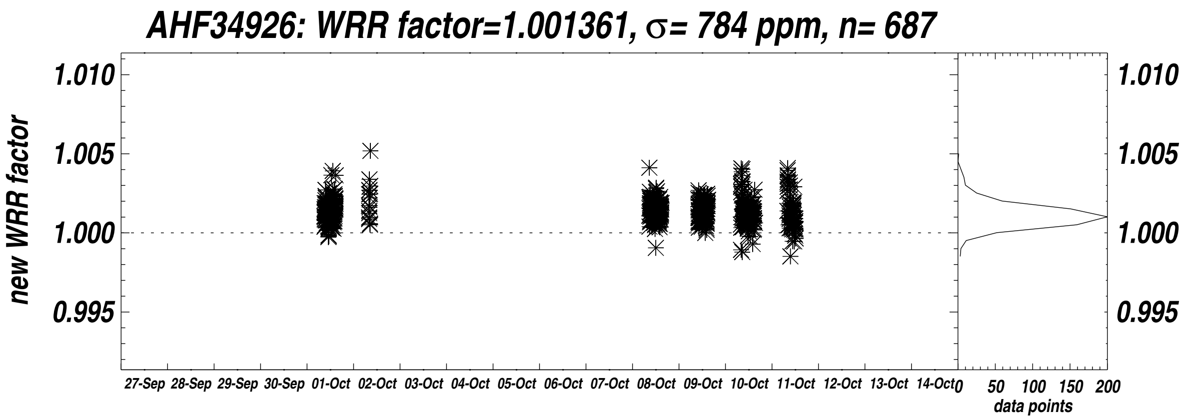
AHF34926: WRR factor=1.001361, σ= 784 ppm, n= 687
new WRR factor
1.010
1.005
1.000
0.995
27-Sep 28-Sep 29-Sep 30-Sep 01-Oct 02-Oct 03-Oct 04-Oct 05-Oct 06-Oct 07-Oct 08-Oct 09-Oct 10-Oct 11-Oct 12-Oct 13-Oct 14-Oct
0 50 100 150 200
data points

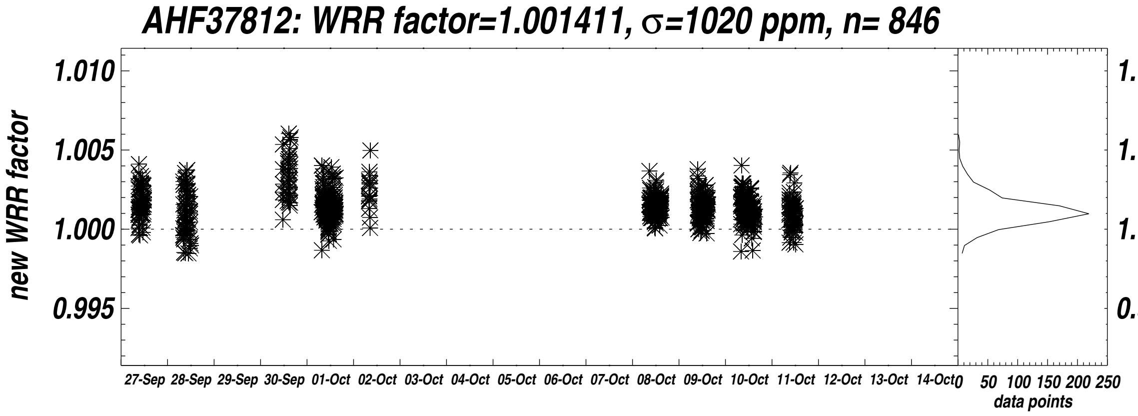
AHF37812: WRR factor=1.001411, σ=1020 ppm, n= 846
new WRR factor
1.010
1.005
1.000
0.995
27-Sep 28-Sep 29-Sep 30-Sep 01-Oct 02-Oct 03-Oct 04-Oct 05-Oct 06-Oct 07-Oct 08-Oct 09-Oct 10-Oct 11-Oct 12-Oct 13-Oct 14-Oct
0 50 100 150 200 250
data points

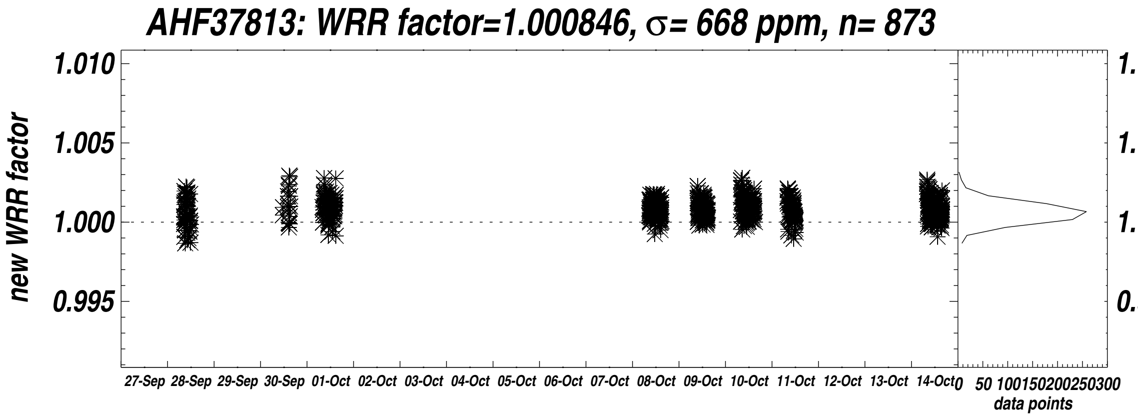
AHF37813: WRR factor=1.000846, σ= 668 ppm, n= 873
new WRR factor
1.010
1.005
1.000
0.995
27-Sep 28-Sep 29-Sep 30-Sep 01-Oct 02-Oct 03-Oct 04-Oct 05-Oct 06-Oct 07-Oct 08-Oct 09-Oct 10-Oct 11-Oct 12-Oct 13-Oct 14-Oct
0 50 100150200250300
data points

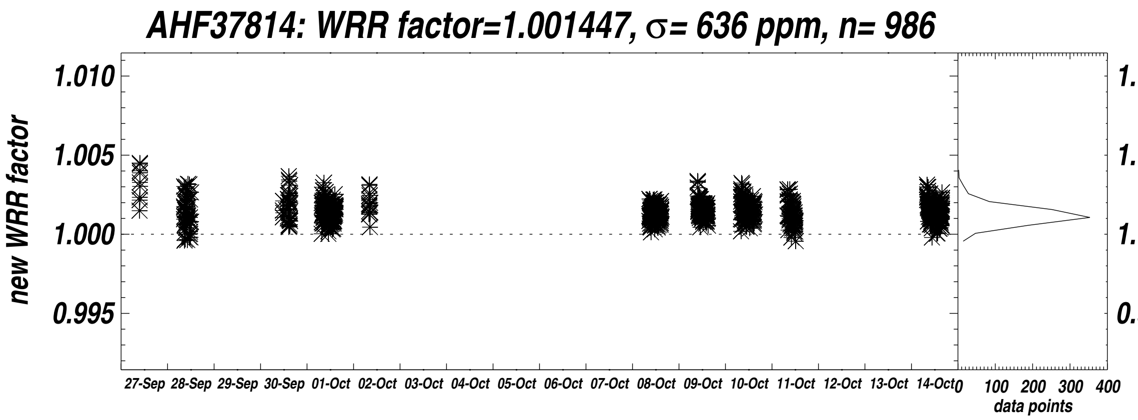
AHF37814: WRR factor=1.001447, σ= 636 ppm, n= 986
new WRR factor
1.010
1.005
1.000
0.995
27-Sep 28-Sep 29-Sep 30-Sep 01-Oct 02-Oct 03-Oct 04-Oct 05-Oct 06-Oct 07-Oct 08-Oct 09-Oct 10-Oct 11-Oct 12-Oct 13-Oct 14-Oct
0 100 200 300 400
data points

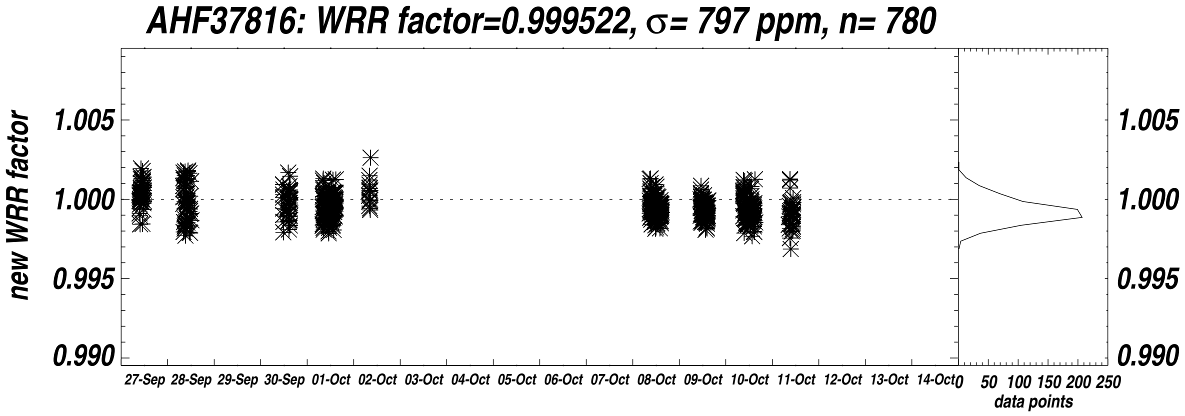
AHF37816: WRR factor=0.999522, σ= 797 ppm, n= 780
new WRR factor
1.005
1.000
0.995
0.990
27-Sep 28-Sep 29-Sep 30-Sep 01-Oct 02-Oct 03-Oct 04-Oct 05-Oct 06-Oct 07-Oct 08-Oct 09-Oct 10-Oct 11-Oct 12-Oct 13-Oct 14-Oct
0 50 100 150 200 250
data points

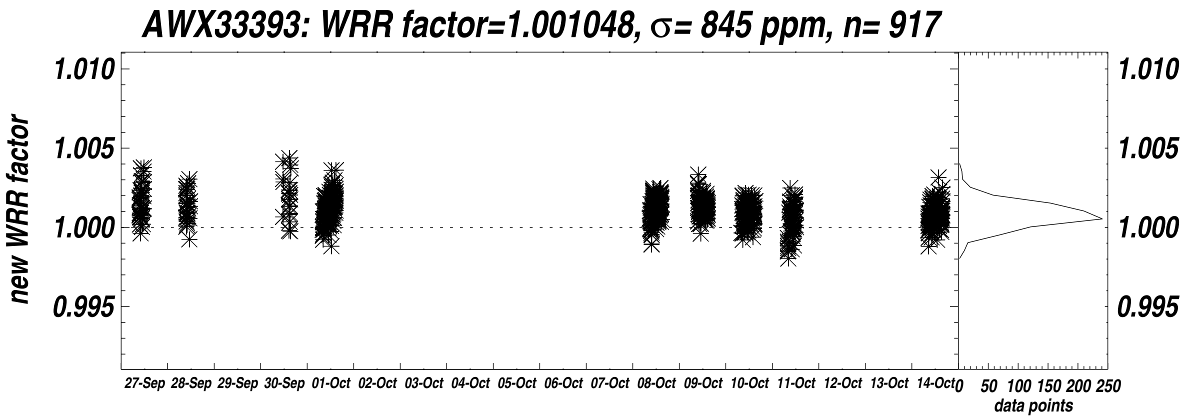
AWX33393: WRR factor=1.001048, σ= 845 ppm, n= 917
new WRR factor
1.010
1.005
1.000
0.995
27-Sep 28-Sep 29-Sep 30-Sep 01-Oct 02-Oct 03-Oct 04-Oct 05-Oct 06-Oct 07-Oct 08-Oct 09-Oct 10-Oct 11-Oct 12-Oct 13-Oct 14-Oct
0 50 100 150 200 250
data points

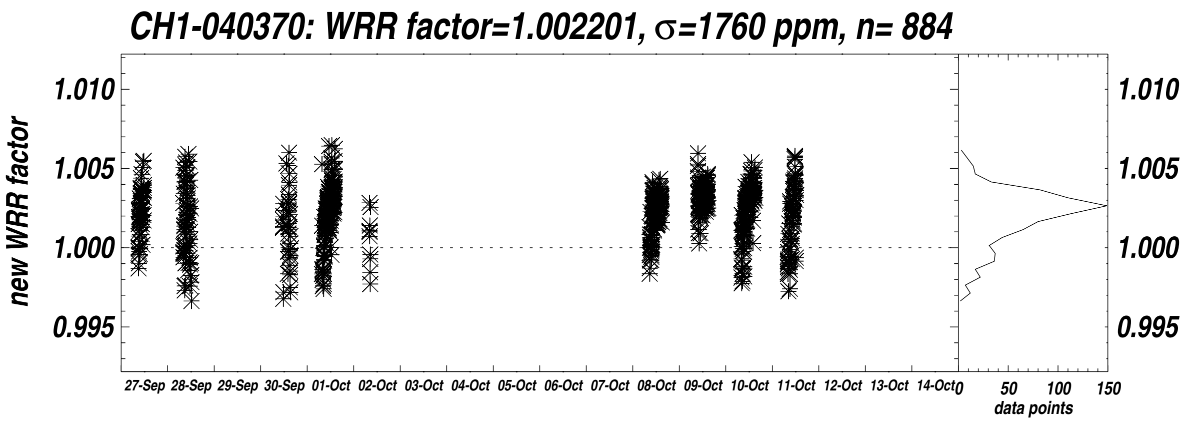
CH1-040370: WRR factor=1.002201, σ=1760 ppm, n= 884
new WRR factor
1.010
1.005
1.000
0.995
27-Sep 28-Sep 29-Sep 30-Sep 01-Oct 02-Oct 03-Oct 04-Oct 05-Oct 06-Oct 07-Oct 08-Oct 09-Oct 10-Oct 11-Oct 12-Oct 13-Oct 14-Oct
0 50 100 150
data points

CH1-060460: WRR factor=1.001348, σ=1773 ppm, n= 897

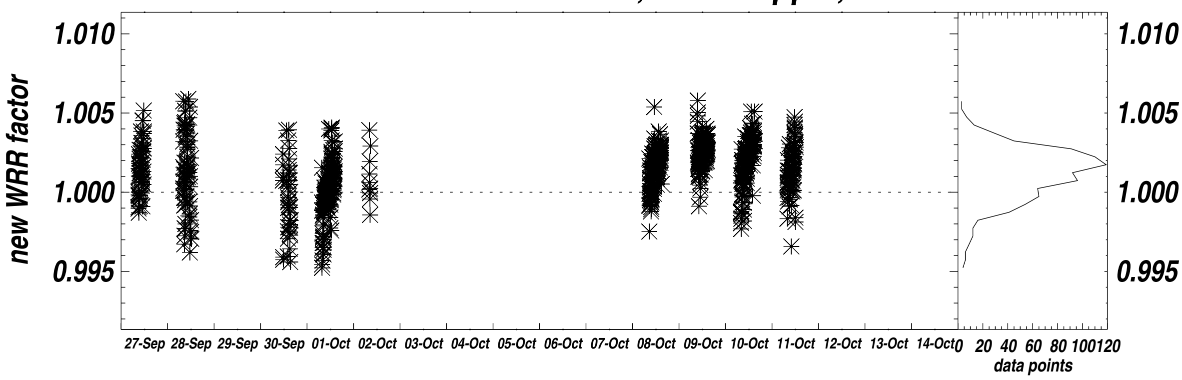

CH1-930018: WRR factor=1.000590, σ=2458 ppm, n= 907

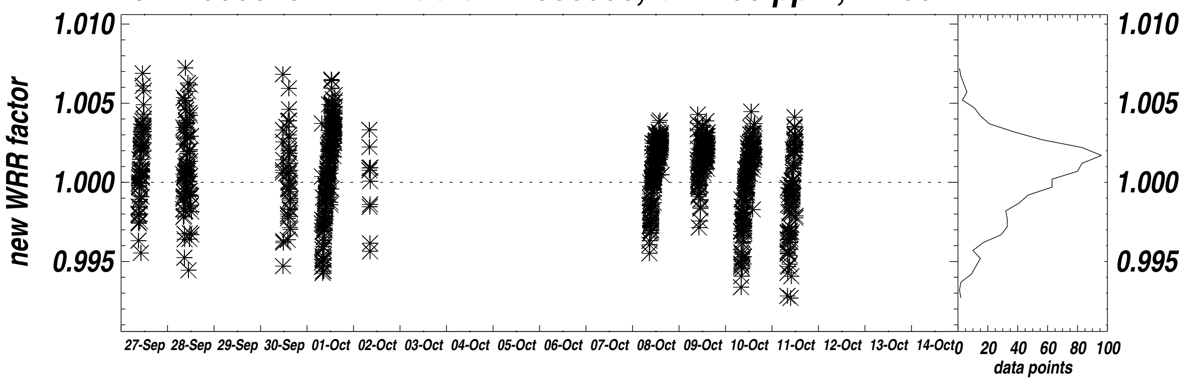

CHP1-110533: WRR factor=0.995962, σ=2463 ppm, n= 891

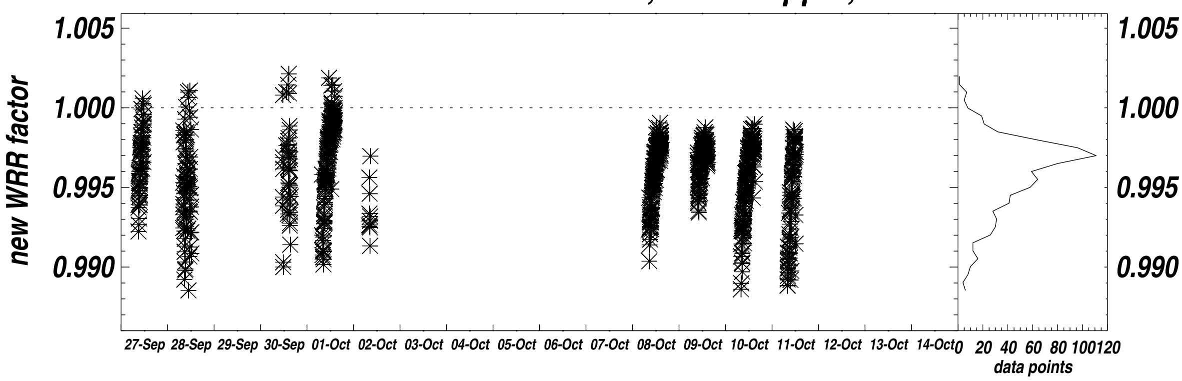

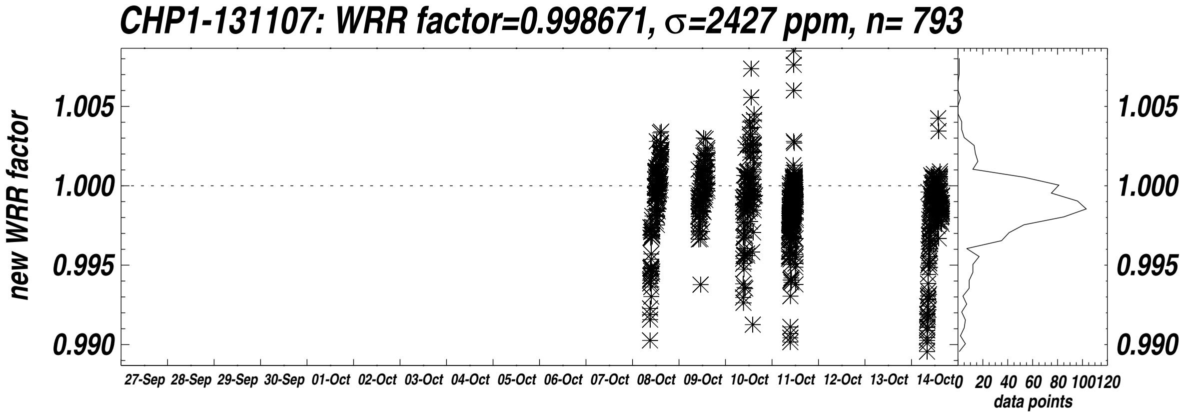
CHP1-131107: WRR factor=0.998671, σ=2427 ppm, n= 793
new WRR factor
1.005
1.000
0.995
0.990
27-Sep 28-Sep 29-Sep 30-Sep 01-Oct 02-Oct 03-Oct 04-Oct 05-Oct 06-Oct 07-Oct 08-Oct 09-Oct 10-Oct 11-Oct 12-Oct 13-Oct 14-Oct
0 20 40 60 80 100120
data points

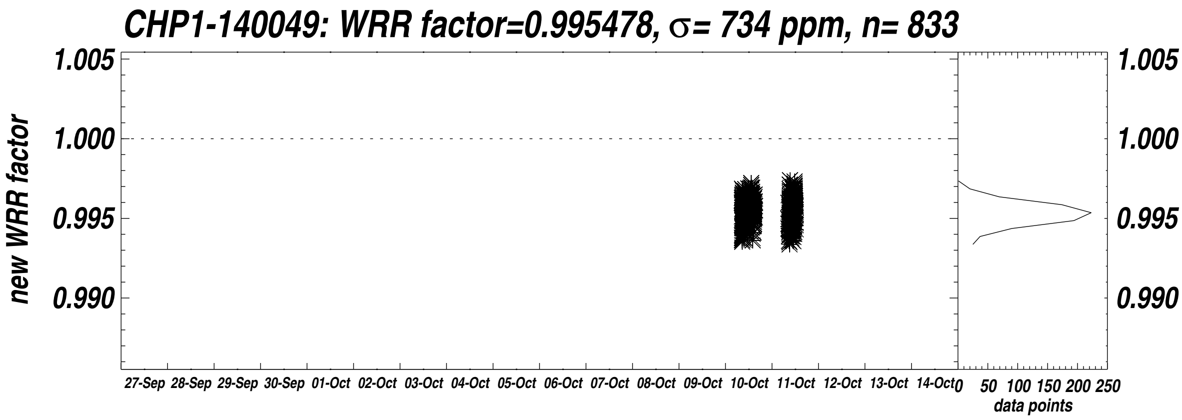
CHP1-140049: WRR factor=0.995478, σ= 734 ppm, n= 833
new WRR factor
1.005
1.000
0.995
0.990
27-Sep 28-Sep 29-Sep 30-Sep 01-Oct 02-Oct 03-Oct 04-Oct 05-Oct 06-Oct 07-Oct 08-Oct 09-Oct 10-Oct 11-Oct 12-Oct 13-Oct 14-Oct
0 50 100 150 200 250
data points


CHP1-150261: WRR factor=0.987260, σ=2762 ppm, n= 778
new WRR factor
0.995
0.990
0.985
0.980
27-Sep 28-Sep 29-Sep 30-Sep 01-Oct 02-Oct 03-Oct 04-Oct 05-Oct 06-Oct 07-Oct 08-Oct 09-Oct 10-Oct 11-Oct 12-Oct 13-Oct 14-Oct
0 50 100 150
data points

CHP1-200837: WRR factor=1.014874, σ=5658 ppm, n=1053

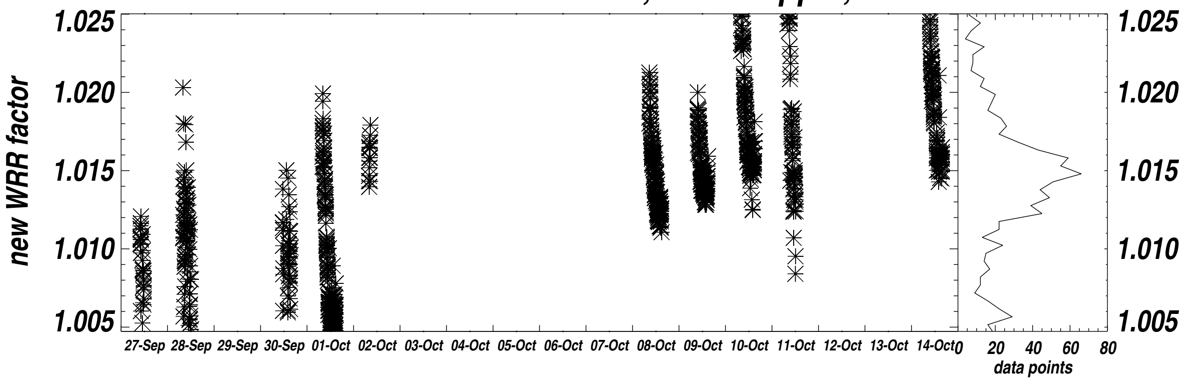

CHP1-200838: WRR factor=1.007458, σ=1412 ppm, n=1023

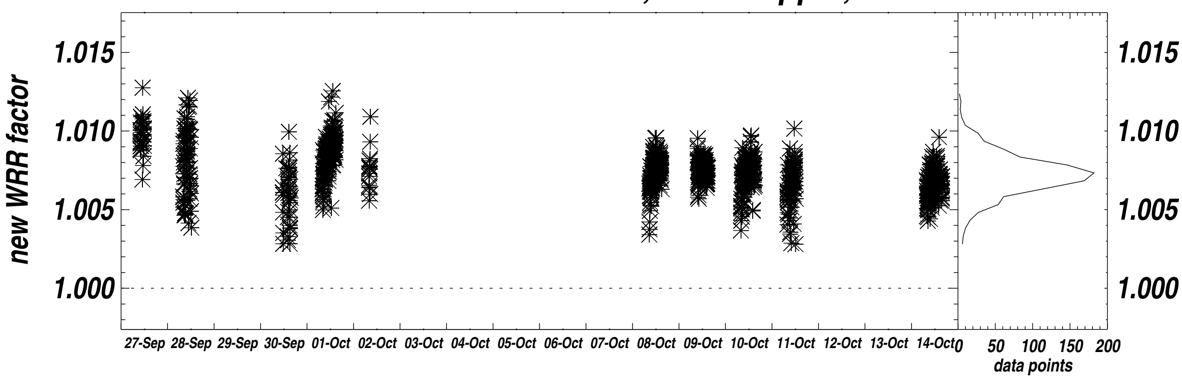

CHP1-REF2: WRR factor=1.005724, σ=1424 ppm, n= 604

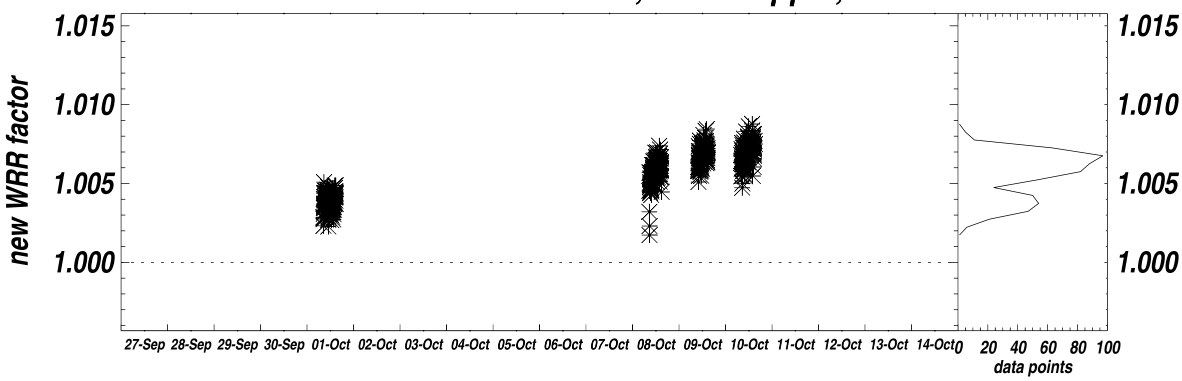

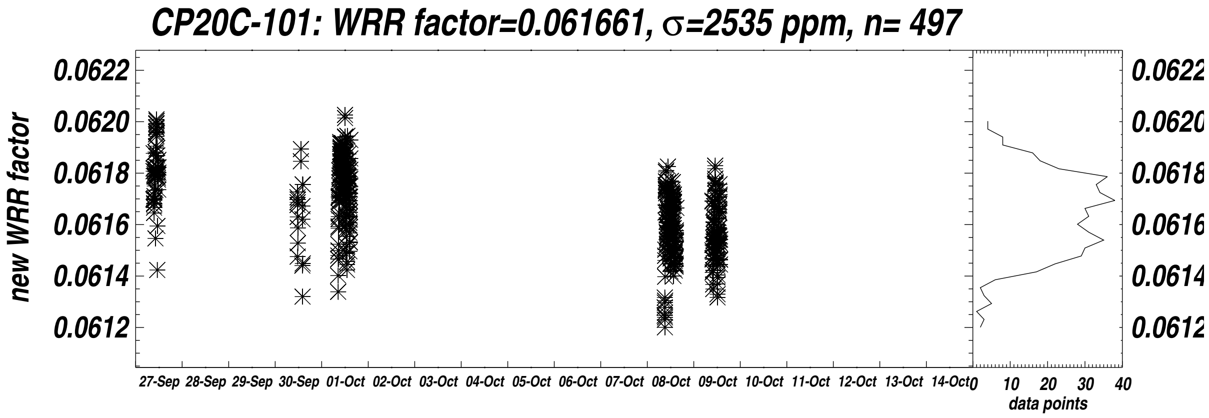
CP20C-101: WRR factor=0.061661, σ=2535 ppm, n= 497
new WRR factor
0.0622
0.0620
0.0618
0.0616
0.0614
0.0612
27-Sep 28-Sep 29-Sep 30-Sep 01-Oct 02-Oct 03-Oct 04-Oct 05-Oct 06-Oct 07-Oct 08-Oct 09-Oct 10-Oct 11-Oct 12-Oct 13-Oct 14-Oct
0 10 20 30 40
data points

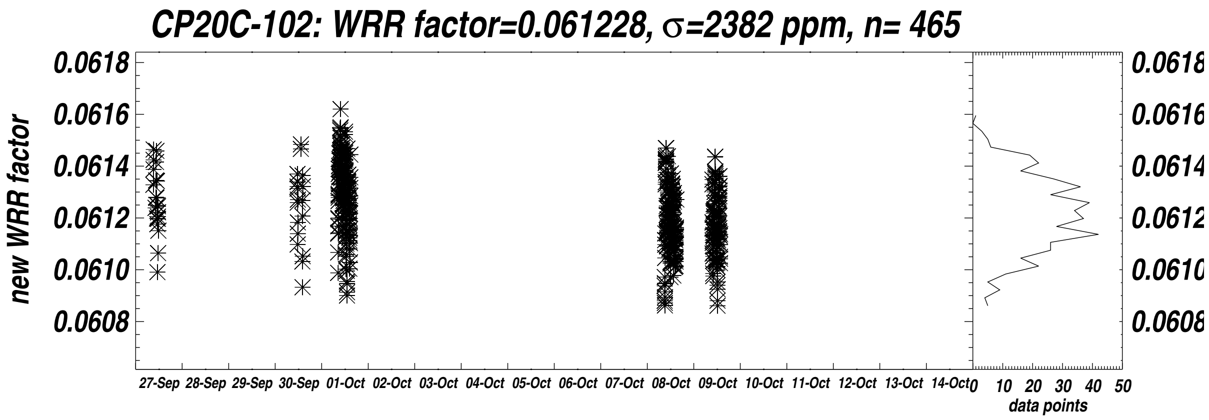
CP20C-102: WRR factor=0.061228, σ=2382 ppm, n= 465
new WRR factor
0.0618
0.0616
0.0614
0.0612
0.0610
0.0608
27-Sep 28-Sep 29-Sep 30-Sep 01-Oct 02-Oct 03-Oct 04-Oct 05-Oct 06-Oct 07-Oct 08-Oct 09-Oct 10-Oct 11-Oct 12-Oct 13-Oct 14-Oct
0 10 20 30 40 50
data points

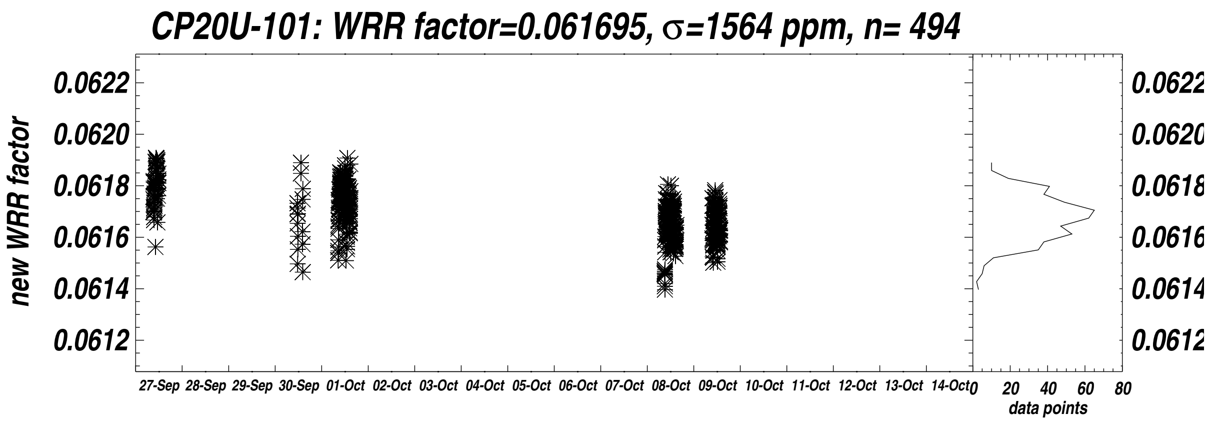
CP20U-101: WRR factor=0.061695, σ=1564 ppm, n= 494
new WRR factor
0.0622
0.0620
0.0618
0.0616
0.0614
0.0612
27-Sep 28-Sep 29-Sep 30-Sep 01-Oct 02-Oct 03-Oct 04-Oct 05-Oct 06-Oct 07-Oct 08-Oct 09-Oct 10-Oct 11-Oct 12-Oct 13-Oct 14-Oct
0 20 40 60 80
data points

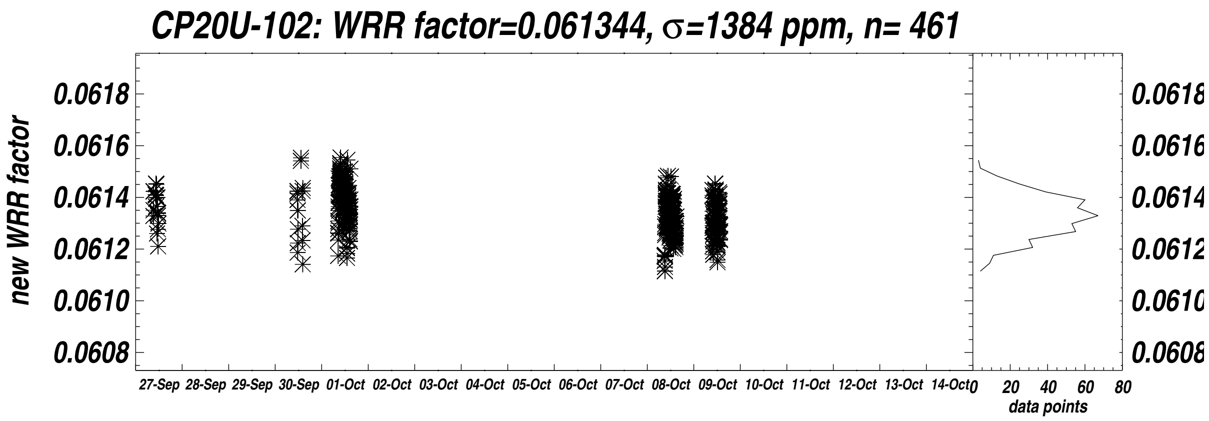
CP20U-102: WRR factor=0.061344, σ=1384 ppm, n= 461
new WRR factor
0.0618
0.0616
0.0614
0.0612
0.0610
0.0608
27-Sep 28-Sep 29-Sep 30-Sep 01-Oct 02-Oct 03-Oct 04-Oct 05-Oct 06-Oct 07-Oct 08-Oct 09-Oct 10-Oct 11-Oct 12-Oct 13-Oct 14-Oct
0 20 40 60 80
data points

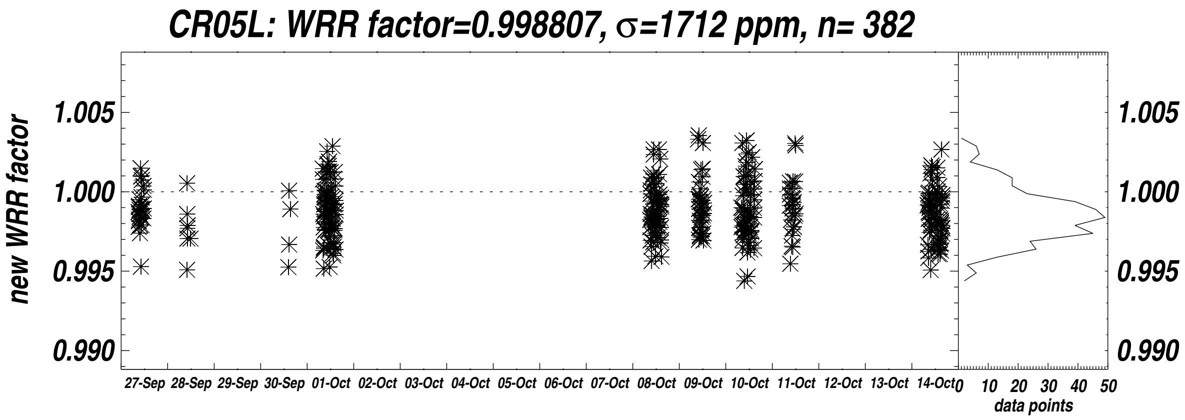
CR05L: WRR factor=0.998807, σ=1712 ppm, n= 382
new WRR factor
1.005
1.000
0.995
0.990
27-Sep 28-Sep 29-Sep 30-Sep 01-Oct 02-Oct 03-Oct 04-Oct 05-Oct 06-Oct 07-Oct 08-Oct 09-Oct 10-Oct 11-Oct 12-Oct 13-Oct 14-Oct
0 10 20 30 40 50
data points

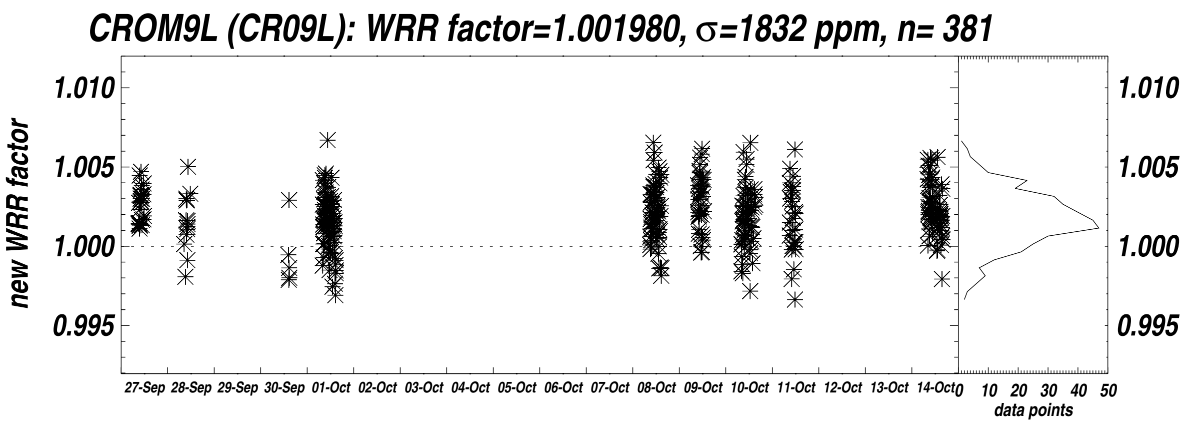
CROM9L (CR09L): WRR factor=1.001980, σ=1832 ppm, n= 381
new WRR factor
1.010
1.005
1.000
0.995
27-Sep 28-Sep 29-Sep 30-Sep 01-Oct 02-Oct 03-Oct 04-Oct 05-Oct 06-Oct 07-Oct 08-Oct 09-Oct 10-Oct 11-Oct 12-Oct 13-Oct 14-Oct
0 10 20 30 40 50
data points

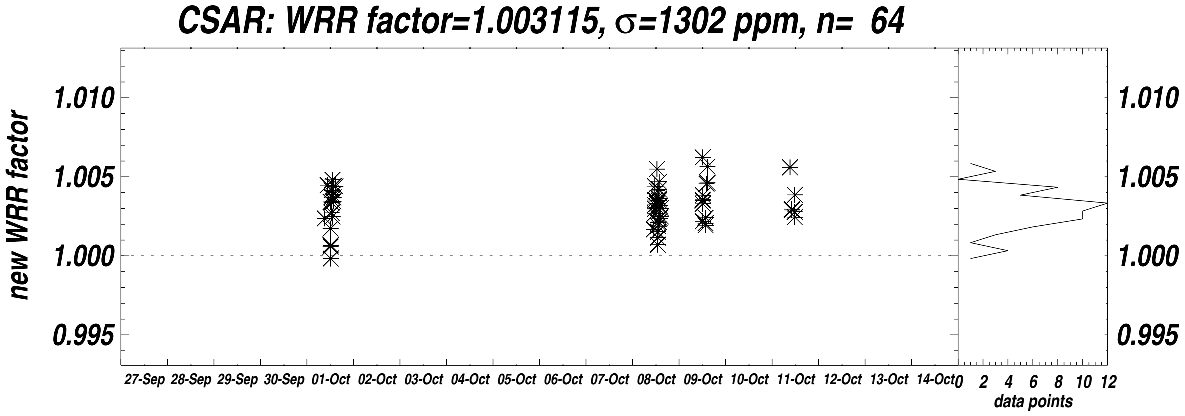
CSAR: WRR factor=1.003115, σ=1302 ppm, n= 64
new WRR factor
1.010
1.005
1.000
0.995
27-Sep 28-Sep 29-Sep 30-Sep 01-Oct 02-Oct 03-Oct 04-Oct 05-Oct 06-Oct 07-Oct 08-Oct 09-Oct 10-Oct 11-Oct 12-Oct 13-Oct 14-Oct
0 2 4 6 8 10 12
data points

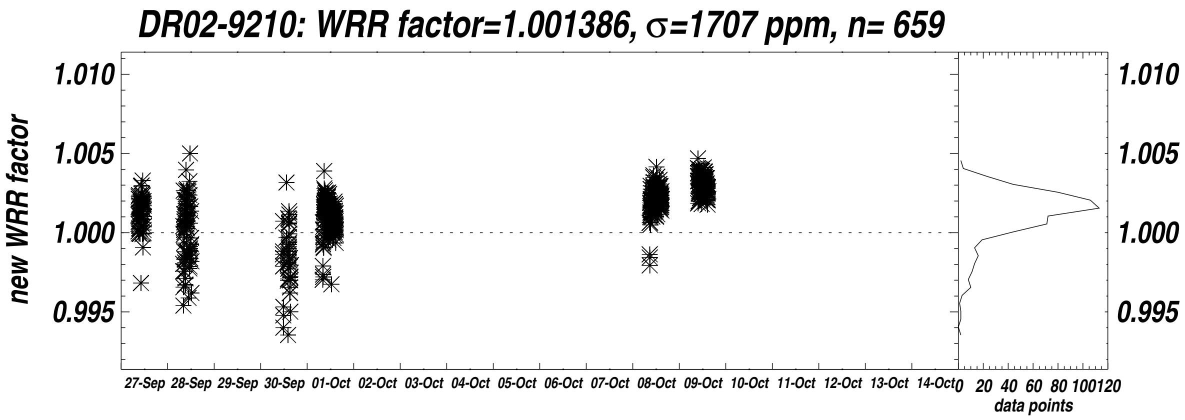
DR02-9210: WRR factor=1.001386, σ=1707 ppm, n= 659
new WRR factor
1.010
1.005
1.000
0.995
27-Sep 28-Sep 29-Sep 30-Sep 01-Oct 02-Oct 03-Oct 04-Oct 05-Oct 06-Oct 07-Oct 08-Oct 09-Oct 10-Oct 11-Oct 12-Oct 13-Oct 14-Oct
0 20 40 60 80 100 120
data points

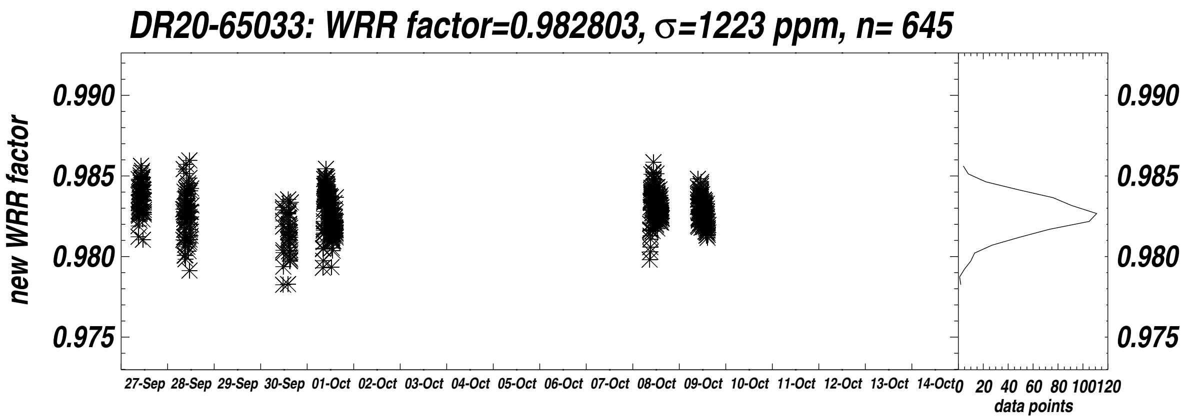
DR20-65033: WRR factor=0.982803, σ=1223 ppm, n= 645
new WRR factor
0.990
0.985
0.980
0.975
27-Sep 28-Sep 29-Sep 30-Sep 01-Oct 02-Oct 03-Oct 04-Oct 05-Oct 06-Oct 07-Oct 08-Oct 09-Oct 10-Oct 11-Oct 12-Oct 13-Oct 14-Oct
0 20 40 60 80 100 120
data points

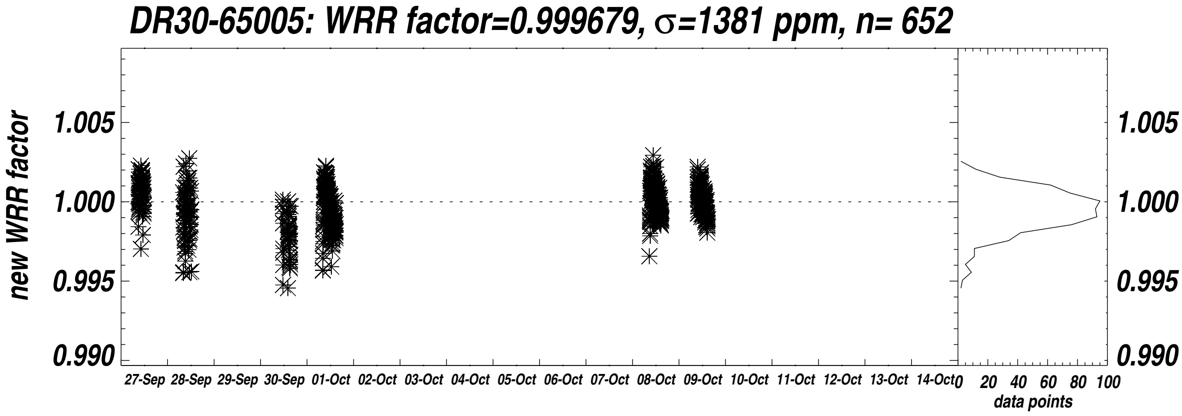
DR30-65005: WRR factor=0.999679, σ=1381 ppm, n= 652
new WRR factor
1.005
1.000
0.995
0.990
27-Sep 28-Sep 29-Sep 30-Sep 01-Oct 02-Oct 03-Oct 04-Oct 05-Oct 06-Oct 07-Oct 08-Oct 09-Oct 10-Oct 11-Oct 12-Oct 13-Oct 14-Oct
0 20 40 60 80 100
data points

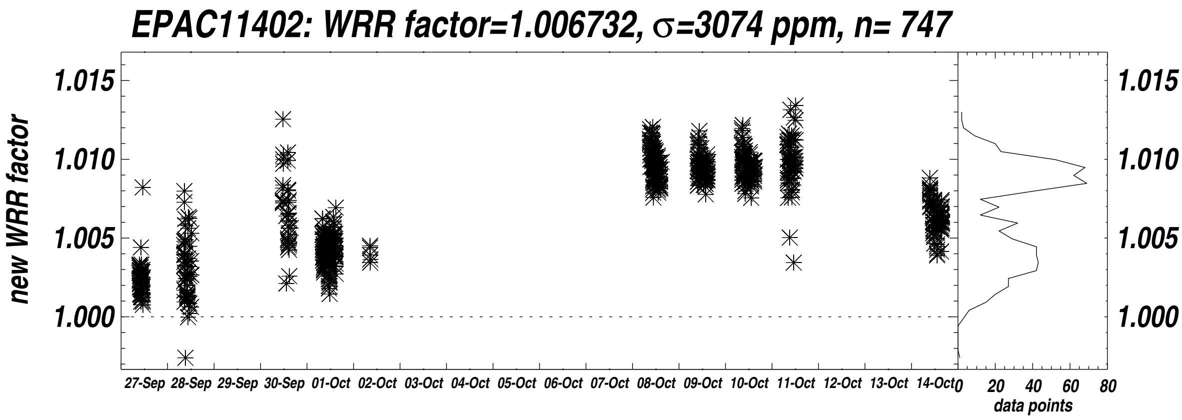
EPAC11402: WRR factor=1.006732, σ=3074 ppm, n= 747
new WRR factor
1.015
1.010
1.005
1.000
27-Sep 28-Sep 29-Sep 30-Sep 01-Oct 02-Oct 03-Oct 04-Oct 05-Oct 06-Oct 07-Oct 08-Oct 09-Oct 10-Oct 11-Oct 12-Oct 13-Oct 14-Oct
0 20 40 60 80
data points

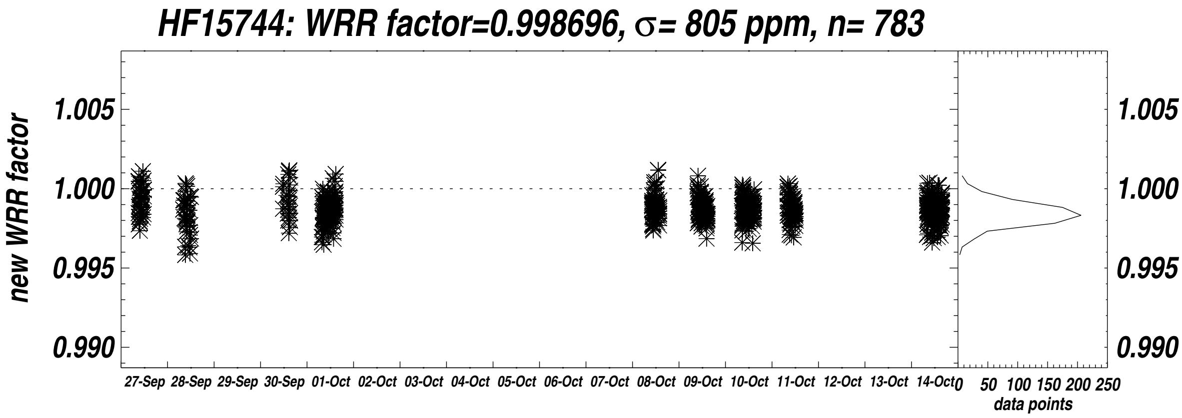
HF15744: WRR factor=0.998696, σ= 805 ppm, n= 783
new WRR factor
1.005
1.000
0.995
0.990
27-Sep 28-Sep 29-Sep 30-Sep 01-Oct 02-Oct 03-Oct 04-Oct 05-Oct 06-Oct 07-Oct 08-Oct 09-Oct 10-Oct 11-Oct 12-Oct 13-Oct 14-Oct
0 50 100 150 200 250
data points

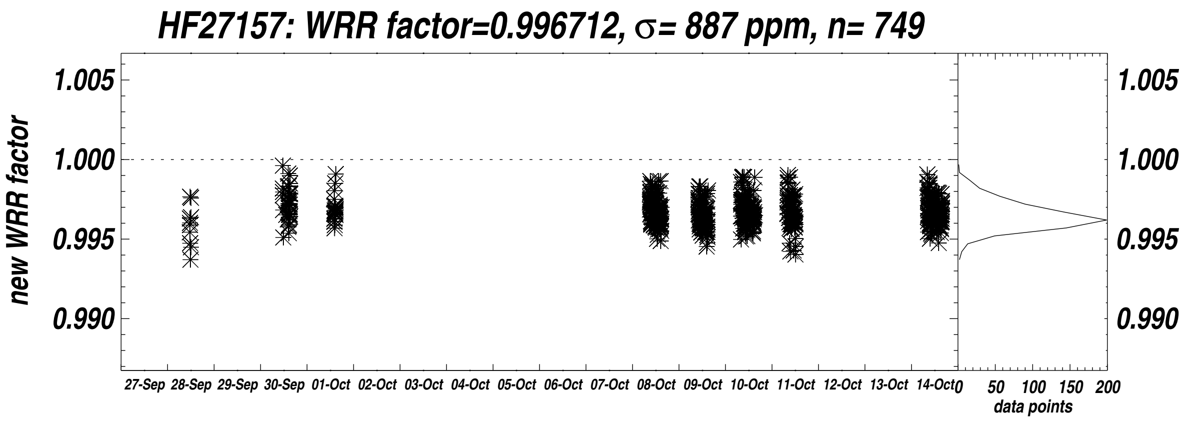
HF27157: WRR factor=0.996712, σ= 887 ppm, n= 749
new WRR factor
1.005
1.000
0.995
0.990
27-Sep 28-Sep 29-Sep 30-Sep 01-Oct 02-Oct 03-Oct 04-Oct 05-Oct 06-Oct 07-Oct 08-Oct 09-Oct 10-Oct 11-Oct 12-Oct 13-Oct 14-Oct
0 50 100 150 200
data points

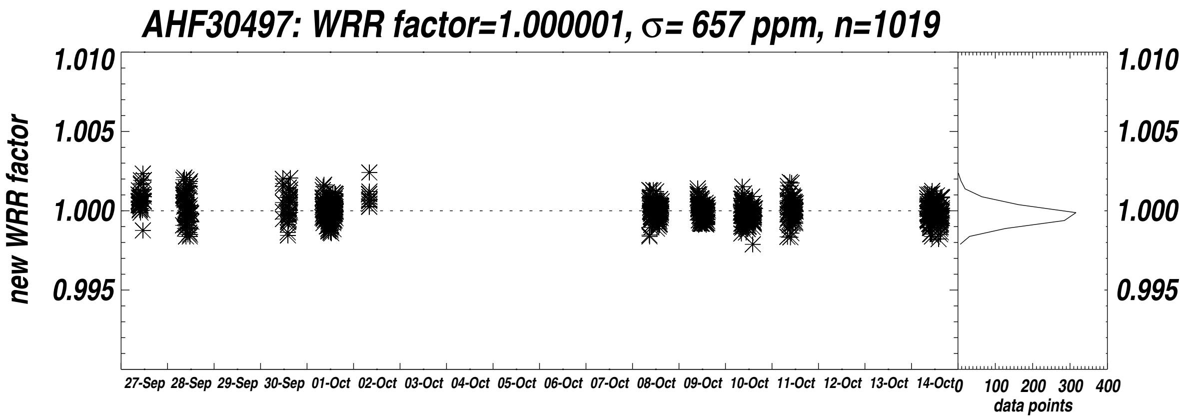
AHF30497: WRR factor=1.000001, σ= 657 ppm, n=1019
new WRR factor
1.010
1.005
1.000
0.995
27-Sep 28-Sep 29-Sep 30-Sep 01-Oct 02-Oct 03-Oct 04-Oct 05-Oct 06-Oct 07-Oct 08-Oct 09-Oct 10-Oct 11-Oct 12-Oct 13-Oct 14-Oct
0 100 200 300 400
data points

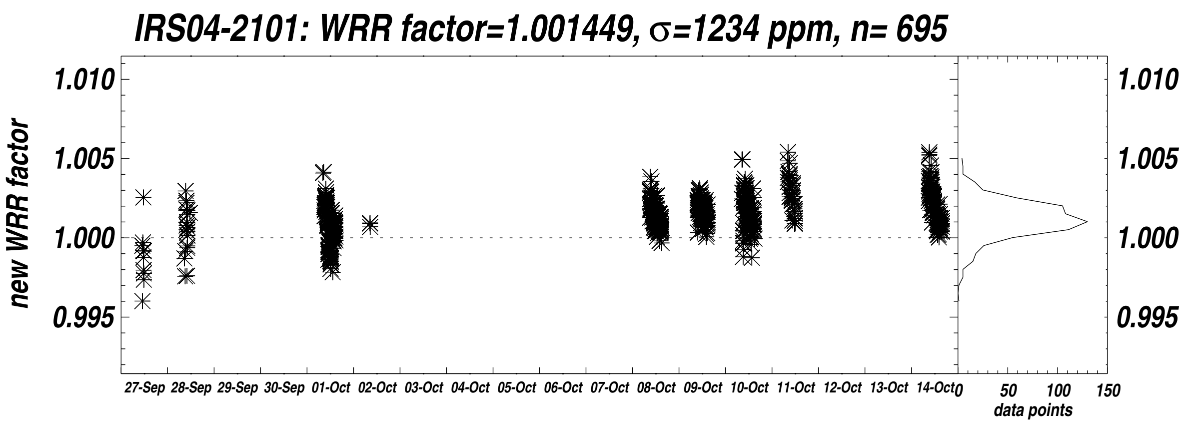
IRS04-2101: WRR factor=1.001449, σ=1234 ppm, n= 695
new WRR factor
1.010
1.005
1.000
0.995
27-Sep 28-Sep 29-Sep 30-Sep 01-Oct 02-Oct 03-Oct 04-Oct 05-Oct 06-Oct 07-Oct 08-Oct 09-Oct 10-Oct 11-Oct 12-Oct 13-Oct 14-Oct
0 50 100 150
data points

IRS04-2102: WRR factor=1.001043, σ=1573 ppm, n= 703

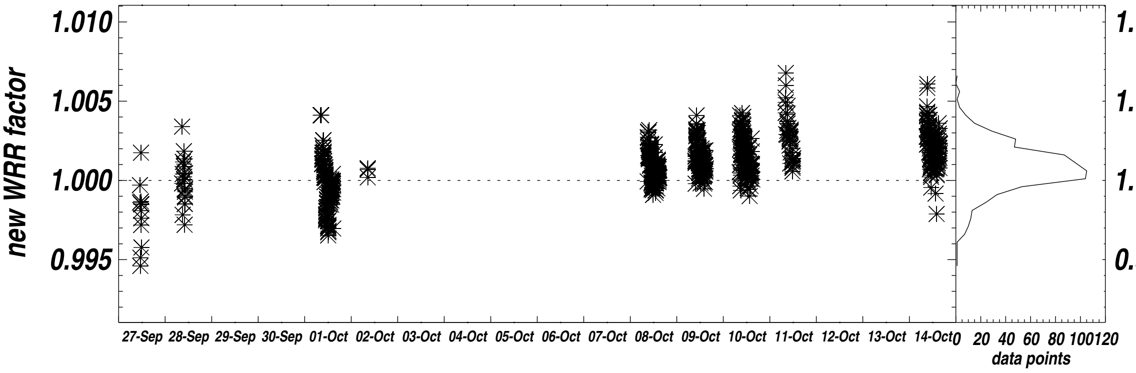

MS56-12036: WRR factor=0.972244, σ=3064 ppm, n= 906

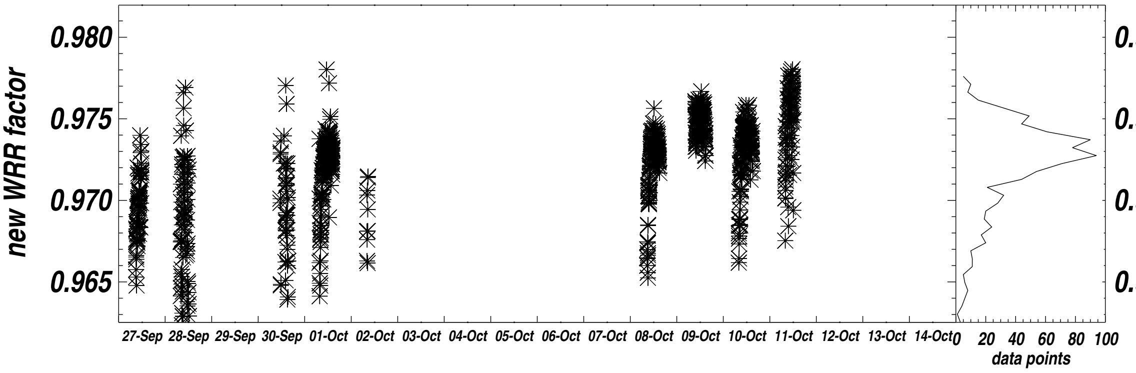

MS56-12039: WRR factor=0.994387, σ=2782 ppm, n= 904

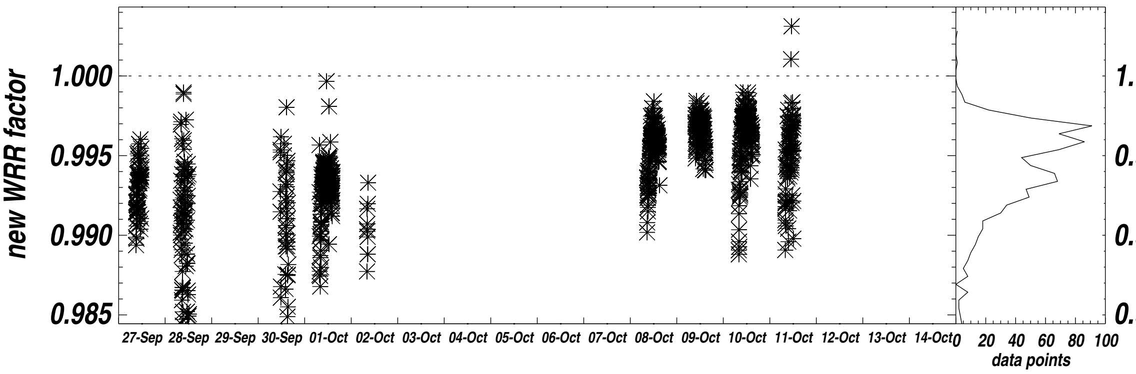

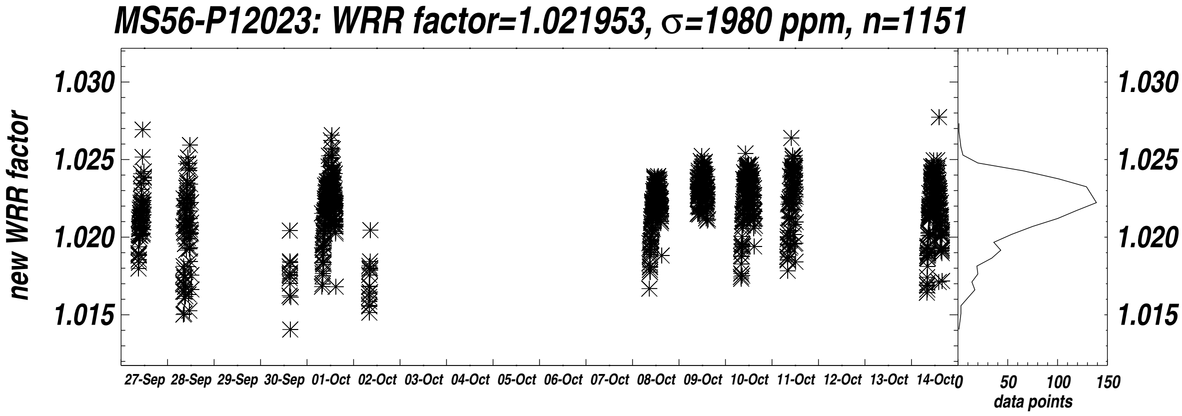
MS56-P12023: WRR factor=1.021953, σ=1980 ppm, n=1151
new WRR factor
1.030
1.025
1.020
1.015
27-Sep 28-Sep 29-Sep 30-Sep 01-Oct 02-Oct 03-Oct 04-Oct 05-Oct 06-Oct 07-Oct 08-Oct 09-Oct 10-Oct 11-Oct 12-Oct 13-Oct 14-Oct
0 50 100 150
data points

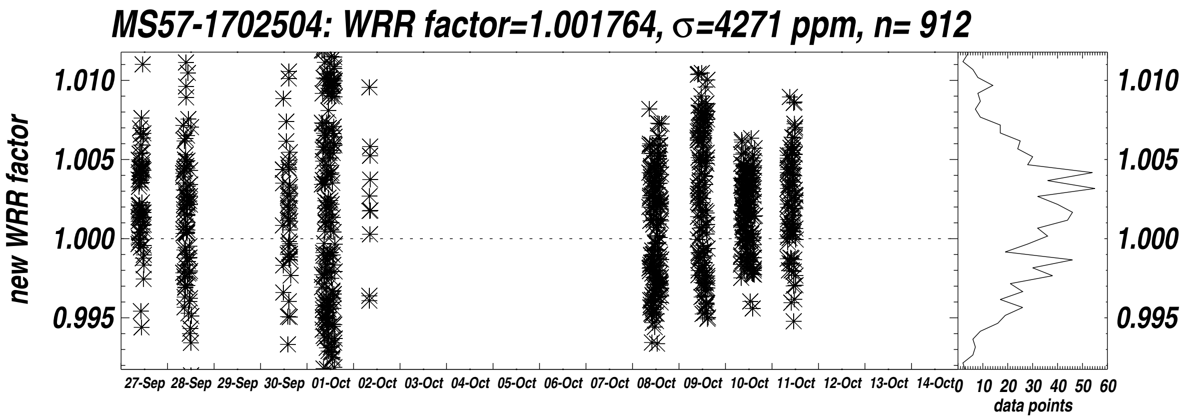
MS57-1702504: WRR factor=1.001764, σ=4271 ppm, n= 912
new WRR factor
1.010
1.005
1.000
0.995
27-Sep 28-Sep 29-Sep 30-Sep 01-Oct 02-Oct 03-Oct 04-Oct 05-Oct 06-Oct 07-Oct 08-Oct 09-Oct 10-Oct 11-Oct 12-Oct 13-Oct 14-Oct
0 10 20 30 40 50 60
data points

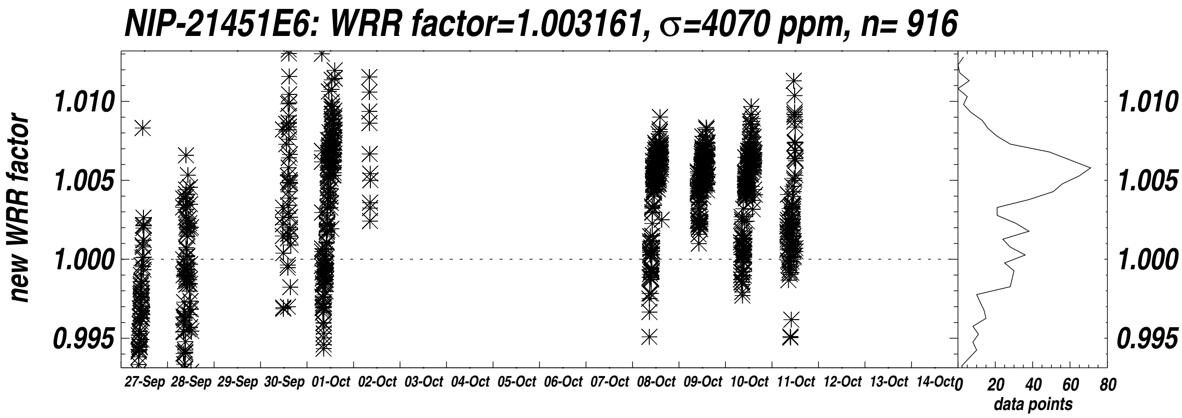
NIP-21451E6: WRR factor=1.003161, σ=4070 ppm, n= 916
new WRR factor
1.010
1.005
1.000
0.995
27-Sep 28-Sep 29-Sep 30-Sep 01-Oct 02-Oct 03-Oct 04-Oct 05-Oct 06-Oct 07-Oct 08-Oct 09-Oct 10-Oct 11-Oct 12-Oct 13-Oct 14-Oct
0 20 40 60 80
data points

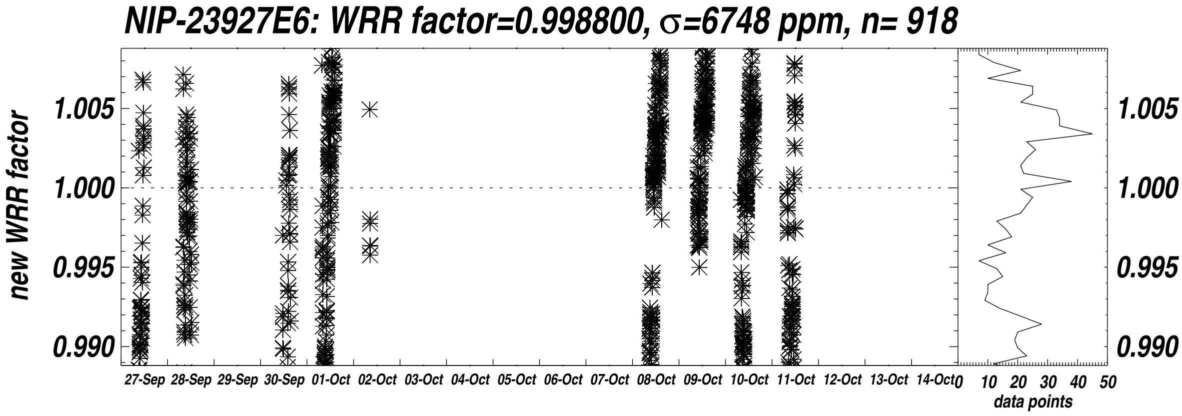
NIP-23927E6: WRR factor=0.998800, σ=6748 ppm, n= 918
new WRR factor
1.005
1.000
0.995
0.990
27-Sep 28-Sep 29-Sep 30-Sep 01-Oct 02-Oct 03-Oct 04-Oct 05-Oct 06-Oct 07-Oct 08-Oct 09-Oct 10-Oct 11-Oct 12-Oct 13-Oct 14-Oct
0 10 20 30 40 50
data points

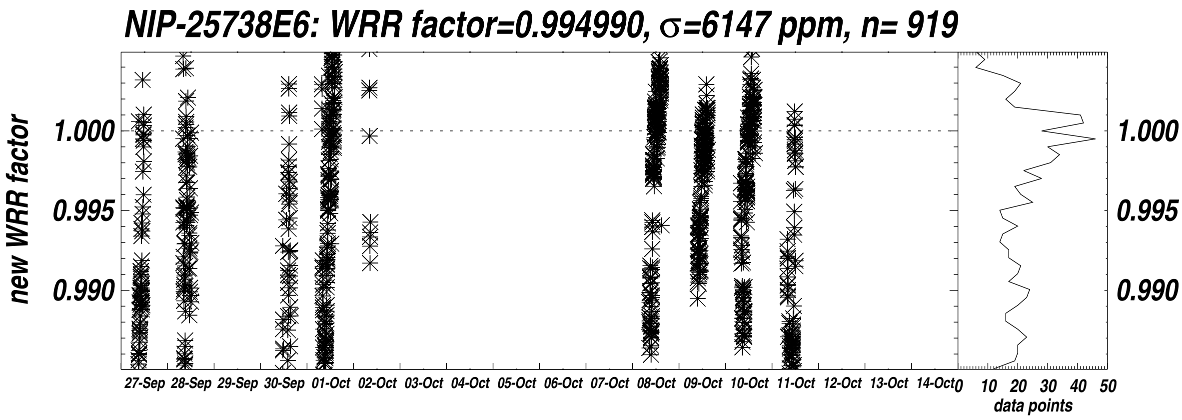
NIP-25738E6: WRR factor=0.994990, σ=6147 ppm, n= 919
new WRR factor
1.000
0.995
0.990
27-Sep 28-Sep 29-Sep 30-Sep 01-Oct 02-Oct 03-Oct 04-Oct 05-Oct 06-Oct 07-Oct 08-Oct 09-Oct 10-Oct 11-Oct 12-Oct 13-Oct 14-Oct
0 10 20 30 40 50
data points

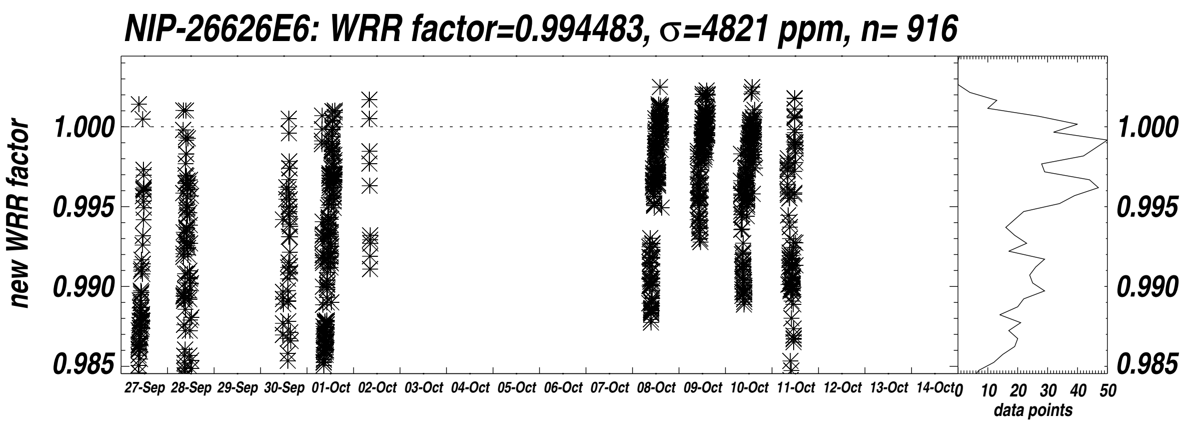
NIP-26626E6: WRR factor=0.994483, σ=4821 ppm, n= 916
new WRR factor
1.000
0.995
0.990
0.985
27-Sep 28-Sep 29-Sep 30-Sep 01-Oct 02-Oct 03-Oct 04-Oct 05-Oct 06-Oct 07-Oct 08-Oct 09-Oct 10-Oct 11-Oct 12-Oct 13-Oct 14-Oct
0 10 20 30 40 50
data points

NIP-31144E6: WRR factor=0.993855, σ=5722 ppm, n=1205

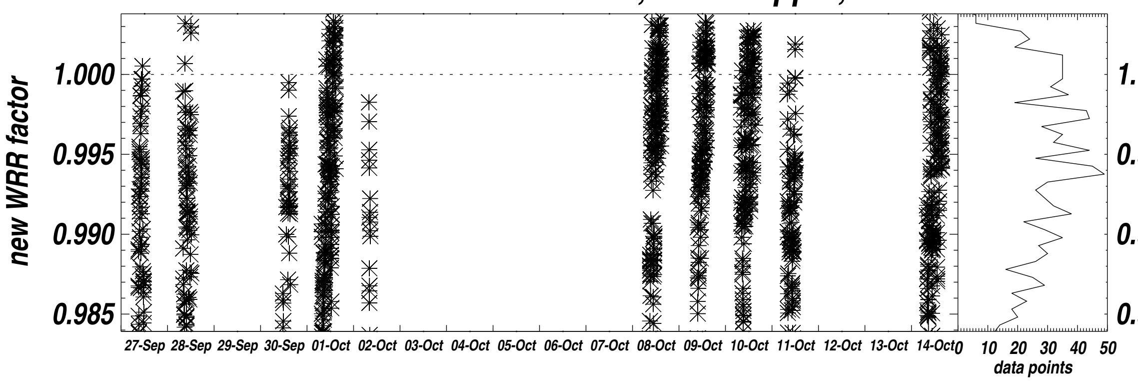

PH1-999991: WRR factor=0.997332, σ=3176 ppm, n= 504

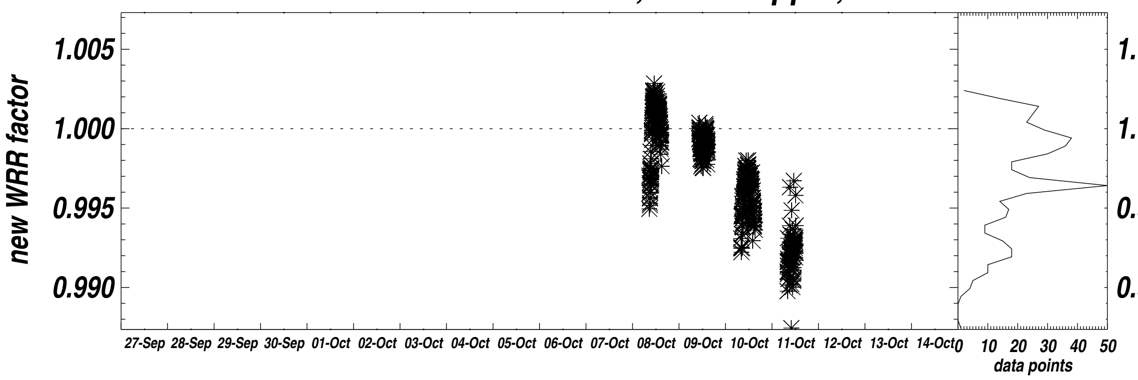

PMO6-0103: WRR factor=0.998913, σ= 609 ppm, n= 611

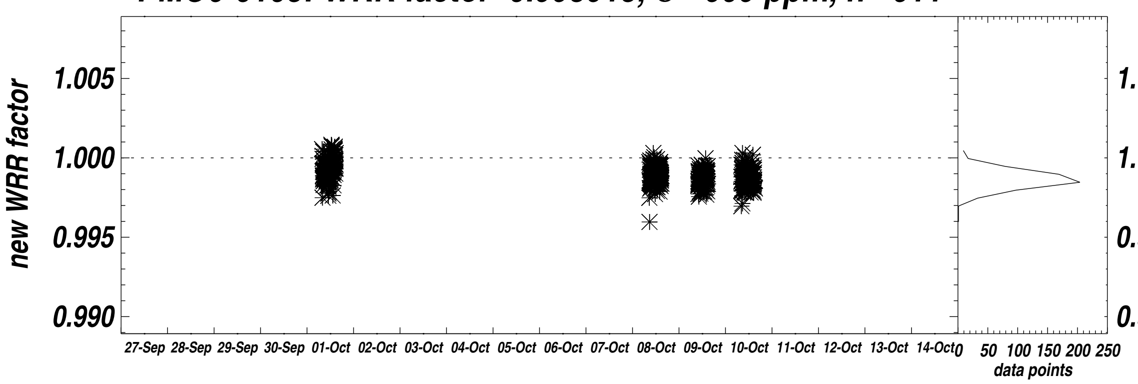

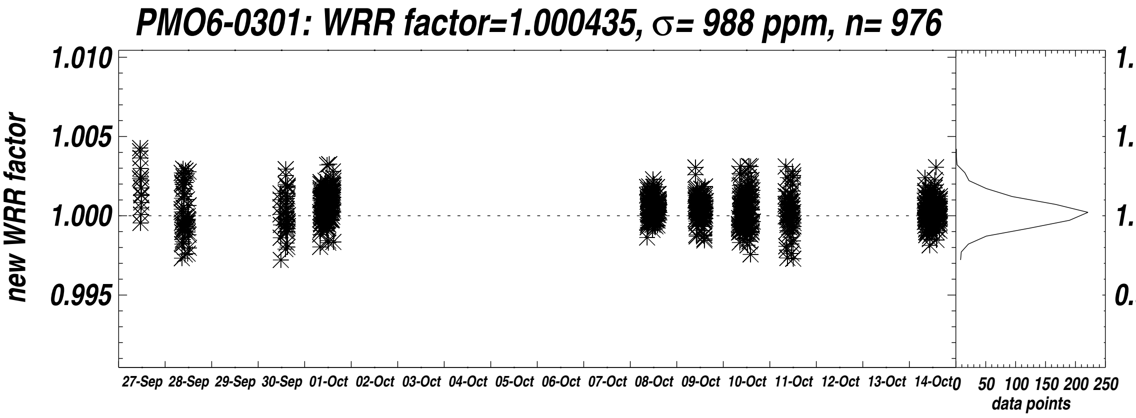
PMO6-0301: WRR factor=1.000435, σ= 988 ppm, n= 976
new WRR factor
1.010
1.005
1.000
0.995
27-Sep 28-Sep 29-Sep 30-Sep 01-Oct 02-Oct 03-Oct 04-Oct 05-Oct 06-Oct 07-Oct 08-Oct 09-Oct 10-Oct 11-Oct 12-Oct 13-Oct 14-Oct
0 50 100 150 200 250
data points

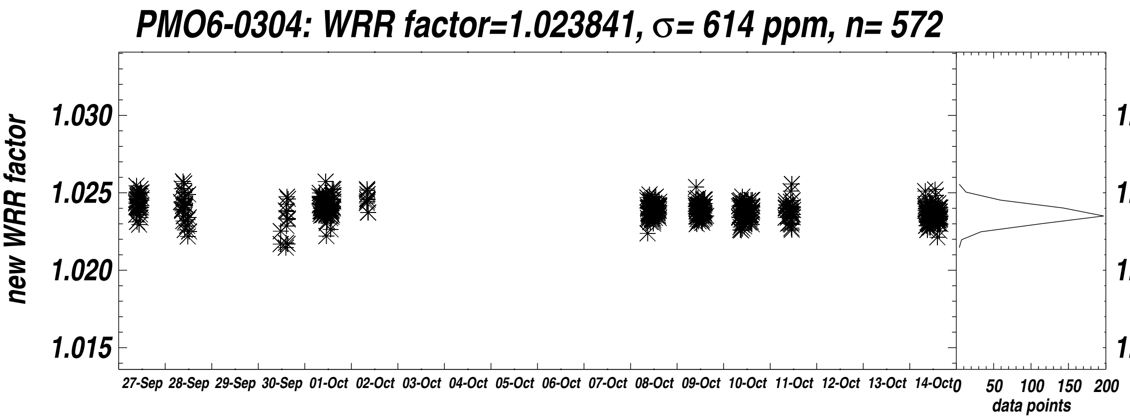
PMO6-0304: WRR factor=1.023841, σ= 614 ppm, n= 572
new WRR factor
1.030
1.025
1.020
1.015
27-Sep 28-Sep 29-Sep 30-Sep 01-Oct 02-Oct 03-Oct 04-Oct 05-Oct 06-Oct 07-Oct 08-Oct 09-Oct 10-Oct 11-Oct 12-Oct 13-Oct 14-Oct
0 50 100 150 200
data points

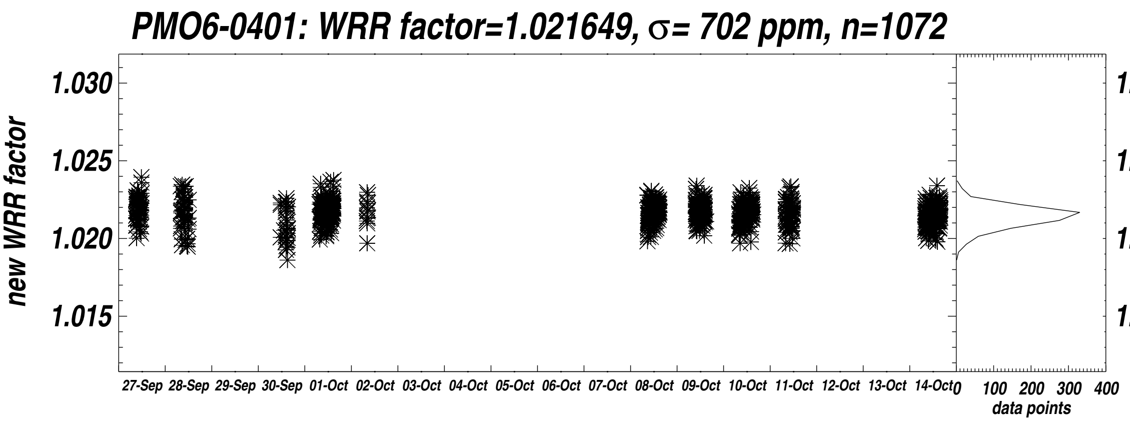
PMO6-0401: WRR factor=1.021649, σ= 702 ppm, n=1072
new WRR factor
1.030
1.025
1.020
1.015
27-Sep 28-Sep 29-Sep 30-Sep 01-Oct 02-Oct 03-Oct 04-Oct 05-Oct 06-Oct 07-Oct 08-Oct 09-Oct 10-Oct 11-Oct 12-Oct 13-Oct 14-Oct
0 100 200 300 400
data points

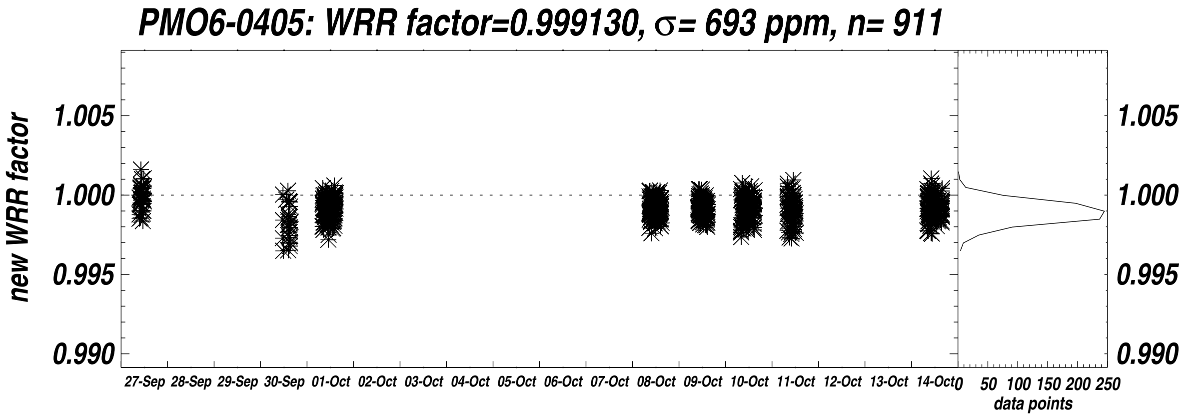
PMO6-0405: WRR factor=0.999130, σ= 693 ppm, n= 911
new WRR factor
1.005
1.000
0.995
0.990
27-Sep 28-Sep 29-Sep 30-Sep 01-Oct 02-Oct 03-Oct 04-Oct 05-Oct 06-Oct 07-Oct 08-Oct 09-Oct 10-Oct 11-Oct 12-Oct 13-Oct 14-Oct
0 50 100 150 200 250
data points

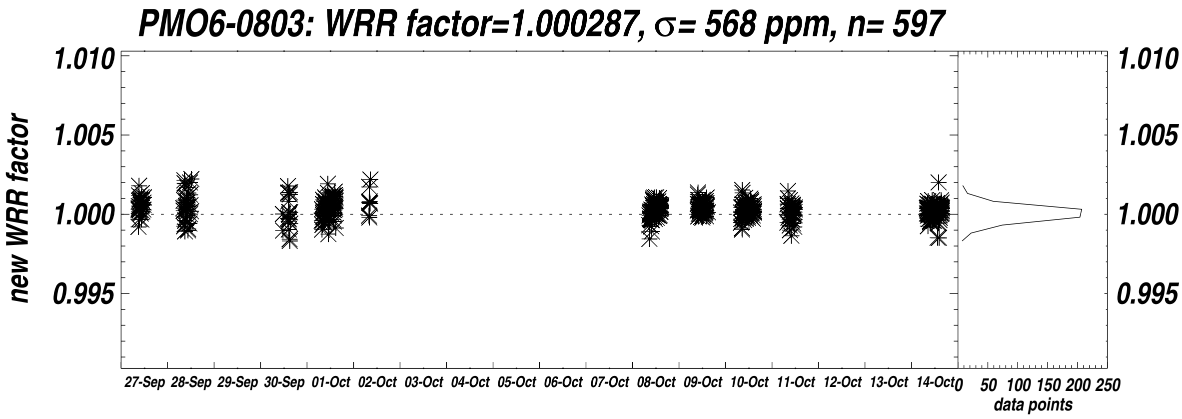
PMO6-0803: WRR factor=1.000287, σ= 568 ppm, n= 597
new WRR factor
1.010
1.005
1.000
0.995
27-Sep 28-Sep 29-Sep 30-Sep 01-Oct 02-Oct 03-Oct 04-Oct 05-Oct 06-Oct 07-Oct 08-Oct 09-Oct 10-Oct 11-Oct 12-Oct 13-Oct 14-Oct
0 50 100 150 200 250
data points

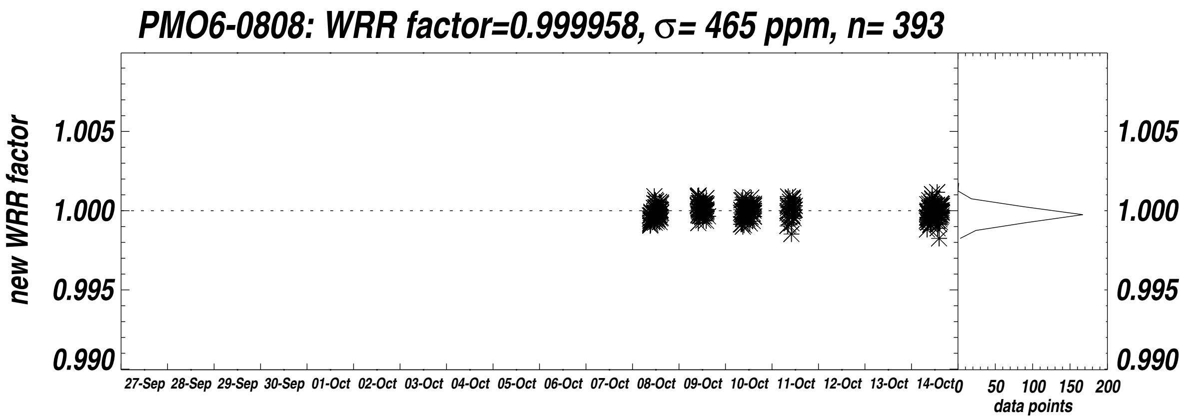
PMO6-0808: WRR factor=0.999958, σ= 465 ppm, n= 393
new WRR factor
1.005
1.000
0.995
0.990
27-Sep 28-Sep 29-Sep 30-Sep 01-Oct 02-Oct 03-Oct 04-Oct 05-Oct 06-Oct 07-Oct 08-Oct 09-Oct 10-Oct 11-Oct 12-Oct 13-Oct 14-Oct
0 50 100 150 200
data points

PMO6-0816: WRR factor=0.999191, σ=1260 ppm, n= 575

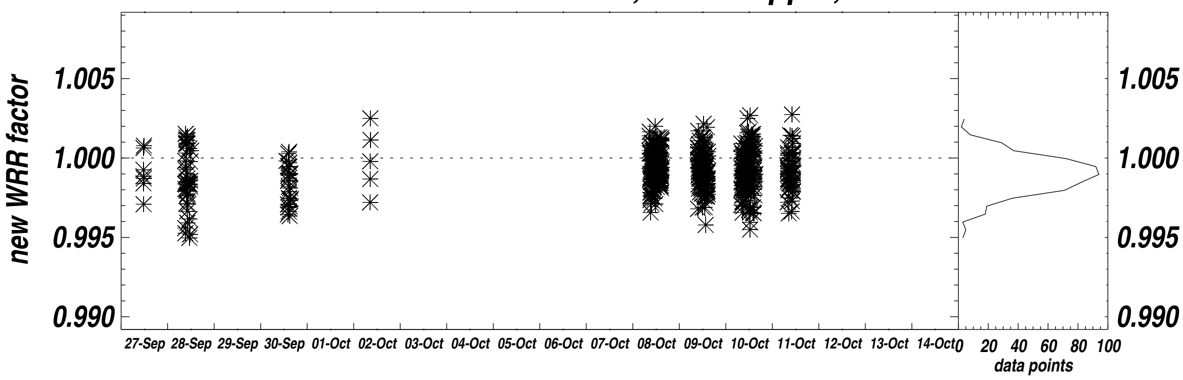

PMO6-0817: WRR factor=0.999957, σ= 762 ppm, n= 941

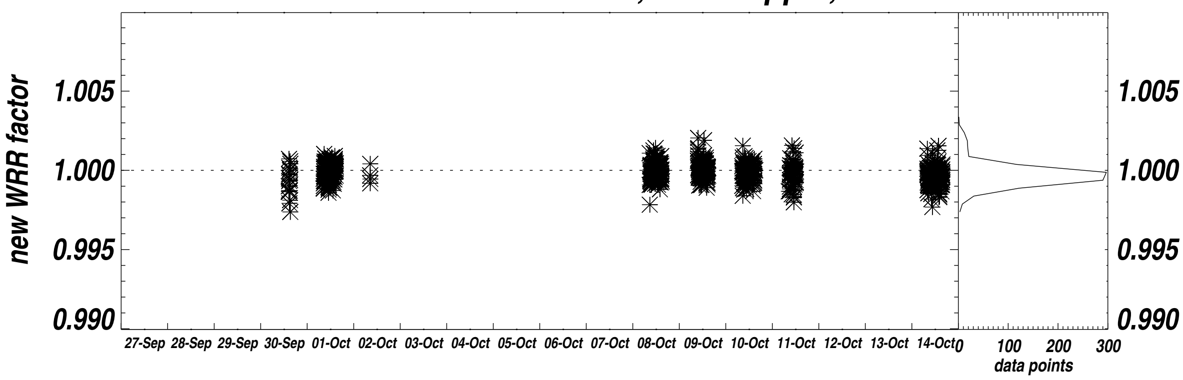

PMO6-1102: WRR factor=0.999367, σ= 802 ppm, n= 777

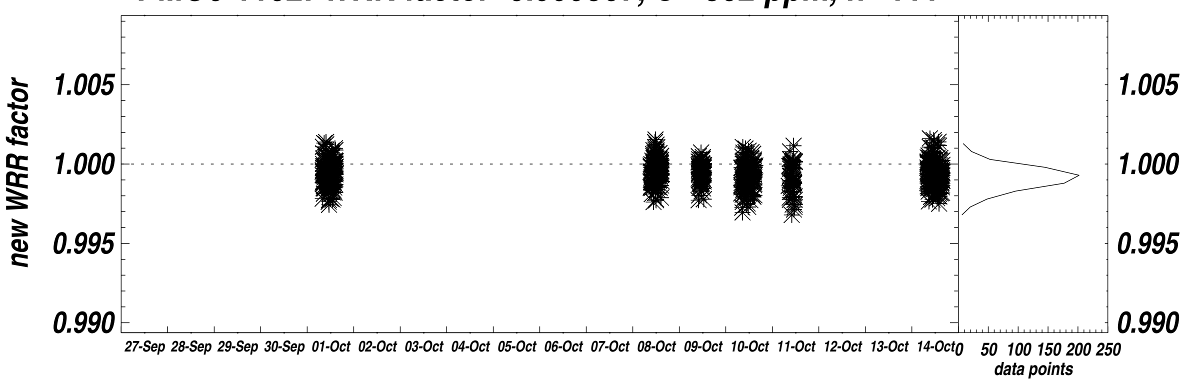

PMO6-1103: WRR factor=0.999661, σ= 557 ppm, n= 596

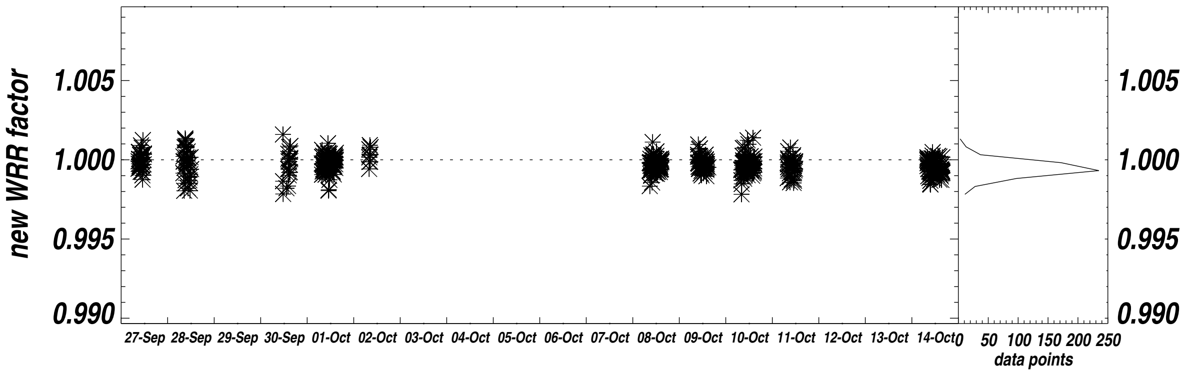

PMO6-1104: WRR factor=1.000427, σ= 881 ppm, n= 580

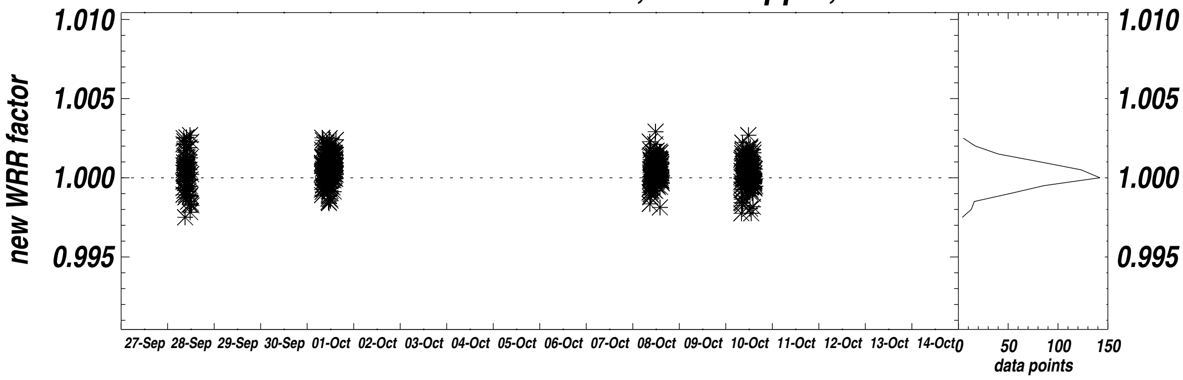

PMO6-1104-L: WRR factor=0.999903, σ=1058 ppm, n= 408

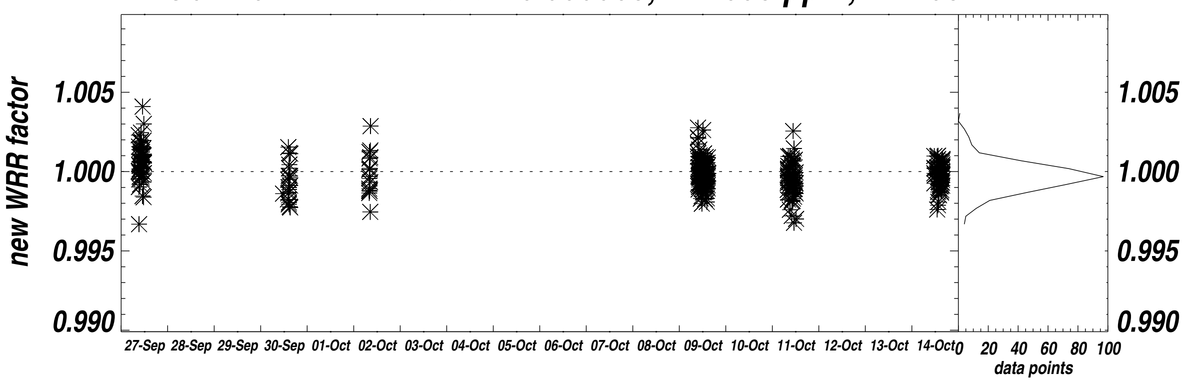

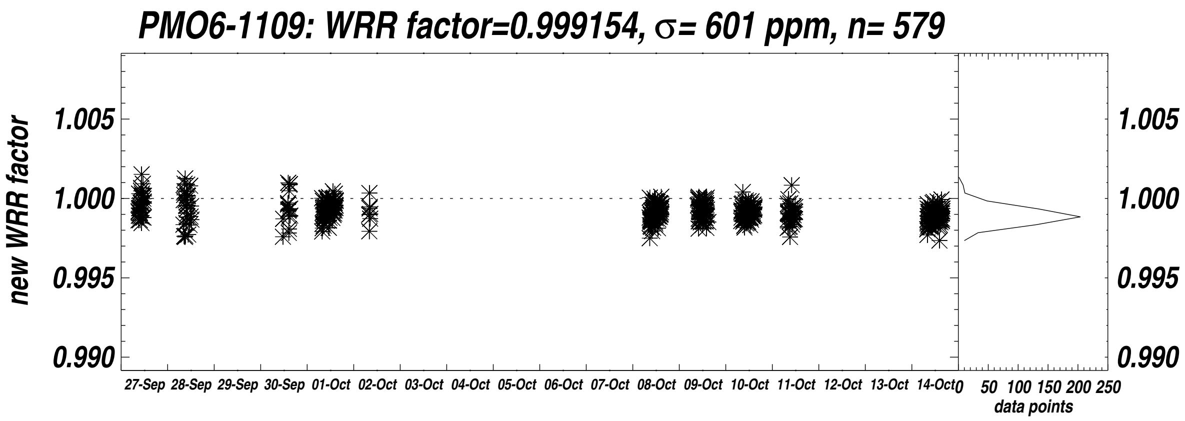
PMO6-1109: WRR factor=0.999154, σ= 601 ppm, n= 579
new WRR factor
1.005
1.000
0.995
0.990
27-Sep 28-Sep 29-Sep 30-Sep 01-Oct 02-Oct 03-Oct 04-Oct 05-Oct 06-Oct 07-Oct 08-Oct 09-Oct 10-Oct 11-Oct 12-Oct 13-Oct 14-Oct
0 50 100 150 200 250
data points

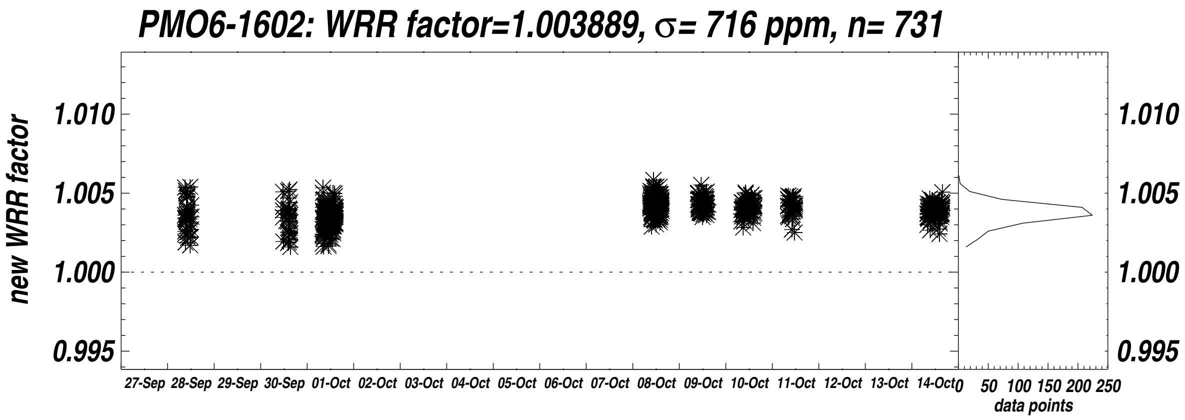
PMO6-1602: WRR factor=1.003889, σ= 716 ppm, n= 731
new WRR factor
1.010
1.005
1.000
0.995
27-Sep 28-Sep 29-Sep 30-Sep 01-Oct 02-Oct 03-Oct 04-Oct 05-Oct 06-Oct 07-Oct 08-Oct 09-Oct 10-Oct 11-Oct 12-Oct 13-Oct 14-Oct
0 50 100 150 200 250
data points

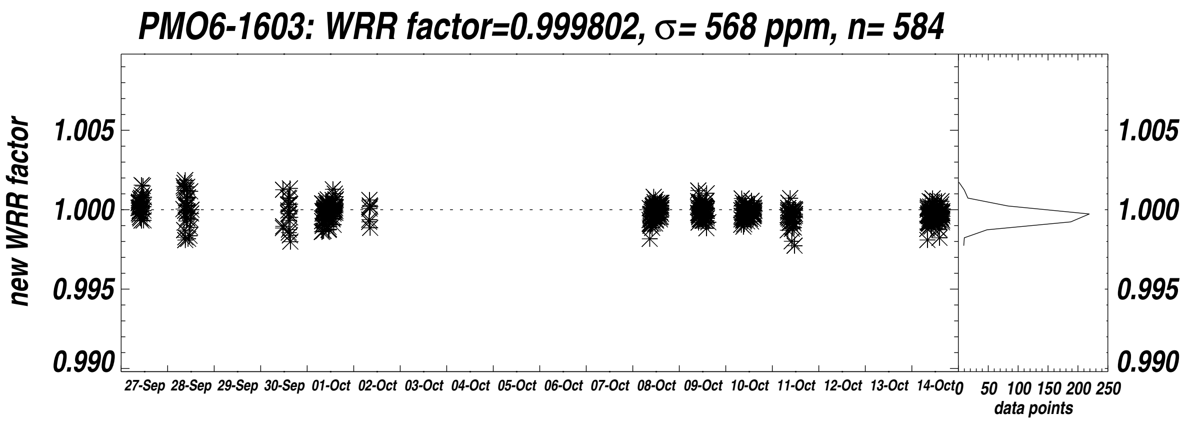
PMO6-1603: WRR factor=0.999802, σ= 568 ppm, n= 584
new WRR factor
1.005
1.000
0.995
0.990
27-Sep 28-Sep 29-Sep 30-Sep 01-Oct 02-Oct 03-Oct 04-Oct 05-Oct 06-Oct 07-Oct 08-Oct 09-Oct 10-Oct 11-Oct 12-Oct 13-Oct 14-Oct
0 50 100 150 200 250
data points

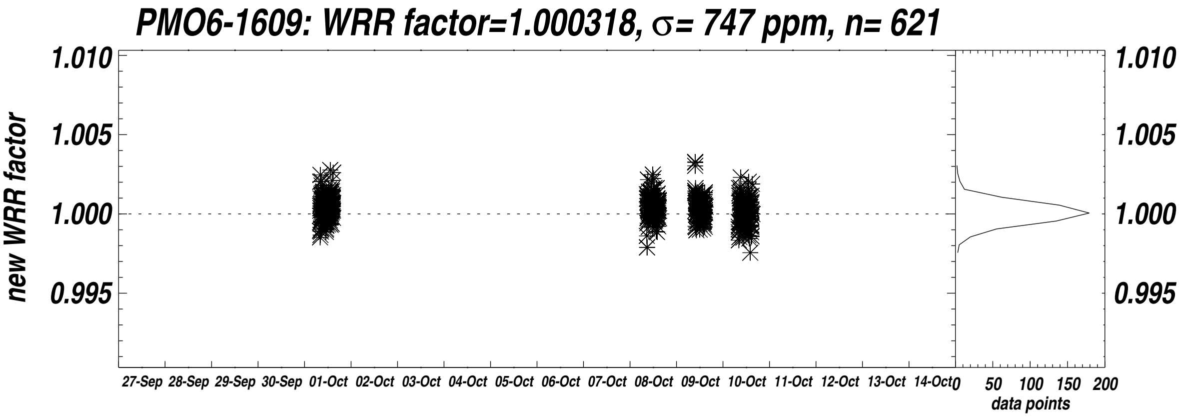
PMO6-1609: WRR factor=1.000318, σ= 747 ppm, n= 621
new WRR factor
1.010
1.005
1.000
0.995
27-Sep 28-Sep 29-Sep 30-Sep 01-Oct 02-Oct 03-Oct 04-Oct 05-Oct 06-Oct 07-Oct 08-Oct 09-Oct 10-Oct 11-Oct 12-Oct 13-Oct 14-Oct
0 50 100 150 200
data points

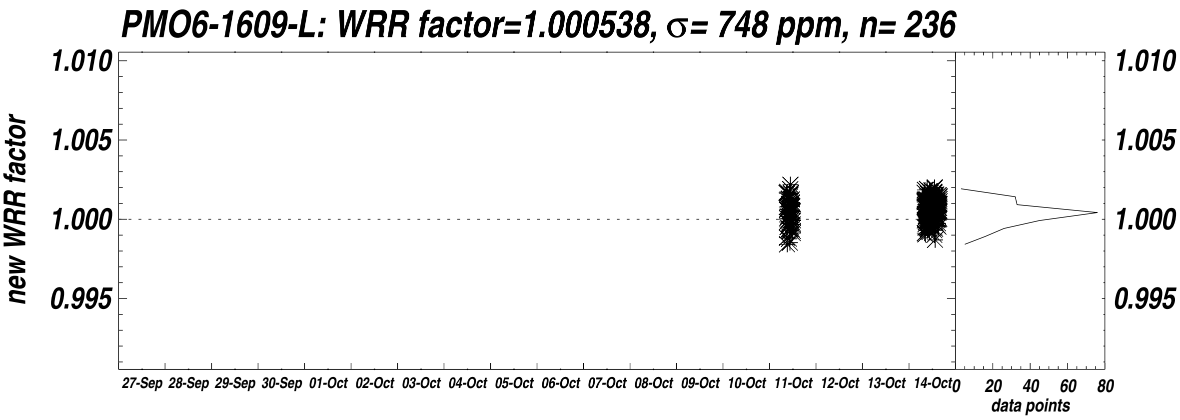
PMO6-1609-L: WRR factor=1.000538, σ= 748 ppm, n= 236
new WRR factor
1.010
1.005
1.000
0.995
27-Sep 28-Sep 29-Sep 30-Sep 01-Oct 02-Oct 03-Oct 04-Oct 05-Oct 06-Oct 07-Oct 08-Oct 09-Oct 10-Oct 11-Oct 12-Oct 13-Oct 14-Oct
0 20 40 60 80
data points

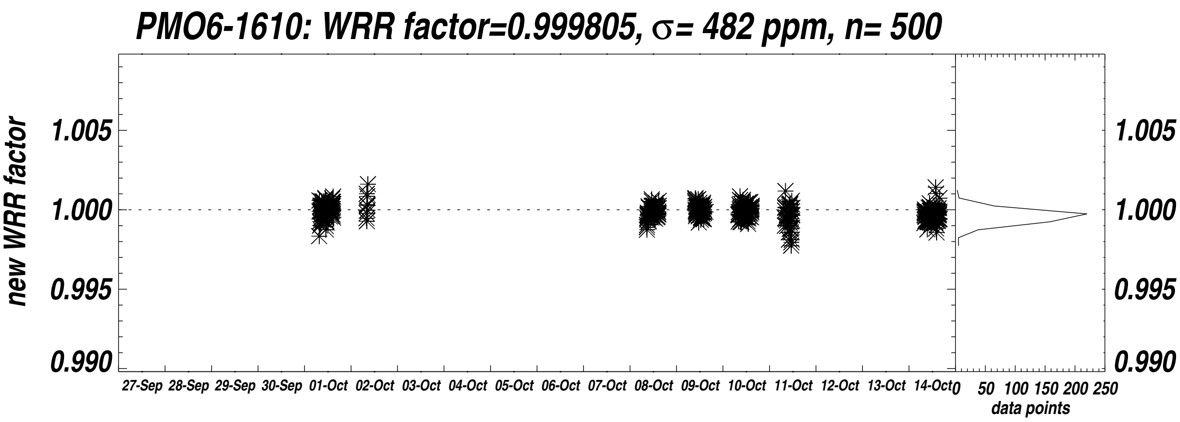
PMO6-1610: WRR factor=0.999805, σ= 482 ppm, n= 500
new WRR factor
1.005
1.000
0.995
0.990
27-Sep 28-Sep 29-Sep 30-Sep 01-Oct 02-Oct 03-Oct 04-Oct 05-Oct 06-Oct 07-Oct 08-Oct 09-Oct 10-Oct 11-Oct 12-Oct 13-Oct 14-Oct
0 50 100 150 200 250
data points

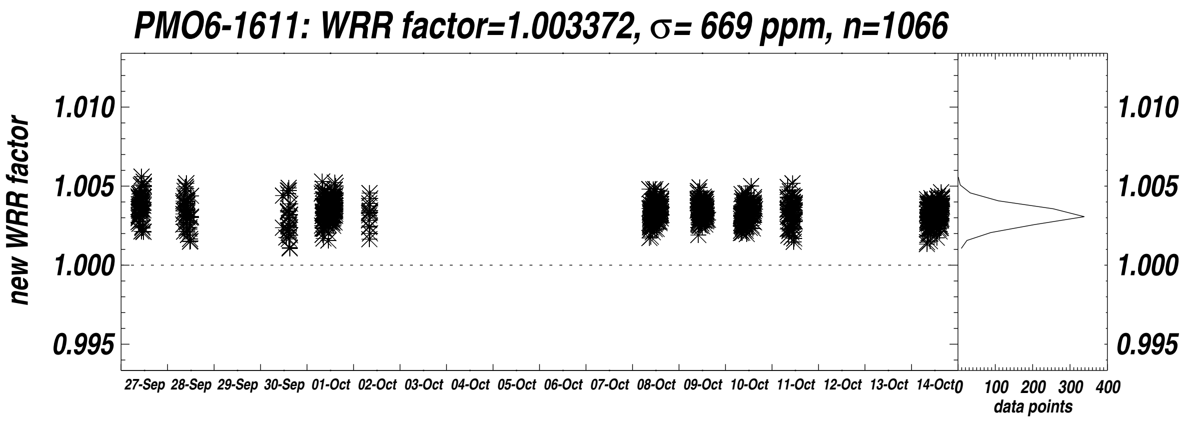
PMO6-1611: WRR factor=1.003372, σ= 669 ppm, n=1066
new WRR factor
1.010
1.005
1.000
0.995
27-Sep 28-Sep 29-Sep 30-Sep 01-Oct 02-Oct 03-Oct 04-Oct 05-Oct 06-Oct 07-Oct 08-Oct 09-Oct 10-Oct 11-Oct 12-Oct 13-Oct 14-Oct
0 100 200 300 400
data points

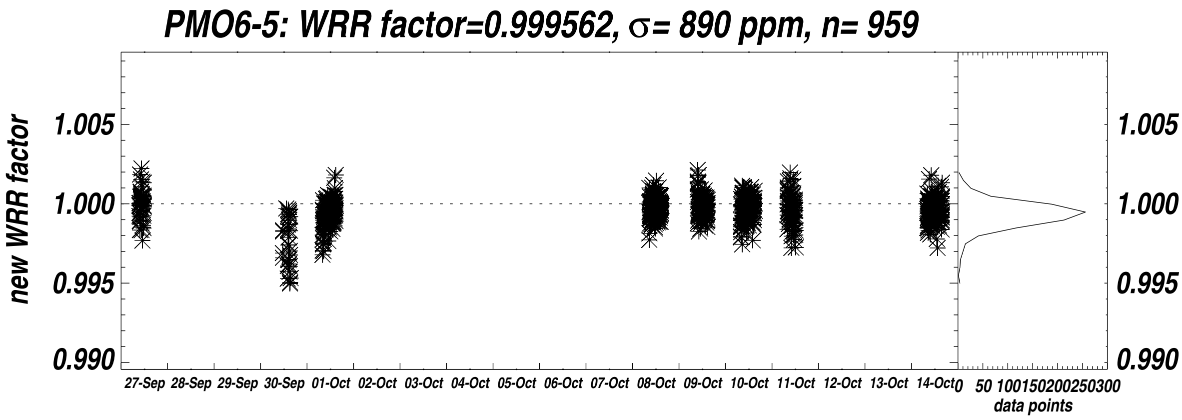
PMO6-5: WRR factor=0.999562, σ= 890 ppm, n= 959
new WRR factor
1.005
1.000
0.995
0.990
27-Sep 28-Sep 29-Sep 30-Sep 01-Oct 02-Oct 03-Oct 04-Oct 05-Oct 06-Oct 07-Oct 08-Oct 09-Oct 10-Oct 11-Oct 12-Oct 13-Oct 14-Oct
0 50 100150200250300
data points

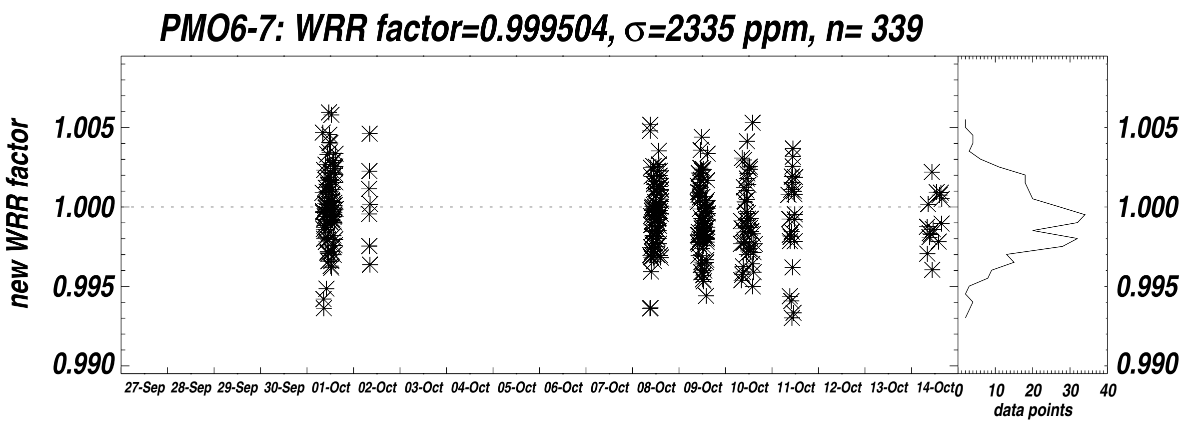
PMO6-7: WRR factor=0.999504, σ=2335 ppm, n= 339
new WRR factor
1.005
1.000
0.995
0.990
27-Sep 28-Sep 29-Sep 30-Sep 01-Oct 02-Oct 03-Oct 04-Oct 05-Oct 06-Oct 07-Oct 08-Oct 09-Oct 10-Oct 11-Oct 12-Oct 13-Oct 14-Oct
0 10 20 30 40
data points

PMO6-79-122: WRR factor=1.002051, σ=2647 ppm, n= 637

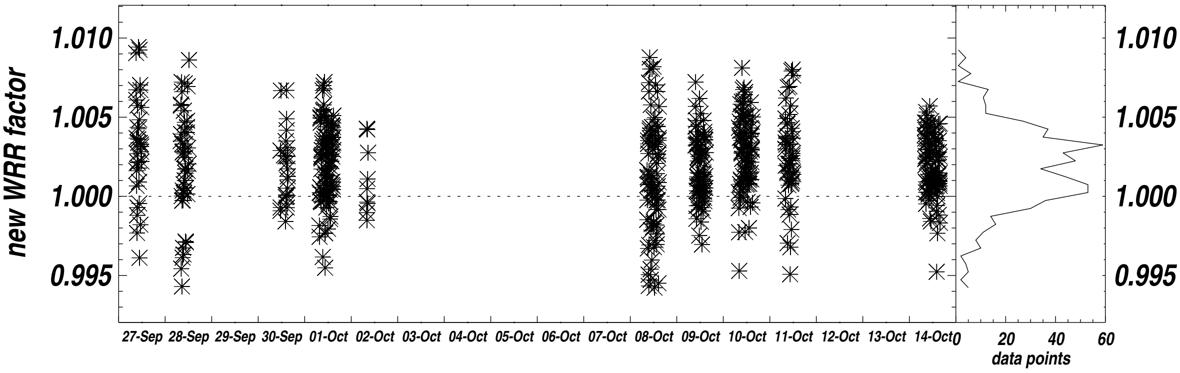

PMO6-81109: WRR factor=0.998599, σ= 706 ppm, n= 872

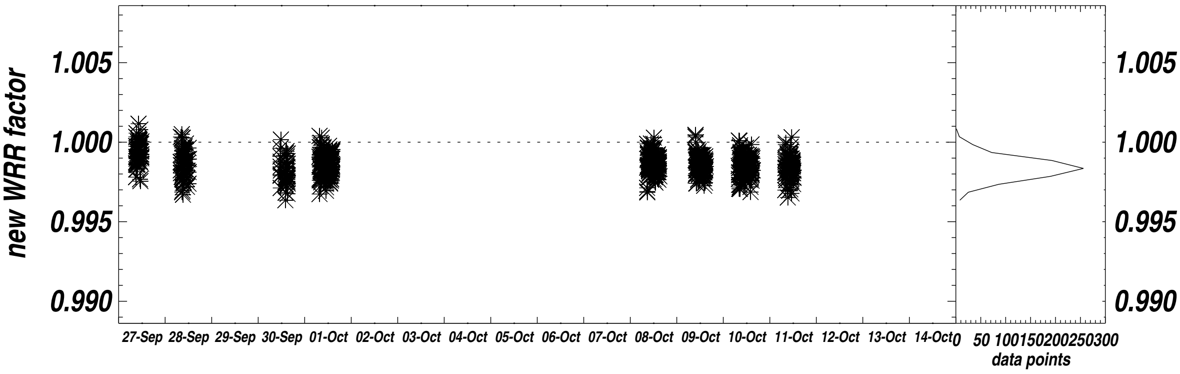

PMO6-911204: WRR factor=1.000612, σ= 871 ppm, n= 862

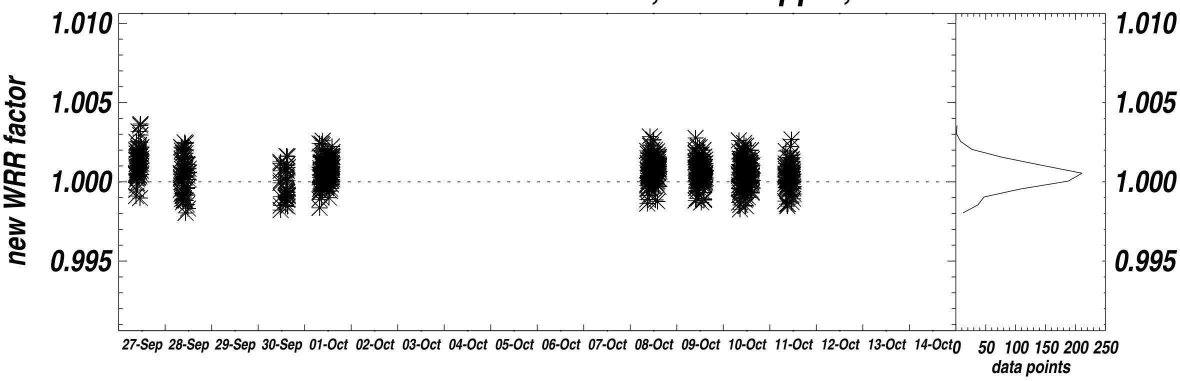

PMO8-F201-001: WRR factor=0.999959, σ= 757 ppm, n= 878

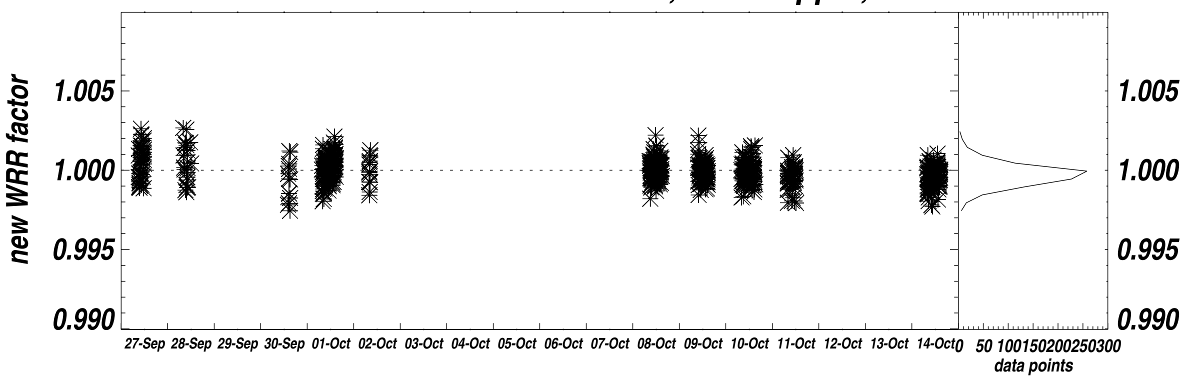

PMO8-F201-002: WRR factor=1.000068, σ= 765 ppm, n= 932

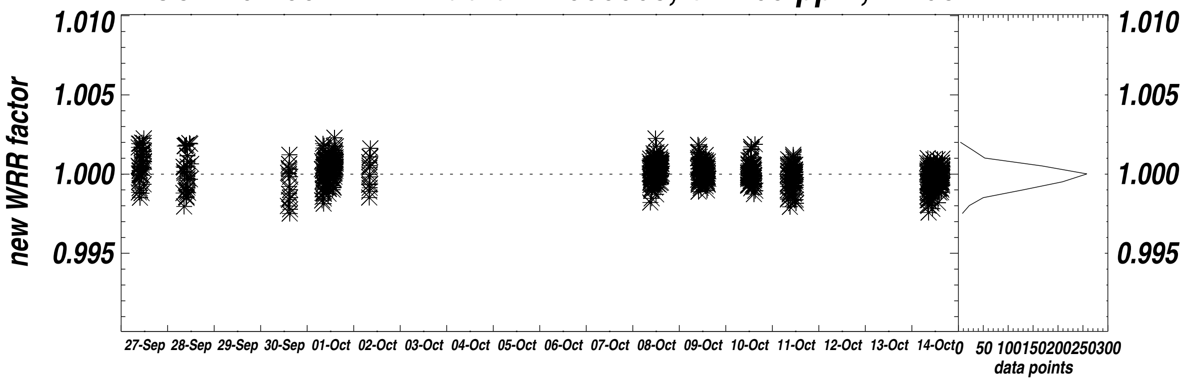

PMO8-F201-006A: WRR factor=1.000082, σ= 702 ppm, n= 947

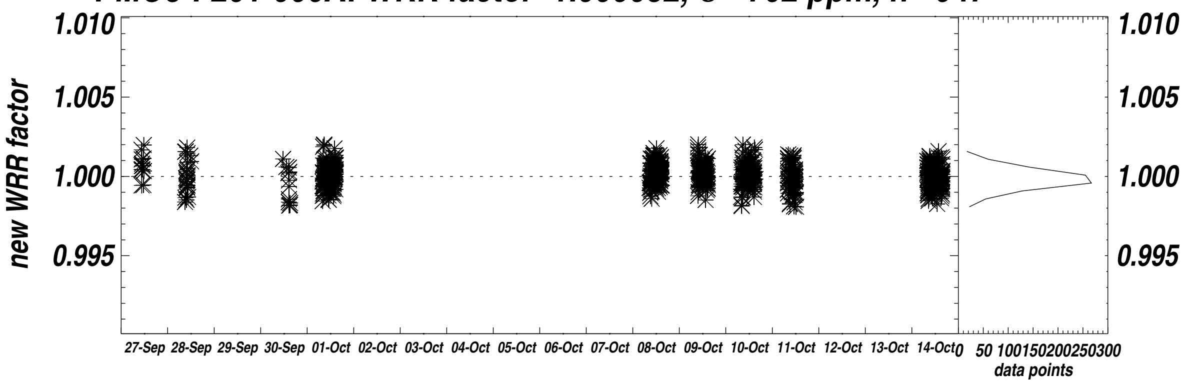

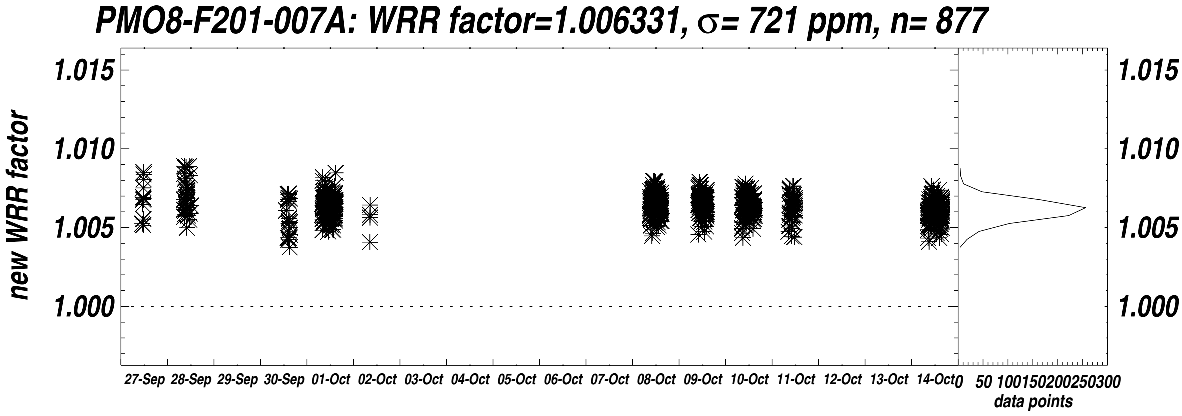
PMO8-F201-007A: WRR factor=1.006331, σ= 721 ppm, n= 877
new WRR factor
1.015
1.010
1.005
1.000
27-Sep 28-Sep 29-Sep 30-Sep 01-Oct 02-Oct 03-Oct 04-Oct 05-Oct 06-Oct 07-Oct 08-Oct 09-Oct 10-Oct 11-Oct 12-Oct 13-Oct 14-Oct
0 50 100 150 200 250 300
data points

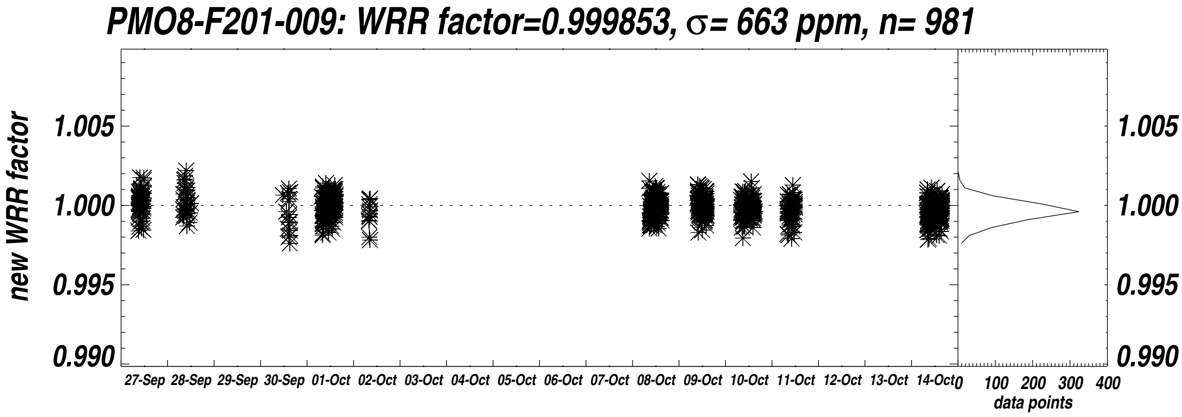
PMO8-F201-009: WRR factor=0.999853, σ= 663 ppm, n= 981
new WRR factor
1.005
1.000
0.995
0.990
27-Sep 28-Sep 29-Sep 30-Sep 01-Oct 02-Oct 03-Oct 04-Oct 05-Oct 06-Oct 07-Oct 08-Oct 09-Oct 10-Oct 11-Oct 12-Oct 13-Oct 14-Oct
0 100 200 300 400
data points

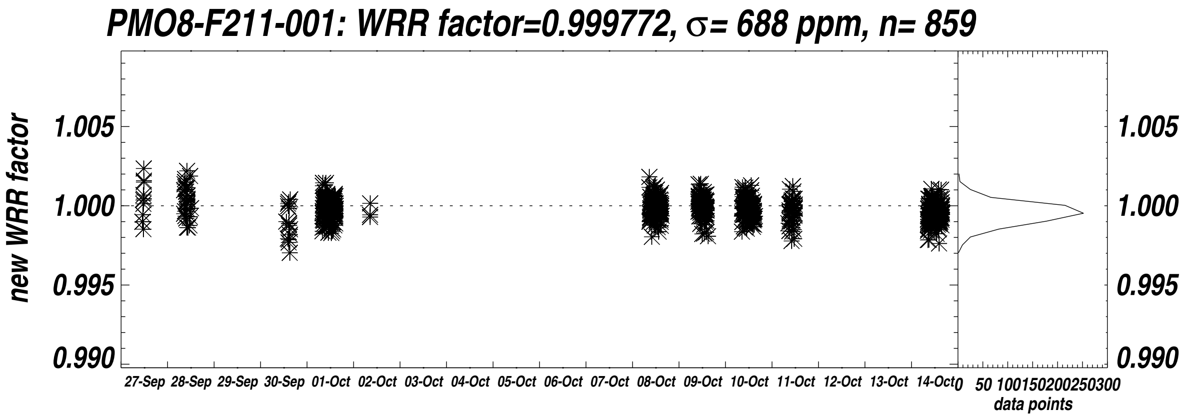
PMO8-F211-001: WRR factor=0.999772, σ= 688 ppm, n= 859
new WRR factor
1.005
1.000
0.995
0.990
27-Sep 28-Sep 29-Sep 30-Sep 01-Oct 02-Oct 03-Oct 04-Oct 05-Oct 06-Oct 07-Oct 08-Oct 09-Oct 10-Oct 11-Oct 12-Oct 13-Oct 14-Oct
0 50 100 150 200 250 300
data points

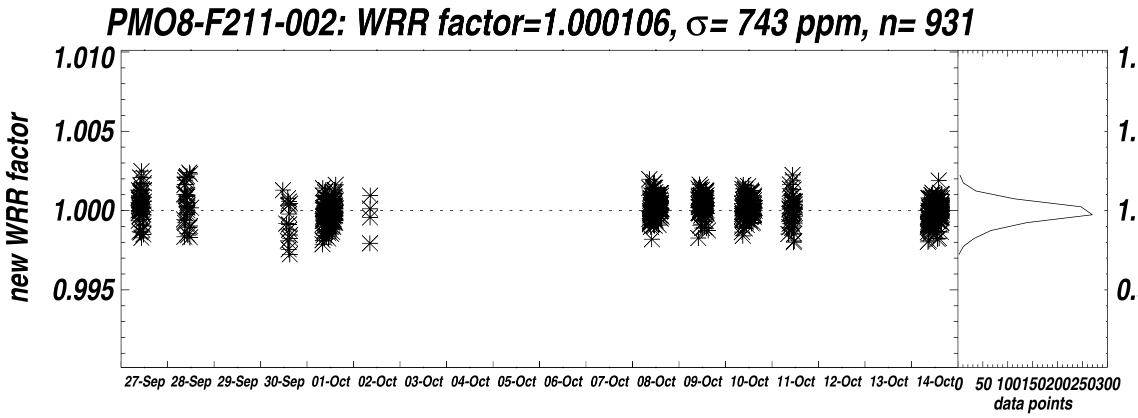
PMO8-F211-002: WRR factor=1.000106, σ= 743 ppm, n= 931
new WRR factor
data points

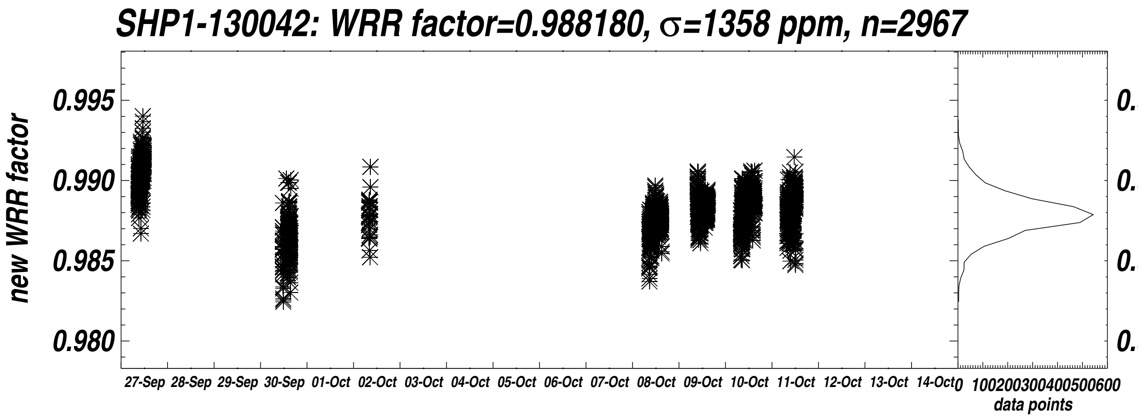
SHP1-130042: WRR factor=0.988180, σ=1358 ppm, n=2967
new WRR factor
data points

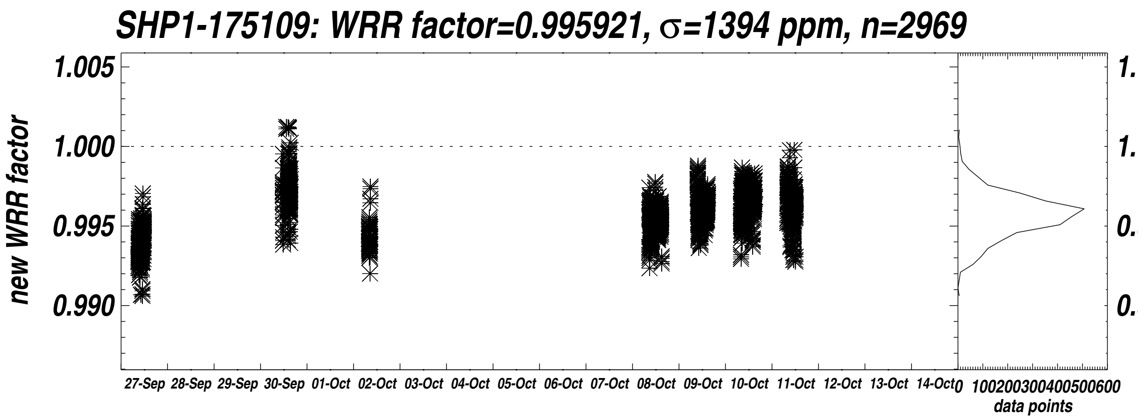
SHP1-175109: WRR factor=0.995921, σ=1394 ppm, n=2969
new WRR factor
data points

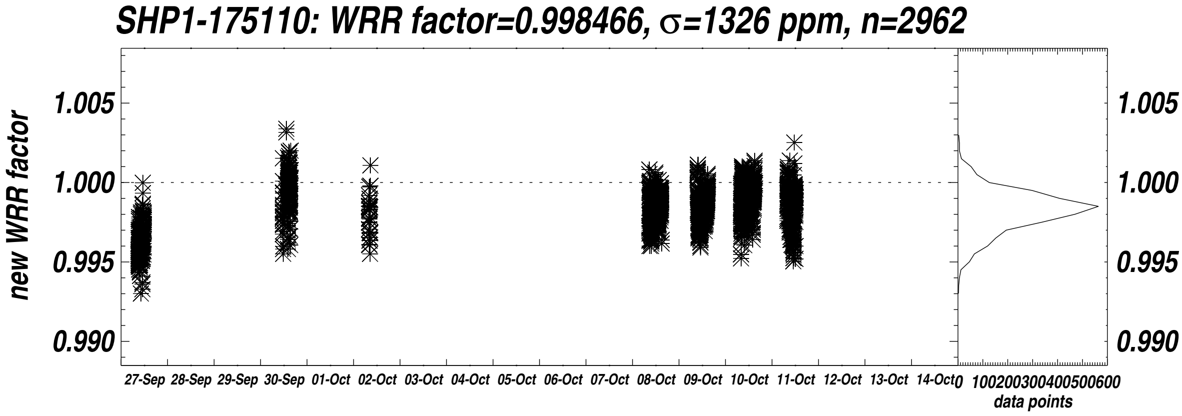
SHP1-175110: WRR factor=0.998466, σ=1326 ppm, n=2962
new WRR factor
1.005
1.000
0.995
0.990
27-Sep 28-Sep 29-Sep 30-Sep 01-Oct 02-Oct 03-Oct 04-Oct 05-Oct 06-Oct 07-Oct 08-Oct 09-Oct 10-Oct 11-Oct 12-Oct 13-Oct 14-Oct
0 100200300400500600
data points

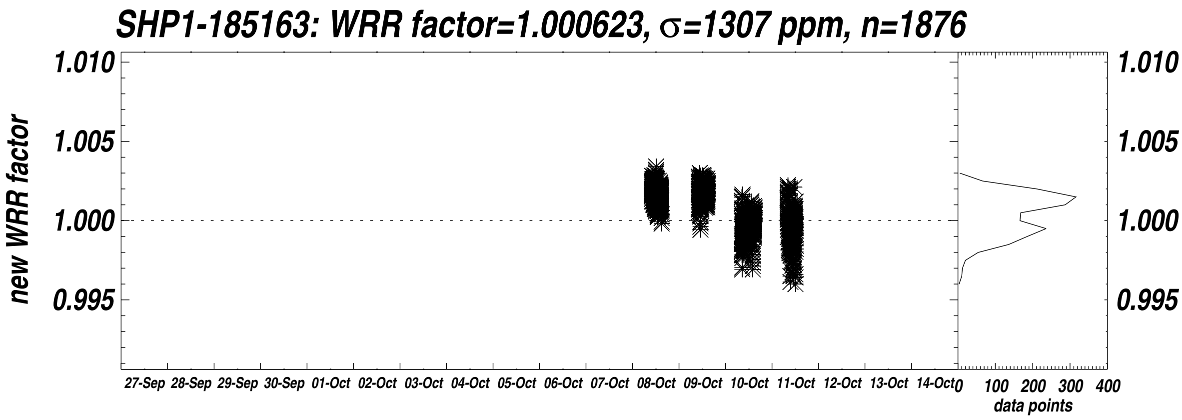
SHP1-185163: WRR factor=1.000623, σ=1307 ppm, n=1876
new WRR factor
1.010
1.005
1.000
0.995
27-Sep 28-Sep 29-Sep 30-Sep 01-Oct 02-Oct 03-Oct 04-Oct 05-Oct 06-Oct 07-Oct 08-Oct 09-Oct 10-Oct 11-Oct 12-Oct 13-Oct 14-Oct
0 100 200 300 400
data points

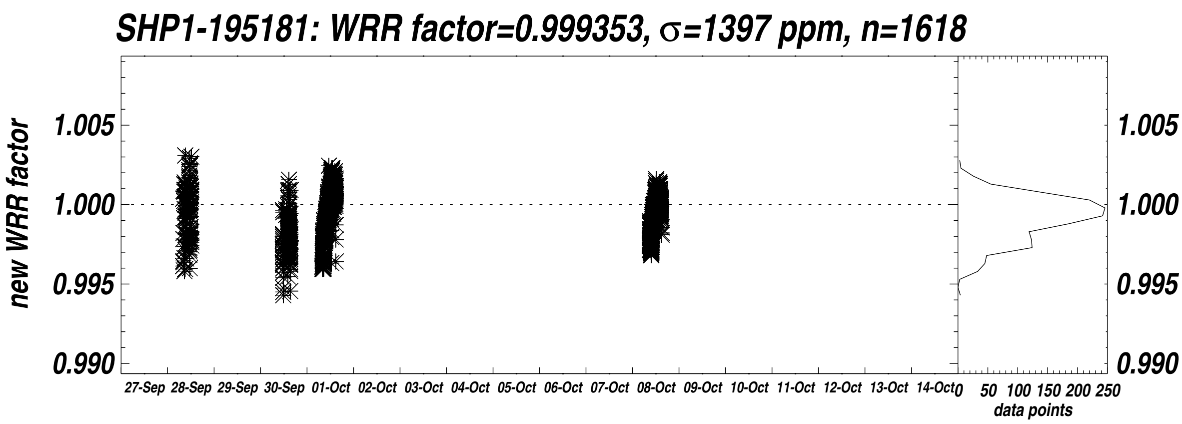
SHP1-195181: WRR factor=0.999353, σ=1397 ppm, n=1618
new WRR factor
1.005
1.000
0.995
0.990
27-Sep 28-Sep 29-Sep 30-Sep 01-Oct 02-Oct 03-Oct 04-Oct 05-Oct 06-Oct 07-Oct 08-Oct 09-Oct 10-Oct 11-Oct 12-Oct 13-Oct 14-Oct
0 50 100 150 200 250
data points

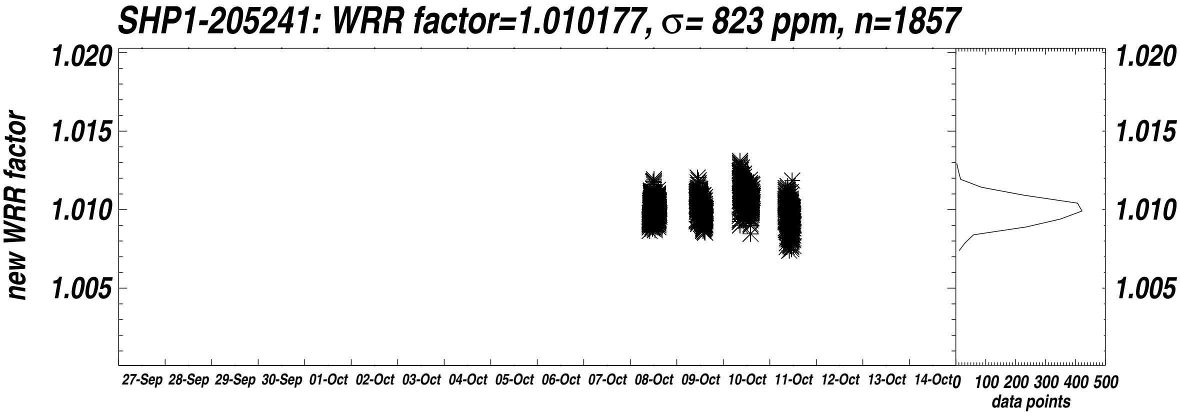
SHP1-205241: WRR factor=1.010177, σ= 823 ppm, n=1857
new WRR factor
1.020
1.015
1.010
1.005
27-Sep 28-Sep 29-Sep 30-Sep 01-Oct 02-Oct 03-Oct 04-Oct 05-Oct 06-Oct 07-Oct 08-Oct 09-Oct 10-Oct 11-Oct 12-Oct 13-Oct 14-Oct
0 100 200 300 400 500
data points

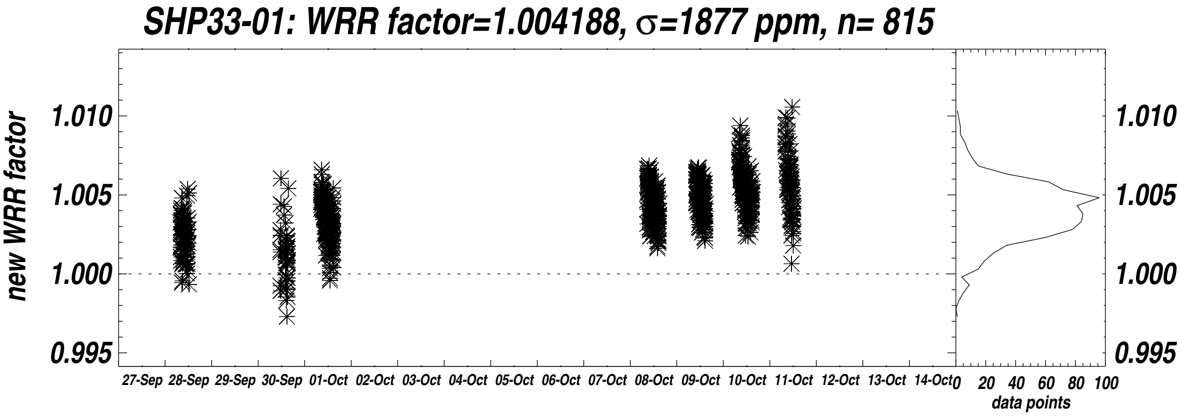
SHP33-01: WRR factor=1.004188, σ=1877 ppm, n= 815
new WRR factor
1.010
1.005
1.000
0.995
27-Sep 28-Sep 29-Sep 30-Sep 01-Oct 02-Oct 03-Oct 04-Oct 05-Oct 06-Oct 07-Oct 08-Oct 09-Oct 10-Oct 11-Oct 12-Oct 13-Oct 14-Oct
0 20 40 60 80 100
data points

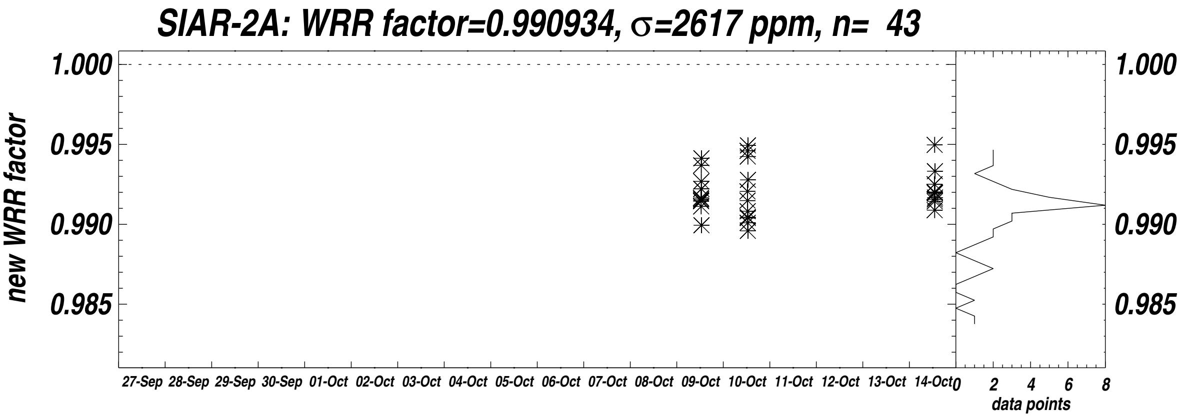
SIAR-2A: WRR factor=0.990934, σ=2617 ppm, n= 43
new WRR factor
1.000
0.995
0.990
0.985
27-Sep 28-Sep 29-Sep 30-Sep 01-Oct 02-Oct 03-Oct 04-Oct 05-Oct 06-Oct 07-Oct 08-Oct 09-Oct 10-Oct 11-Oct 12-Oct 13-Oct 14-Oct
0 2 4 6 8
data points

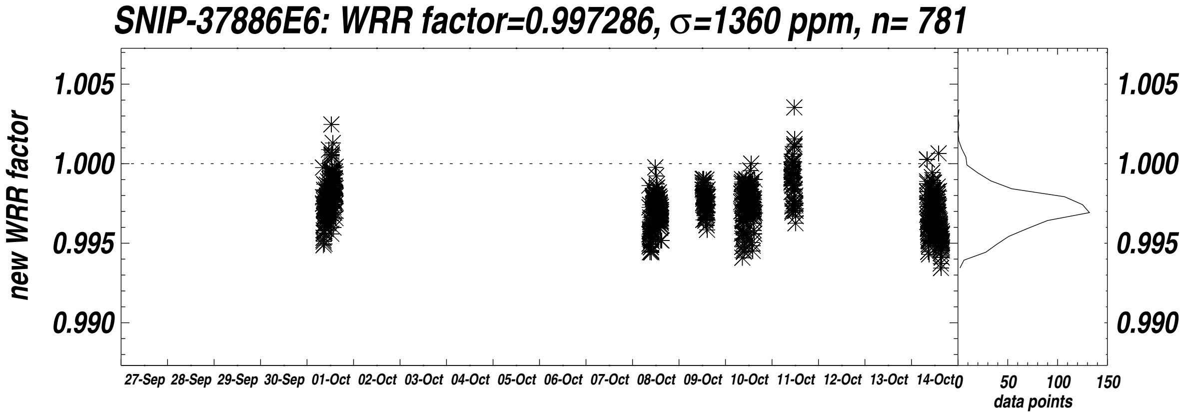
SNIP-37886E6: WRR factor=0.997286, σ=1360 ppm, n= 781
new WRR factor
1.005
1.000
0.995
0.990
27-Sep 28-Sep 29-Sep 30-Sep 01-Oct 02-Oct 03-Oct 04-Oct 05-Oct 06-Oct 07-Oct 08-Oct 09-Oct 10-Oct 11-Oct 12-Oct 13-Oct 14-Oct
0 50 100 150
data points

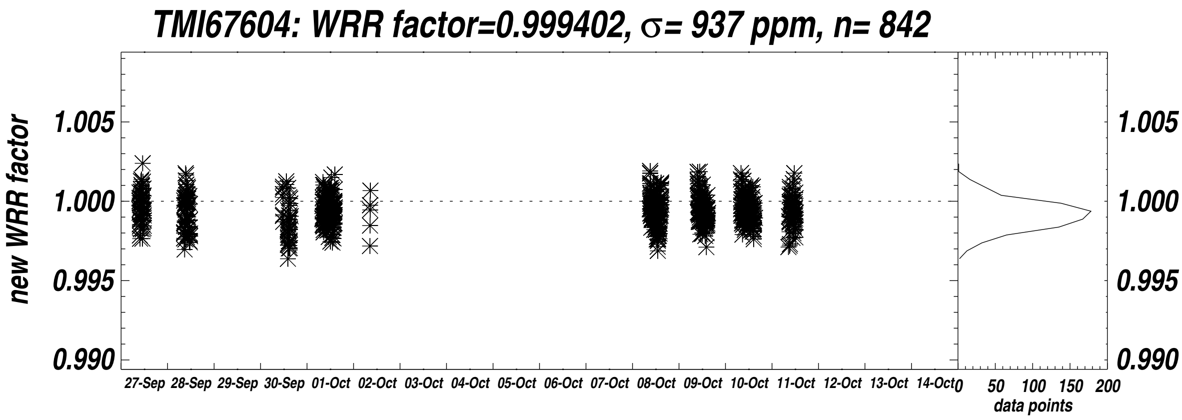
TMI67604: WRR factor=0.999402, σ= 937 ppm, n= 842
new WRR factor
1.005
1.000
0.995
0.990
27-Sep 28-Sep 29-Sep 30-Sep 01-Oct 02-Oct 03-Oct 04-Oct 05-Oct 06-Oct 07-Oct 08-Oct 09-Oct 10-Oct 11-Oct 12-Oct 13-Oct 14-Oct
0 50 100 150 200
data points

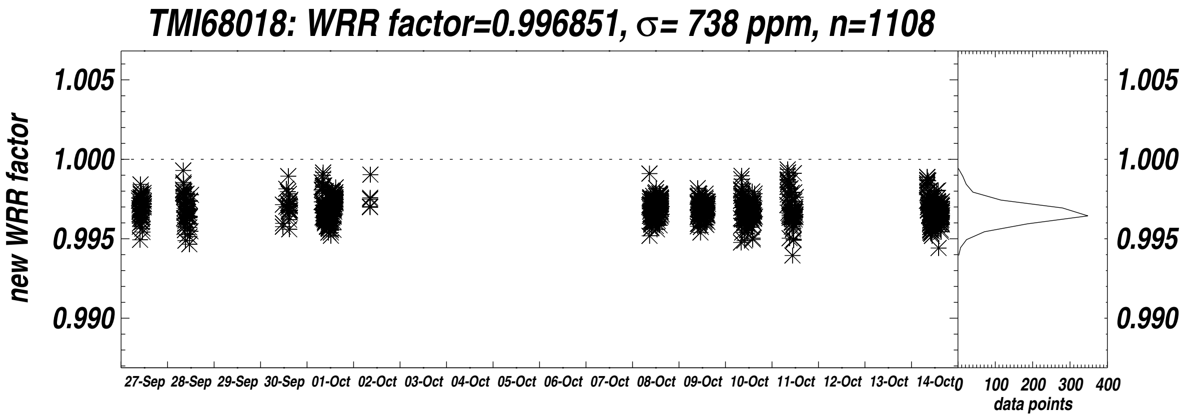
TMI68018: WRR factor=0.996851, σ= 738 ppm, n=1108
new WRR factor
1.005
1.000
0.995
0.990
27-Sep 28-Sep 29-Sep 30-Sep 01-Oct 02-Oct 03-Oct 04-Oct 05-Oct 06-Oct 07-Oct 08-Oct 09-Oct 10-Oct 11-Oct 12-Oct 13-Oct 14-Oct
0 100 200 300 400
data points

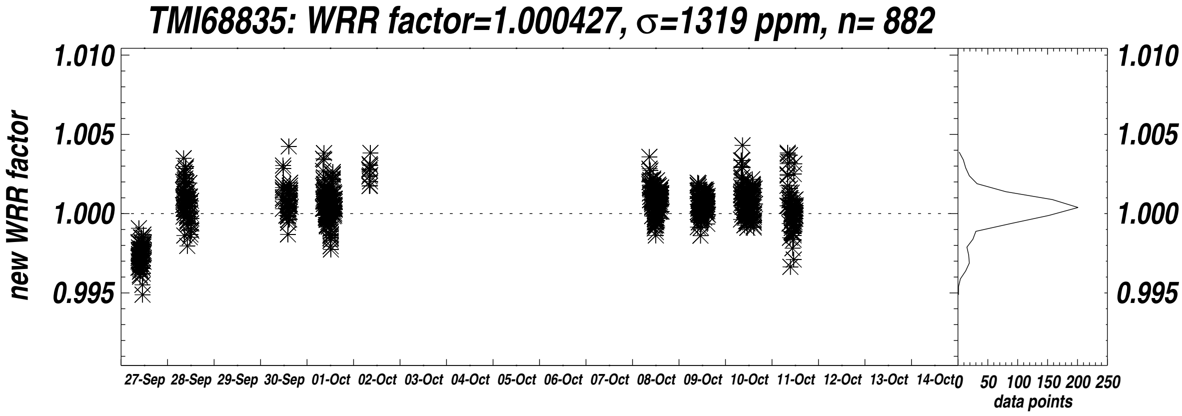
TMI68835: WRR factor=1.000427, σ=1319 ppm, n= 882
new WRR factor
1.010
1.005
1.000
0.995
27-Sep 28-Sep 29-Sep 30-Sep 01-Oct 02-Oct 03-Oct 04-Oct 05-Oct 06-Oct 07-Oct 08-Oct 09-Oct 10-Oct 11-Oct 12-Oct 13-Oct 14-Oct
0 50 100 150 200 250
data points

Chapter 4 Auxiliary Data

The wind speed and AOD measurements were used for selecting valid data points (cf. Sect. 2.1). Meteorological parameters and irradiance levels are plotted for reference only.

4.1 Direct and Diffuse Irradiance

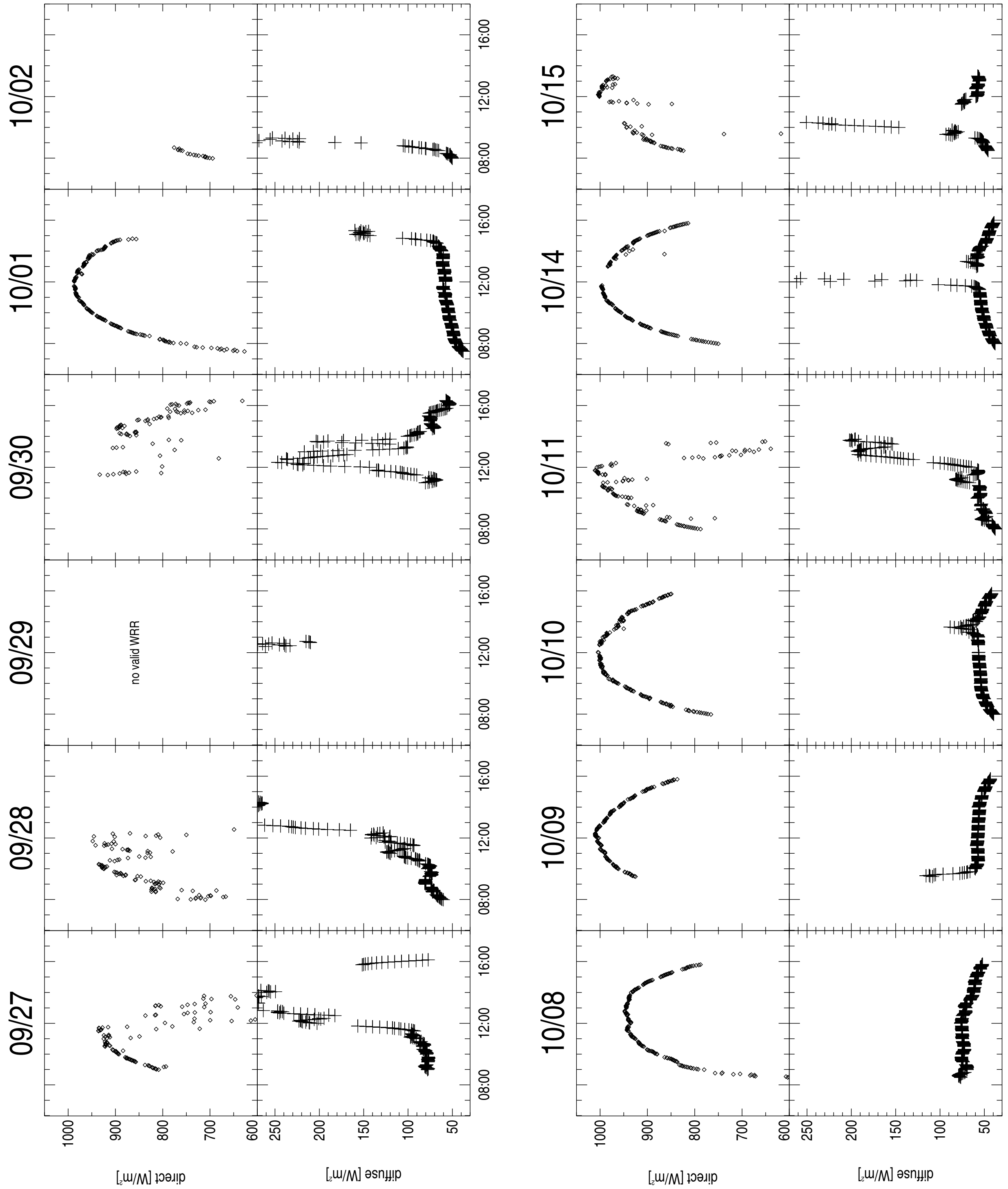

Direct (WRR) and diffuse irradiance (shaded K&Z CM22 S/N 020059).

4.2 Airmass and Aerosol Optical Depth (AOD)

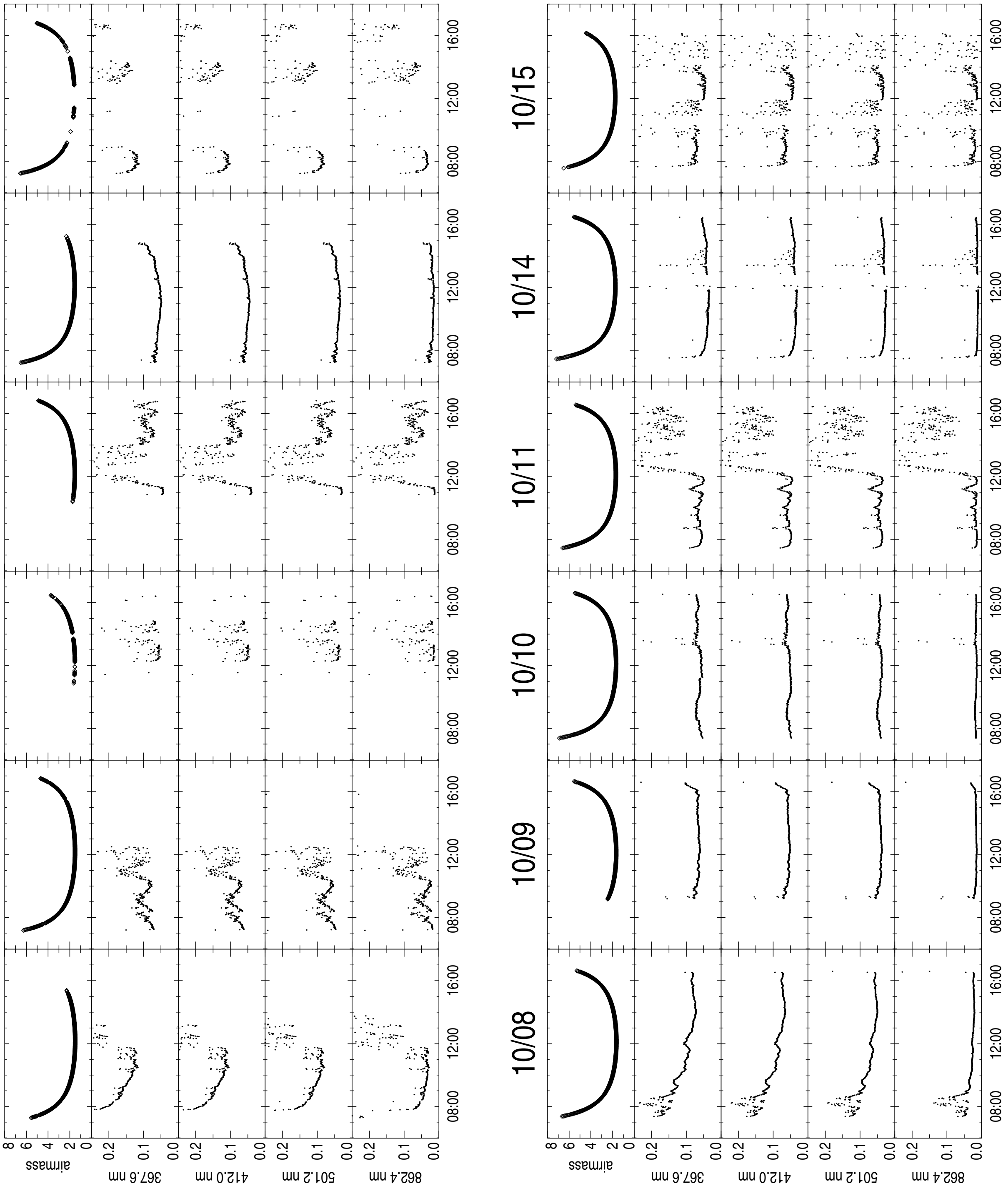

A four-channel Precision Filter Radiometer (PFR) was used to determine AOD.

4.3 Wind Speed

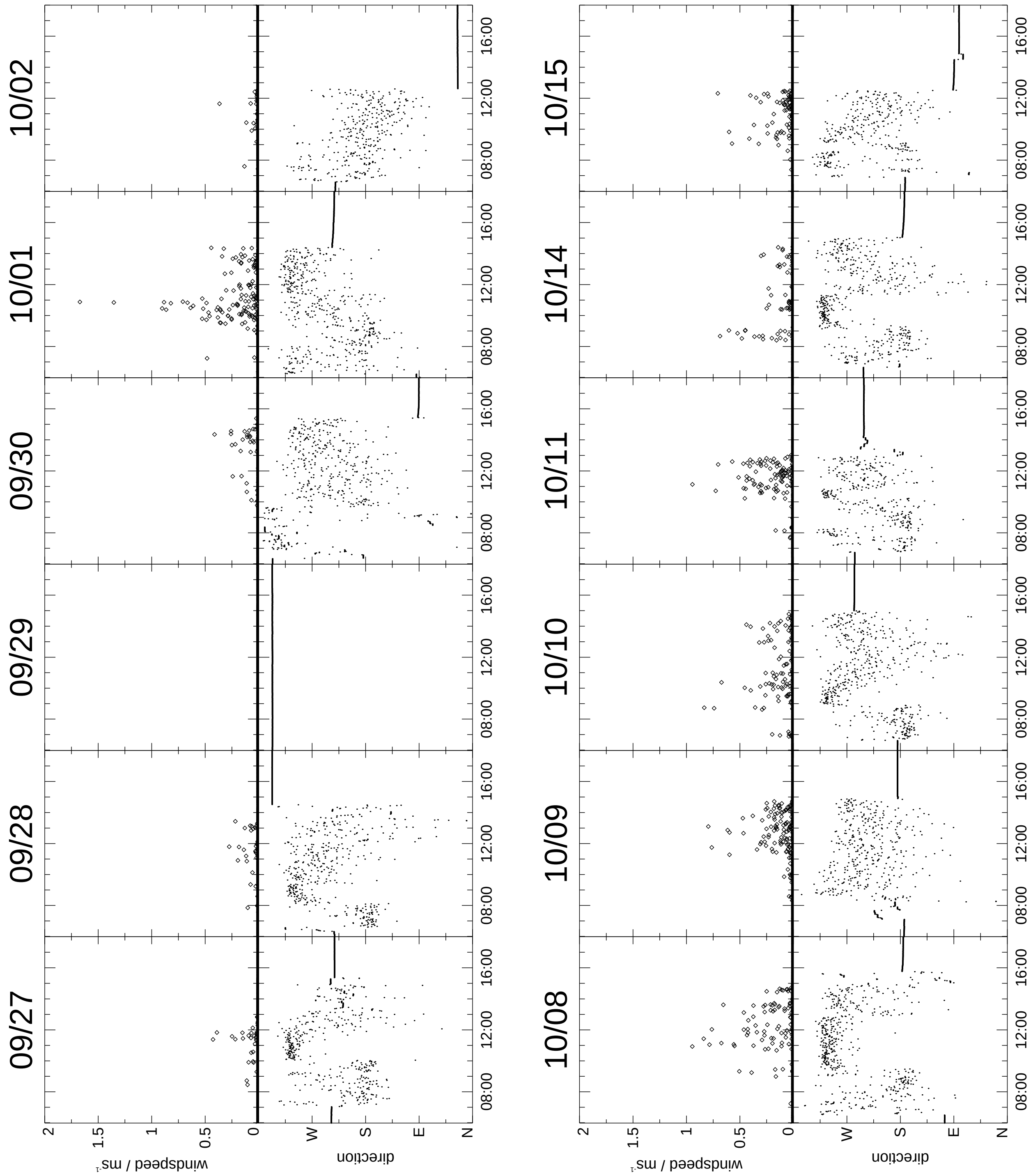

The wind speed and direction above the WSG tracker.

4.4 Meteorological Data

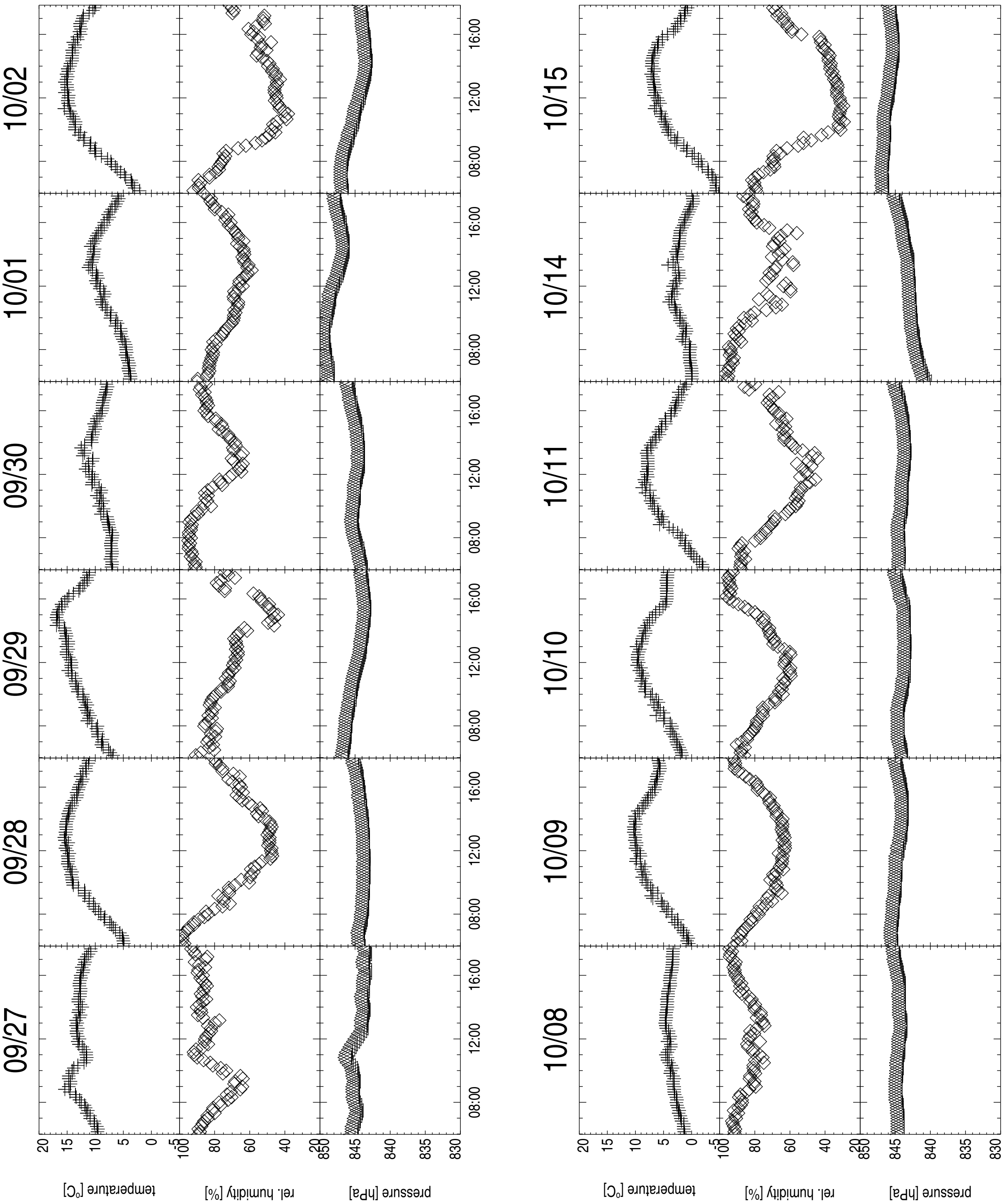

Meteorological parameters measured by the SwissMetNet Davos station of MeteoSwiss (adjacent to IPC-XIII measuring field).

Chapter 5 Symposium

5.1 To Build and Share Knowledge

On cloudy, overcast, or rainy days when no measurements were possible the IPC-XIII symposium was held. Radiation experts from PMOD/WRC as well as many IPC-XIII participants presented their work and/or national radiation infrastructure in order to share and build knowledge.

All presentations are publicly accessable on https://community.wmo.int/publications-and-iom-reports/ipc-xiii-proceedings [8].

Chapter 6 Supplementary Information

6.1 Addresses of Participants

AlAdwani Abdullah
King Abdullah City for Atomic And Renewable Energy
Saudi Arabia - Riyadh
2022 Riyadh
Saudi Arabia
email: a.adwani@energy.gov.sa

AlQahtani Saad
King Abdullah City for Atomic And Renewable Energy
Saudi Arabia - Riyadh
2022 Riyadh
Saudi Arabia
email: s.qahtani@energy.gov.sa
phone: 966507441114

Amand Julien
RMIB
Av. Circulaire 3
1180 Brussels
Belgium
email: julien.amand@meteo.be

Andersson Anne
RISE Research Institute of Sweden
Brinellgatan 4, Box 857
50115 Borås
Sweden
email: anne.andersson@ri.se
phone: '+46703749944

Andreas Afshin
National Renewable Energy Laboratory (NREL)
15013 Denver West Parkway
80401 Golden
USA
email: afshin.andreas@nrel.gov

BEN MOHAMMED MOHAMED ELOUALID
Office National de la METEOROLOGIE
P.O BOX 31 METEO Tamanrasset 11000 ALGERIA
11000 TAMANRASSET
ALGERIA
email: dmrstam11@gmail.com
phone: 213667429778

Büchel Valeria
Davos Instruments AG
Am Kurpark 3
7270 Davos Platz
Switzerland
email: valeria.buechel@davos-instruments.ch

Balenzategui Jose
CIEMAT
Avenida Complutense, 40
28040 MADRID
Spain
email: jl.balenzategui@ciemat.es
phone: '+34 91 496 2509

Barreto Africa
Izaña Atmospheric Research Center (AEMET)
Calle La Marina no 20
38001 Santa Cruz de Tenerife
Spain
email: abarretov@aemet.es
phone: 0034 922151718

Becker Ralf
Deutscher Wetterdienst / Meteorologisches Observatorium Lindenberg (DWD/MOL-RAO)
Am Observatorium 12
15248 Tauche, OT: Lindenberg
Germany
email: ralf.becker@dwd.de

BinDayil Abdulhakim
King Abdullah City for Atomic And Renewable Energy
Saudi Arabia - Riyadh
2022 Riyadh
Saudi Arabia
email: a.bindayil@energy.gov.sa

Buchli Jon
Davos Instruments AG
Am Kurpark 3
7270 Davos Platz
Switzerland
email: jon.buchli@davos-instruments.ch

Carlund Thomas
Swedish Meteorological and Hydrological Institute (SMHI)
Folkborgsvägen 17
60176 Norrköping
Sweden
email: thomas.carlund@smhi.se
phone: '+46114958229

Chevalier André
RMIB (part-2)
Av circulaire 3
1180 Brussels
Belgium
email: andy@meteo.be

Conscience Christian
RMIB
Av. Circulaire 3
1180 Brussels
Belgium
email: cch@meteo.be

Cordero Raúl
Universidad de Santiago de Chile
Av. Libertador Bernardo O'Higgins 3363
9170022 Santiago
Chile
email: raul.cordero@usach.cl

Donkers Chiel
Hukseflux Thermal Sensors B.V.
Delftechpark 31
2628XJ Delft
The Netherlands
email: chiel@hukseflux.com

Doppler Lionel
Deutscher Wetterdienst / Meteorologisches Observatorium Lindenberg (DWD/MOL-RAO)
Am Observatorium 12
15248 Tauche, OT: Lindenberg
Germany
email: lionel.doppler@dwd.de

Essnid Akram
Libyan Center for Solar Energy Research and Studies
Sidi Abdulkareem St, Tajora, Tripoli, Libya
218 Tripoli
Libya
email: sneeda74@yahoo.com
phone: 218918998566

Friedrich Dirk
Physikalisch-Technische Bundesanstalt
Bundesallee 100
38116 Braunschweig
Deutschland
email: dirk.friedrich@ptb.de
phone: 495315924141

Galleano Roberto
3, Via Santorre die Santarosa
10064 Pinerolo
Italy
email: roberto.galleano@protonmail.com
phone: +39 3333225876

Gonzalez Adriana Elizabeth
Universidad Nacional Autónoma de México
Av. Universidad 3000
4510 Mexico City
Mexico
email: gonzalezc@igeofisica.unam.mx
phone: +52 5556224139

Gotseff Peter
National Renewable Energy Laboratory (NREL)
15013 Denver West Parkway
80401 Golden
USA
email: Peter.Gotseff@nrel.gov

Hendriks Hendrik
KNMI
PO Box 201
3730 AE De Bilt
Netherlands
email: izzy.hendriks@knmi.nl

Hiscock David
Met Office
Met Office, FitzRoy Road
EX1 3PB Exeter
UK
email: david.hiscock@metoffice.gov.uk

Hoogendijk Kees
EKO Instruments Europe B.V.
Lulofsstraat 55, u28
2521 AL Den Haag
Netherlands
email: kees.hoogendijk@eko-eu.com

Iakovlev Vladislav
Voeikov Main Geophysical Observatory (Voeikov MGO)
Karbysheva st. 7
194021 St. Petersburg
Russian Federation
email: vadosprod@gmail.com

Jensen Adam
Technical University of Denmark, Kgs. Lyngby
Brovej, building 118
2800 Kgs. Lyngby
Denmark
email: arajen@byg.dtu.dk
phone: +4552747411

Jorquera José
Universidad de Santiago de Chile
Av. Libertador Bernardo O'Higgins 3363
Santiago
Chile
email: jorqueratorres@gmail.com

Källberg Stefan
RISE Research Institute of Sweden
Brinellgatan 4, Box 857
50115 Borås
Sweden
email: stefan.kallberg@ri.se

Kalantan Abdullah
King Abdullah City for Atomic And Renewable Energy
Saudi Arabia - Riyadh
2022 Riyadh
Saudi Arabia
email: s.qahtani@energy.gov.sa

Khaled Wael
Egyptian Meteorological Authority (EMA)
El Khalifa El Maamoun Street - Kobri El kobba
11321 Cairo
Egypt
email: wael.khaled@gmail.com
phone: +201006072166

Kirk Tom
The Eppley Laboratory, Inc.
12 Sheffield Avenue
2871 Newport
United States
email: info@eppleylab.com
phone: 4018471020

Knap Wouter
KNMI
PO Box 201
3730 AE De Bilt
Netherlands
email: wouter.knap@knmi.nl
phone: +31646254013

Konings Jörgen
Hukseflux Thermal Sensors B.V.
Delftechpark 31
2628XJ Delft
The Netherlands
email: jorgen@hukseflux.com

Laguarda Agustín
Laboratorio de Energía Solar, Universidad de la República.
Av. Luis Batlle Berres km 508 (ex-Ruta 3), Salto Grande
50000 Salto
Uruguay
email: agu.laguarda@gmail.com
phone: +59899123346

Lindgren Mikael
RISE Research Institute of Sweden
Brinellgatan 4, Box 857
50115 Borås
Sweden
email: mikael.lindgren@ri.se

Müllejans Harald
European Commission - DG JRC - Directorate C - Energy, Transport and Climate
Building 45, TP450 , Via Fermi, 2749
I-21027 Ispra (Va)
ITALY
email: harald.muellejans@ec.europa.eu

Malcorps Pierre
RMIB (part-2)
Av circulaire 3
1180 Brussels
Belgium
email: pierre.malcorps@meteo.be

McGee Major
ATLAS Material Testing Technology LLC
45601 North 47th Ave.,
85087-7042 Phoenix
United States
email: major.mcgee@ametek.com
phone: 1 (843) 230-7802

Mes Joop
Kipp & Zonen (Ott hydromet)
Delftechpark 36
2628XH Delft
The Netherlands
email: joop.mes@otthydromet.com
phone: +31-628638174

Miklavžina Iztok
Slovenian Environment Agency
Vojkova 1b
1000 Ljubljana
Slovenia
email: iztok.miklavzina@gov.si

Molema Tijmen
KNMI
PO Box 201
3730 AE De Bilt
Netherlands
email: tijmen.molema@knmi.nl

Nagel Erik
Kipp & Zonen (Ott hydromet)
Delftechpark 36
2628XH Delft
The Netherlands
email: erik.nagel@otthydromet.com

Naranen Erik
ISO-Cal North America
36610 N 20th Street
Arizona, 85086 Phoenix
United States
email: enaranen@isocalnorthamerica.com
phone: 001+623-693-2153

Nelson Donald
Eppley Laboratory
6136 Misty Way, Longmont CO 80503, United States
80503 Longmont
United States
email: donaldnelson@mac.com
phone: 1 3037750443

Nevens Stijn
RMIB
Av. Circulaire 3
1180 Brussels
Belgium
email: stijn.nevens@meteo.be
phone: +32 (0) 485 50 38 44

Ohkubo Kazuhiko
ISHIKAWA TRADING CO., LTD.
4-6-10 Shinkawa
181-0004 Mitaka-shi
Japan
email: ohkubo@ishikawa-sangyo.co.jp

Pó Mário
EKO
Lulofsstraat 55, unit 28
2521 AL The Hague
Netherlands
email: mario.po@eko-instruments.com
phone: +31628838831

Pavanello Diego
European Commission - DG JRC - Directorate C - Energy, Transport and Climate
Building 45, TP450 , Via Fermi, 2749
I-21027 Ispra (Va)
ITALY
email: diego.pavanello@ec.europa.eu

Peterson Josh
University of Oregon, Solar Radiation Monitoring Lab
361 Onyx Bridge, Department of Physics
97403 Eugene
United States
email: jpeters4@uoregon.edu
phone: 5413464745

Pokorny Jiri
Czech Hydrometeorological Institute
Zamecek 456
500 08 Hradec Kralove
Czech Republic
email: jiri.pokorny@chmi.cz
phone: +420 495 279 261

Premec Krunoslav
WMO
7bis, avenue de la Paix
CH-1211 Geneva
Switzerland
email: kpremec@wmo.int

Pribullová Anna
Slovak Hydrometeorological Institute
Aerological and solar radiation measurement centre
SHMU
058 01 Poprad-Ganovce 178
Slovakia
email: apribull@ta3.sk
phone: +421908635343

Rüedi Isabelle
WMO
7bis, Avenue de la Paix
1211 Geneva 2
Switzerland
email: iruedi@wmo.int
phone: +41 22 730 82 78

Rea Anthony
WMO
7bis, Avenue de la Paix
1211 Geneva 2
Switzerland
email: area@wmo.int

Reda Ibrahim
National Renewable Energy Laboratory (NREL)
15013 Denver West Parkway
80401 Golden
USA
email: Ibrahim.Reda@nrel.gov
phone: 13033846385

Riveros-Rosas David
Universidad Nacional Autonoma de Mexico
Av Universidad 3000
4510 Coyoacán
Mexico
email: driveros@igeofisica.unam.mx
phone: +52 (55) 23409797

Rodionov Artem
Voeikov Main Geophysical Observatory (Voeikov MGO)
Karbysheva st. 7
194021 St. Petersburg
Russian Federation
email: rodionov.artm@gmail.com
phone: 7 952 237 48 30

Russo Paola
UdelaR
Phisics Department, Solar Energy Laboratory, Av. Luis Batlle Berres km 508 (ex-Ruta 3), Salto Grande
50000 Salto
Uruguay
email: paolarussoganon@gmail.com
phone: +59899112041

Sanghera Sandeep
Met Office
Met Office, FitzRoy Road
EX1 3PB Exeter
UK
email: sandeep.sanghera@metoffice.gov.uk
phone: +44 (0)7525387627

Schifano Luca
RMIB
Av. Circulaire 3
1180 Brussels
Belgium
email: Luca.schifano@meteo.be

Sepúlveda Edgardo
Universidad de Santiago de Chile
Av. Libertador Bernardo O'Higgins 3363
9170022 Santiago
Chile
email: edgardo.sepulvedaa@usach.cl
phone: +56977690532

Suter Markus
Davos Instruments AG
Am Kurpark 3
7270 Davos Platz
Switzerland
email: markus.suter@davos-instruments.ch

Svetličič Marko
Slovenian Environment Agency
Vojkova 1b
1000 Ljubljana
Slovenia
email: marko.svetlicic@gov.si
phone: +386 1 478 44 64

Vuilleumier Laurent
Federal Office of Meteorology and Climatology MeteoSwiss
Ch. de l'Aérologie 1
1530 Payerne
Switzerland
email: laurent.vuilleumier@meteoswiss.ch
phone: +41 58 460 95 41

Wacker Stefan
Deutscher Wetterdienst / Meteorologisches Observatorium Lindenberg (DWD/MOL-RAO)
Am Observatorium 12
15248 Tauche, OT: Lindenberg
Germany
email: stefan.wacker@dwd.de
phone: +49680625860

Webb Craig
Argonne National Lab ARM/DOE
1702 S 3rd St
74631 Blackwell
United States
email: craigw@ops.sgp.arm.gov
phone: 13313183354 or 1-580-262-2306

Zaaiman Willem
European Commission - DG JRC - Directorate C - Energy, Transport and Climate
Building 45, TP450 , Via Fermi, 2749
I-21027 Ispra (Va)
ITALY
email: willem.zaaiman@ec.europa.eu
phone: +39 0332 785750

de Jager Mario
GeoSUN
21 Quantum Street, Techno Park
7600 Stellenbosch
South Africa
email: mario@geosun.co.za
phone: +27 21 882 8354

6.2 Glossary

- (A)HF: Hickey-Frieden self-calibrating pyrheliometer. A type of cavity pyrheliometer originally developed by J.R. Hickey and R.G. Frieden [3], marketed by EPLAB.
- AWX: All-weather AHF. A windowed AHF-type pyrheliometer with electric body heater.
- CH(P)1: A type of field pyrheliometer built and marketed by Kipp & Zonen (OTT HydroMet B.V.).
- CP20: A type of field pyrheliometer built by Hukseflux Thermal Sensors.
- CR: CROM pyrheliometer. A type of cavity pyrheliometer developed by D. Crommelynck.
- CSAR: Cryogenic Solar Absolute Radiometer. A prototype cavity pyrheliometer operating at ~ 30 K. The CSAR was developed and built by PMOD, NPL, and METAS [6].
- DRxx: A type of field pyrheliometer built and marketed by Hukseflux Thermal Sensors.
- MSxx: A type of field pyrheliometer built and marketed by EKO Instruments Co..
- NIP: Normal Incidence Pyrheliometer. A type of field pyrheliometer built and marketed by EPLAB.
- PAC3: PACRAD 3 pyrheliometer. A prototype cavity pyrheliometer developed by J.M. Kendall and C.M. Berdahl [1].
- PMOD: The Physikalisch-Meteorologisches Observatorium Davos, a research institute focusing on radiation and climate research. It was established in 1907 at Davos, Switzerland.
- PMOx: PMO-type pyrheliometer. A type of cavity radiometer originally developed by R.W. Brusa, C. Fröhlich, and J.M. Kendall (PMO1, PMO2, PMO3) [2, 5]. Later iterations of the type were developed by C. Fröhlich and R. Brusa (PMO4, PMO5, PMO6) [4], and M. Suter (PMO8), marketed by Davos Instruments AG.
- SHP1: A type of field pyrheliometer similar to CHP1 with digital connectivity built and marketed by Kipp & Zonen (OTT HydroMet B.V.).
- SNIP: A type of field pyrheliometer similar to the NIP with digital connectivity built and marketed by EPLAB.
- SIAR: SIAR pyrheliomoeter. A type of cavity pyrheliometer developed and built by CIOMP/CAS.
- TMI: TMI pyrheliometer. A type of cavity pyrheliometer developed by J.M. Kendall and C.M. Berdahl, built and marketed by Technical Measurements, Inc..
- WMO: The World Meteorological Organisation (https:/wmo.int)
- WRC: The World Radiation Centre. The WRC was established at PMOD in 1971, it is mandated by WMO [9].
- WRR: The World Radiometric Reference. A concept introduced in 1977 by WMO to standardize solar irradiance measurements [9].
- WSG: The World Standard Group of pyrheliometers. It serves as the physical realization of the WRR [9].

Bibliography

[1] J.M. Kendal Sr. and C.M. Berdahl. "Two Blackbody Radiometers of High Accuracy". In: *Applied Optics* 9.5 (1970).

[2] R.W. Brusa and C. Fröhlich. *Entwicklung eines neuen Absolutradiometers*. Tech. rep. 1. WRC, 1972.

[3] J.R. Hickey; R.G Frieden; F.J. Griffin; S.A. Cone; R.H. Maschoff and J. Gniady. "The Self-Calibrating Sensor of the Eclectice Satellite Pyrheliometer (ESP) Program". In: Proceedings of the Annual Meeting. ASES. 1977.

[4] R.W. Brusa and C. Fröhlich. "Absolute radiometrers (PMO6) and their experimental characterization". In: *Applied Optics* 25.22 (1986).

[5] A.A. Kmito and Yu.A. Sklyarov. *Pyrheliometry*. Translated from Russian. Amerind Publishing Co. Pvt. Ltd., New Delhi, 1987.

[6] R. Winkler. "Cryogenic Solar Absolute Radiometer a potential SI standard for solar irradiance". PhD thesis. University College London, 2013.

[7] W. Finsterle. *IPC-XII Final Report*. IOM Report No. 124. WMO, 2016.

[8] *IPC-XIII/FRC-V/IPgC-III Symposium*. IOM Report No. 138. WMO, 2023.

[9] *Guide to Instruments and Methods of Observation*. WMO-No. 8.

For more information, please contact:

World Meteorological Organization

7 bis, avenue de la Paix – P.O. Box 2300 – CH 1211 Geneva 2 – Switzerland

Communication and Public Affairs Office

Tel.: +41 (0) 22 730 83 14 – Fax: +41 (0) 22 730 81 71

E-mail: cpa@wmo.int

public.wmo.int